GOETHE UNIVERSITÄT FRANKFURT AM MAIN

Master Thesis

Investigation of the Heavy-Light Tetraquark System $\bar{b}\bar{b}ud$ Using Lattice NRQCD

Martin Pflaumer

Institut für Theoretische Physik
Goethe-Universität
Frankfurt am Main

26 September 2018

Supervisor and 1st Examiner
Prof. Dr. Marc Wagner
Goethe-Universität
Frankfurt am Main

2nd Examiner
Prof. Dr. Stefan Meinel
University of Arizona
Tucson, Arizona

Erklärung nach § 30 (12) Ordnung für den Bachelor- und Masterstudiengang

Hiermit erkläre ich, dass ich die Arbeit selbständig und ohne Benutzung anderer als der angegebenen Quellen und Hilfsmittel verfasst habe. Alle Stellen der Arbeit, die wörtlich oder sinngemäß aus Veröffentlichungen oder aus anderen fremden Texten entnommen wurden, sind von mir als solche kenntlich gemacht worden. Ferner erkläre ich, dass die Arbeit nicht - auch nicht auszugsweise - für eine andere Prüfung verwendet wurde.

Frankfurt am Main, 26. September 2018 Martin Pflaumer

Abstract

In this thesis, we focus on the heavy-light tetraquark system with the quark content $\bar{b}\bar{b}ud$. We established the formulation of non-relativistic QCD and derived the required expressions for a non-relativistic treatment of the tetraquark system. In the framework of NRQCD, we consider several creation operators for generating a $\bar{b}\bar{b}ud$ state in the $I(J^P) = 0(1^+)$ channel and construct the associated correlation matrix. Afterwards, searching for bound states in this system, we extract the effective masses and compare them to the BB^* threshold in order to make reliable statements about stable states. Performing a detailed analysis including different lattice gauge link ensembles and extrapolating these results to the physical pion mass, we find a bound $\bar{b}\bar{b}ud$ state with a binding energy of $E_{\bar{b}\bar{b}ud} = -99\,^{+39}_{-39}$ MeV.

Contents

Chapter 1

Introduction

Mankind has been searching for insight into the deepest and smallest components of our world as long as anyone can remember. Even Goethe's Faust desired to discover "what holds the world together at its core". In contrast to Goethe's era, nowadays we have a much better understanding of the fundamental principles of nature, described by the *Standard Model of Nature*.

Therein, the basic constituents of matter are the so-called *quarks*. All particles composed of quarks are named *hadrons*. We distinguish between *baryons* and *mesons*: Baryons on the one hand are half-integer spin particles while the most common ones are composed of a set of three quarks (or three anti-quarks). Mesons on the other hand have an integer spin and are built of quark-antiquark pairs.
There are six different types of quarks, called *flavours*, which are classified in three generations. The first generation contains the light up (u) and down (d) quark, which are the constituents of the most common elementary particles: the proton (uud), the neutron (udd), and the three pions ($u\bar{d}, d\bar{u}, u\bar{u} - d\bar{d}$). The second generation covers the strange (s) and charm (c) quark, which are a few hundred times heavier than the light ones. Finally, in the third generation we find the heavy bottom (b) and top (t) quark whose masses are several thousands times heavier than the light u/d quarks [1].

In the Standard Model, quarks are assumed to be point-like fundamental particles without any spatial extent. They interact with all four fundamental forces, that means electromagnetic, weak, strong, and gravitational. The electric charge of quarks assumes non-integer values ($+2/3$ or $-1/3$) which are combined to integers by forming hadrons. The binding of hadrons is described by the strong force with the associated colour charge. In contrast to the electromagnetic force where two different charges (positive/negative) exist, the colour charge comprises three, usually named green, blue, and red. Furthermore, also the gluons acting as the exchange particles of this theory carry colour charge.

In the mathematical approach, this theory is formulated by a non-abelian SU(3)-gauge theory called *Quantum Chromo Dynamics (QCD)*. Due to the charged gluons, there are self-interaction effects. Hence, computing quark interactions becomes extremely challenging and therefore QCD observables at low energy cannot be extracted easily with an analytical computation. One well-established approach for performing non-pertubative QCD calculations from first principles is provided by lattice QCD. For this purpose, the four dimensional space-time is discretized to a finite-sized Euclidean lattice with a defined

lattice spacing. In this way, physical observables can be computed numerically without further assumptions from first principals using high performance computers. For our theoretical studies, we are applying methods of lattice QCD.

Talking about hadrons, one refers usually to the well-established baryons built of three quarks (qqq) or mesons consisting of a quark-antiquark pair ($q\bar{q}$). Additionally the Standard Model predicts some exotic hadrons, e.g. glueballs, hybrid mesons, tetraquarks or pentaquarks. However, these states are experimentally extremely difficult to observe since they are often resonances and rapidly decay to non-exotic hadrons. Even theoretical investigation of exotic states is quite challenging.

Considering tetraquarks was first initiated by the experimental observations of states like the $a_0(980)$ which could not be identified with known structures. Today, there are studies suggesting that the $a_0(980)$ meson corresponds to a two meson scattering resonance (cf. e.g. [46]).
Nowadays, plenty of possible tetraquark candidates are known experimentally. In 2003, the temporarily stable charmonium-like $X(3872)$ was found [3]. Followed by further tetraquark candidates like the $Z(4430)$ [4, 5, 6, 7] or the bottomonium-like $Z_b(10610)$ and $Z_b(10650)$ [8], the first independently confirmed tetraquark resonance is the $Z_c(3900)$ found in 2013 [9, 10, 11, 12]. Recently, further possible tetraquark candidates have been announced mentioning here only the $X(5568)$ [13] whose existence, however, has not been confirmed yet.
Obviously, the search for exotic hadrons especially tetraquarks is an ongoing topic with auspicious possibilities of gaining a deeper insight into QCD.

In this thesis, we theoretically investigate heavy-light four-quark systems containing bottom quarks. Especially, we focus on the promising tetraquark candidates with quark content $\bar{b}\bar{b}ud$ which might form a bound state. In contrast to the previously mentioned Z_b state which is supposed to contain a heavy quark b, a heavy antiquark $\bar{b}$ and the associated light quarks, we are considering two heavy antiquarks $\bar{b}\bar{b}$. Using two heavy antiquarks is theoretically less complicated to investigate but experimentally more challenging to generate and detect.

In recent years, many efforts have been made to investigate this tetraquark system by means of lattice calculations and great progress has been made in understanding this system and extracting important properties (cf. [14, 15, 16, 17, 18, 19, 20, 21, 22, 23, 24]). In my thesis, I will continue to work on the heavy-light tetraquark $\bar{b}\bar{b}ud$ by proceeding as follows:

In Chapter 2 we start to study the theoretical background of heavy quarks on the lattice. Introducing an effective theory which is in our case non-relativistic QCD (NRQCD), we discuss how to treat heavy quarks on the lattice, derive the NRQCD-Lagrangian and present how to compute heavy quark propagators.
The lattice setup including all lattice gauge configurations used is described in Chapter 3. Moreover the methods used for error analysis are discussed. In addition to statistical error analysis, also quantification of systematic uncertainties is presented in a subsection.
In Chapter 4 we perform a first NRQCD calculation considering the bottomonium states $\eta_B(1S)$ and $\Upsilon(1S)$. Using these less complicated systems, we demonstrate computing quantum numbers, determining the correlation functions and extracting the masses and mass splitting. We examine how to extract physical masses and how to set the scale.

Chapter 5 focuses on a four-quark system consisting of four bottom quarks ($\bar{b}\bar{b}bb$). We compute the mass of the system and compare it to the masses of its constituents from the previous chapter in order to investigate possible bound states.
The principal part of this work is presented in Chapter 6 investigating the $\bar{b}\bar{b}ud$ system. The possible creation operator structures are discussed in detail as well as the components of the correlation matrix. Finally the results obtained in the framework of NRQCD are presented.
To conclude, in Chapter 7 we summarize our results and give an outlook about possible further projects.

Chapter 2

Effective Theories for Heavy Quarks

The quark model includes six different quark flavours which can be grouped in light quarks and heavy quarks. Talking about heavy quarks refers in this context to the hadronic energy scale and involves the charm (c), bottom (b), and top (t) quarks. However, even if the top quark is the heaviest one, it decays rapidly and thus can be treated perturbatively. Therefore, when mentioning heavy quarks in this work, we are talking about the charm and the bottom quark.
Considering the most common particles in nature, like protons, neutrons or pions, we recognize that light quarks seem to dominate our world. Nevertheless, systems containing heavy quarks play an important role in understanding elementary features of QCD. Some reasons to mention can be found in [25]: Heavy quark physics is elementary for a deeper understanding of the Standard Model's flavour structure involving also the CP violation mechanism. Studying decay processes of mesons containing charm or bottom quarks gives evidence about the flavour mixing in QCD and therefore enables us to precisely determine the Cabibbo-Kobayashi-Maskawa (CKM) matrix elements. In addition to that, one can use heavy quark physics as a starting point for physics beyond the Standard Model: The relevant loop effects can be examined by considering flavour-changing neutral current processes, e.g. rare B decays. These processes are suppressed in the Standard Model due to the Glashow-Iliopuolos-Maiani (GIM) mechanism.

In this thesis, we will work with quark systems containing heavy quarks - especially the heavy-light $\bar{b}\bar{b}ud$ - and therefore have to establish a formalism to treat these heavy quarks adequately in lattice QCD simulations. Compared to lattice formulations involving only light quarks, studying heavy quarks in lattice calculations requires special techniques. These are based on an effective Lagrangian which will be the non-relativistic QCD Lagrangian in this work. The reason why it is feasible as well as necessary to treat these systems in the mentioned framework will be illustrated in the next sections.

2.1 Why Using an Effective Theory

Considering heavy quarks, i.e. charm or bottom quarks, the assigned masses in the $\overline{MS}$-scheme are ([26, 27]):

$$m_c \approx 1.27(9) \text{ GeV} \tag{2.1}$$
$$m_b \approx 4.20(12) \text{ GeV} \tag{2.2}$$

We now consider the Compton wavelength, which is proportional to the inverse quark mass m_Q, so $\lambda_C \propto \frac{1}{m_Q}$. Comparing the Compton wavelength to the lattice spacing a gives evidence about the quality of a simulation: If the Compton wavelength is smaller or in a comparable magnitude like the lattice spacing, there will occur serious discretization errors. Consequently, for the two heavy quarks λ_C becomes:

$$\frac{1}{m_c} \approx 0.16 \text{ fm} \tag{2.3}$$
$$\frac{1}{m_b} \approx 0.05 \text{ fm} \tag{2.4}$$

Therefore, an adequate lattice spacing a should be smaller than 0.05 fm for bottom and smaller than 0.16 fm for charm quarks to guarantee a well-working lattice computation with small discretization errors. The motivation to develop an effective theory can be found in the past of lattice theory: The minimal lattice spacing was restricted and could not be created sufficiently small. Even nowadays, commonly used lattice spacings often are of the same magnitude as the Compton wavelength (e.g. 0.1 fm).
However, choosing a sufficiently small lattice spacing causes some additional challenges. For studying hadrons on the lattice, we need an adequate total lattice extent of at least 2 fm: The spatial volume must be large enough to accommodate the hadron while the temporal extent has to enable us to study the Euclidean propagators and to extract masses. Concerning these issues, a lattice with small a has to contain about $\mathcal{O}(100)^4$ lattice points. Hence, the numerical computation becomes extremely expansive.
In short, using the standard lattice QCD methods does not seem to be the optimal approach for studying heavy quarks, so consequently a new concept had to be established.

2.2 Dynamics of Heavy Quarks

Aiming for an improved approach to compute heavy quarks on the lattice, we will examine their dynamics. Having discussed the challenges with regard to heavy quarks on the lattice, we can recognize one big advantage: We can treat heavy quarks non-relativistically. For example, we consider the spatial velocity of the charmonium state ψ $(c\bar{c})$ or the bottomonium state Υ $(b\bar{b})$. One can assume that the mass difference between the $2S$ and the $1S$ splitting coincides approximately with the average kinetic energy $\sim m_Q v^2$ while m_Q is the quark mass. For the charmonium, the mass splitting is $\psi(2S) - \psi(1S) \sim 700$ MeV

while $m_\psi \sim 3$ GeV, so $v^2 \sim 0.3$. Analogously, for the bottomonium, $\Upsilon(2S) - \Upsilon(1S) \sim 600$ MeV and $m_\Upsilon \sim 9$ GeV, thus $v^2 \sim 0.1$. In a concentrated form this is:

$$v^2 \sim \begin{cases} 0.1 & \text{for } \Upsilon \\ 0.3 & \text{for } \psi \end{cases} \tag{2.5}$$

This involves two important consequences for systems containing heavy quarks (cf. [31]): First, since the radiation of gluons is proportional to v, we can neglect radiated low-energetic gluons. Second, an exchanged gluon's momentum is of order of the quark momenta and therefore the gluon's energy is by a factor of $1/v$ greater than the quark's kinetic energy: $E_g \sim p_g \sim p_Q \gg E_Q$. As a consequence, gluon exchange and thus the interaction between quark and antiquark is almost immediate.
For quarkonium states, one has to consider three different energy scales in the system:

- the mass $\sim m_Q$
- the spatial momentum $\sim m_Q v$
- the kinetic energy $\sim m_Q v^2$

Since the quarks are non-relativistic, we can deduce: $m_Q \gg m_Q v \gg m_Q v^2$. Consequently, the expansion parameter for an effective theory in a non-relativistic approximation is the spatial velocity v or rather the spatial momentum $\mathbf{k}$. Accordingly, we will perform a separation of scales for $|\mathbf{k}| \ll m_Q$ with m_Q being the heavy quark mass. An important consequence of this separation is that heavy pair creation will be neglected. However, for a detailed analysis one has to distinguish between systems containing only one heavy quark and systems with more than one heavy quark. This will be considered in Sec. 2.4 when focusing on power counting.
We will continue by deriving the effective Lagrangian in the non-relativistic approximation in Sec. 2.3. The resulting theory is well-known as *non-relativistic QCD (NRQCD)*. In this work, we will apply the Foldy-Wouthuysen-Tani (FWT) transformation to derive this effective Lagrangian in the continuum.

We would like to emphasise that there exist several effective theories. Another prominent example is the *heavy quark effective theory (HQET)*, which is applied when only one heavy quark is present. However, in this thesis we always consider at least two heavy quarks and thus work solely in the non-relativistic framework. Therefore, we put our main focus on NRQCD and the associated effective Lagrangian. Nevertheless, the FWT transformation is strictly formal and can be applied for both theories, HQET and NRQCD in consideration of the scaling behaviour. In Sec. 2.4, we illuminate the differences when discussing power counting.

2.3 Foldy-Wouthuysen-Tani (FWT) Transformation

The Foldy-Wouthuysen-Tani transformation is a well-established formalism to derive the effective Lagrangian. This paragraph is based on [21, 28]. The initial idea of the FWT transformation is strongly related to the derivation of the Pauli equation: We aim to split the Lagrangian into a particle and an antiparticle equation.
Therefore, we will summarize the computation of the Pauli equation to motivate the following approach for the FWT transformation.

2.3.1 Derivation of Pauli Equation

The starting point for this calculation is the well-known Dirac equation for a particle in an electromagnetical field [29], namely:

$$\left(i\gamma^\mu D_\mu - m_Q\right)\Psi = 0 \tag{2.6}$$

with $D_\mu = \partial_\mu - iqA_\mu$.

For solving it, we use the ansatz: $\Psi = \begin{pmatrix} \varphi(p) \\ \chi(p) \end{pmatrix} \mathrm{e}^{-ip_\mu x^\mu}$. In the limit of small velocities, we can use:

$$E = \left(m_Q^2 + |p|^2\right)^{\frac{1}{2}} = m_Q\left(1 + \frac{|p|^2}{m_Q^2}\right)^{\frac{1}{2}} = m_Q\left(1 + \frac{|p|^2}{2m_Q^2} + \mathcal{O}\left(\frac{|p|^4}{m_Q^4}\right)\right) \approx m_Q \tag{2.7}$$

So, the exponential function can be written as:

$$\mathrm{e}^{-ip_\mu x^\mu} = \mathrm{e}^{-iEt}\mathrm{e}^{i\mathbf{px}} \approx \mathrm{e}^{-im_Q t}\mathrm{e}^{i\mathbf{px}} \tag{2.8}$$

which makes it possible to transform the spinor to:

$$\Psi = \begin{pmatrix} \varphi(x) \\ \chi(x) \end{pmatrix} \mathrm{e}^{-im_Q t} \tag{2.9}$$

Inserting this into the Dirac-equations results in:

$$\begin{aligned} 0 &= \left(i\gamma^\mu D_\mu - m_Q\right)\Psi = \left(i\gamma^0 D_0 - i\gamma^j D_j - m_Q\right)\Psi \\ &= \left(i\gamma^0 D_0 - i\gamma^j D_j - m_Q\right)\begin{pmatrix} \varphi(x) \\ \chi(x) \end{pmatrix}\mathrm{e}^{-im_Q t} \\ &= \left[i\begin{pmatrix} 1 & 0 \\ 0 & -1 \end{pmatrix} D_0 - i\begin{pmatrix} 0 & \sigma^j \\ -\sigma^j & 0 \end{pmatrix} D_j - m_Q\begin{pmatrix} 1 & 0 \\ 0 & 1 \end{pmatrix}\right]\begin{pmatrix} \varphi(x) \\ \chi(x) \end{pmatrix}\mathrm{e}^{-im_Q t} \end{aligned} \tag{2.10}$$

This leads to the two equations:

$$\begin{aligned} iD_0\varphi(x)\mathrm{e}^{-im_Qt} - i\sigma^j D_j\chi(x)\mathrm{e}^{-im_Qt} - m_Q\varphi(x)\mathrm{e}^{-im_Qt} = 0 \\ -iD_0\chi(x)\mathrm{e}^{-im_Qt} + i\sigma^j D_j\varphi(x)\mathrm{e}^{-im_Qt} - m_Q\chi(x)\mathrm{e}^{-im_Qt} = 0 \end{aligned} \tag{2.11}$$

Inserting the derivative for $\varphi(x)$

$$iD_0\varphi(x)\mathrm{e}^{-im_Qt} = i\left(D_0\varphi(x)\right)\mathrm{e}^{-im_Qt} + i\left(-im_Q\right)\varphi(x)\mathrm{e}^{-im_Qt} \tag{2.12}$$

and analogous for $\chi(x)$ yields to:

$$\begin{aligned} iD_0\varphi(x) - i\sigma^j D_j\chi(x) &= 0 \\ -iD_0\chi(x) - 2m_Q\chi(x) + i\sigma^j D_j\varphi(x) &= 0 \end{aligned} \tag{2.13}$$

and can be consequently expressed as:

$$\begin{aligned} iD_0\varphi(x) &= i\sigma^j D_j\chi(x) \\ \left(iD_0 + 2m_Q\right)\chi(x) &= i\sigma^j D_j\varphi(x) \end{aligned} \tag{2.14}$$

Note that $\chi(x)$ is smaller than $\varphi(x)$ by a factor $2m_Q$. We can now neglect the term $iD_0\chi(x)$, so the second equation is reduced to:

$$\begin{aligned} iD_0\varphi(x) &= i\sigma^j D_j\chi(x) \\ \chi(x) &= \frac{i}{2m_Q}\sigma^j D_j\varphi(x) \end{aligned} \tag{2.15}$$

If we combine both equations from 2.15, we get:

$$iD_0\varphi(x) = \frac{-1}{2m_Q}\sigma^j D_j\sigma^k D_k\varphi(x) \tag{2.16}$$

With the relation for the Pauli matrices $\sigma^j\sigma^k = \delta^{jk} + i\epsilon_{jkl}\sigma^l$ this can be evaluated in the following way:

$$\begin{aligned} iD_0\varphi(x) =& \frac{-1}{2m_Q}\left(\delta^{jk} + i\epsilon_{jkl}\sigma^l\right)D_jD_k\varphi(x) \\ =& \frac{-1}{2m_Q}\left(D_jD^j + i\epsilon_{jkl}D_jD_k\sigma^l\right)\varphi(x) \end{aligned} \tag{2.17}$$

Using the extended expression for the covariant derivative, we get:

$$\begin{aligned} & i\epsilon_{jkl}D_jD_k\sigma^l\varphi(x) = i\epsilon_{jkl}\left(\partial_j - iqA_j\right)\left(\partial_k - iqA_k\right)\sigma^l\varphi(x) \\ =& i\epsilon_{jkl}\Big[\partial_j\partial_k\varphi(x) - iq\left(\partial_jA_k\right)\varphi(x) - iqA_k\partial_j\varphi(x) \\ & -iqA_j\partial_k\varphi(x) + qA_jqA_k\varphi(x)\Big]\sigma^l \\ =& \epsilon_{jkl}q\left(\partial_jA_k\right)\sigma^l\varphi(x) = q\mathrm{B}_l\sigma^l\varphi(x) \end{aligned} \tag{2.18}$$

Inserting this into (2.17) yields:

$$iD_0\varphi(x) = \frac{-1}{2m_Q}\left(D_jD^j + q\mathrm{B}_l\sigma^l\right)\varphi(x) \tag{2.19}$$

Finally, rewriting this expression in vector notation, we receive the well-know Pauli equation in (2.20):

$$\left(iD_0 + \frac{\mathbf{D}^2}{2m_Q} + \frac{q}{2m_Q}q\boldsymbol{\sigma}\cdot\mathbf{B}\right)\varphi(x) = 0 \tag{2.20}$$

Note that the particle and anti-particle solutions are decoupled.

2.3.2 Derivation of FWT Transformation

We will use a similar approach to derive the effective Lagrangian for QCD in the non-relativistic limit. Note that the Pauli equation has been decoupled into particle and anti-particle solution. We will use a related strategy to decouple particle and anti-particle components of the Dirac Lagrangian for heavy quarks to a given order in the expansion parameter $1/m$. This parameter is strictly formal, for a more detailed view on this parameter, see Sec. 2.4. One additional remark to this approach should be mentioned at this state: Since we are decoupling particles and anti-particles, we are removing quark-antiquark pair production from our effective theory.

We are using the particle / anti-particle projectors

$$P_{\pm} = \frac{1}{2}\left(1 \pm \gamma^0\right) \tag{2.21}$$

and the Dirac-Lagrangian

$$\mathcal{L} = \overline{\Psi}\left(i\gamma^0 D_0 - i\gamma^j D_j - m_Q\right)\Psi \tag{2.22}$$

written in Minkowski space.
A transformation decoupling particle and anti-particle solution consequently removes all contributions from the Lagrangian that do not commute with γ^0. Considering (2.22), the only term which does not commute is $i\gamma^j D_j$. At this point, we introduce redefined spinors:

$$\begin{aligned}\Psi &= \exp\left(-\frac{1}{2m_Q} i\gamma^j D_j\right)\Psi_{(1)} \\ \overline{\Psi} &= \overline{\Psi}_{(1)} \exp\left(-\frac{1}{2m_Q} i\gamma^j D_j\right)\end{aligned} \tag{2.23}$$

This redefinition cancels the non-commuting term but introduces an infinite number of terms with higher powers in $\frac{1}{m_Q}$. For leading order, the Lagrangian $\mathcal{L}_{(1)0}$ is given by:

$$\begin{aligned}\mathcal{L}_{(1)0} =& \overline{\Psi}_{(1)} \exp\left(-\frac{1}{2m_Q} i\gamma^j D_j\right)\left(i\gamma^0 D_0 - i\gamma^j D_j - m_Q\right)\exp\left(-\frac{1}{2m_Q} i\gamma^j D_j\right)\Psi_{(1)} \\ =& \overline{\Psi}_{(1)}\left(1 - \frac{1}{2m_Q} i\gamma^j D_j + \ldots\right)\left(i\gamma^0 D_0 - i\gamma^j D_j - m_Q\right)\left(1 - \frac{1}{2m_Q} i\gamma^j D_j + \ldots\right)\Psi_{(1)} \\ =& \overline{\Psi}_{(1)}\left(i\gamma^0 D_0 - m_Q - i\gamma^j D_j + \frac{1}{2} i\gamma^j D_j + \frac{1}{2} i\gamma^j D_j\right)\Psi_{(1)} + \mathcal{O}\left(\frac{1}{m_Q}\right) \\ =& \overline{\Psi}_{(1)}\left(i\gamma^0 D_0 - m_Q\right)\Psi_{(1)} + \mathcal{O}\left(\frac{1}{m_Q}\right)\end{aligned} \tag{2.24}$$

The redefined Lagrangian up to $\mathcal{O}\left(\frac{1}{m_Q^3}\right)$ including the detailed derivation can be found in Appendix B.1.

The Lagrangian in closed form in terms of the new spinors reads:

$$\mathcal{L} = \overline{\Psi}_{(1)} \left(i\gamma^0 D_0 - m_Q \right) \Psi_{(1)} + \sum_{n=1}^{\infty} \frac{1}{m_Q^n} \overline{\Psi}_{(1)} O_{(1)n} \Psi_{(1)} \tag{2.25}$$

where $O_{(1)n}$ with $n \geq 1$ describes the contributions with higher orders in $1/m_Q$ which do not commute with γ^0. For calculating $O_{(1)1}$, we have to include the term $\mathcal{O}\left(\frac{1}{m_Q}\right)$ in (2.24), which is given by (see Appendix B.1):

$$O_{(1)1} = +\frac{1}{2}\gamma^j D_j \gamma^0 D_0 + \frac{1}{2}\gamma^0 D_0 \gamma^j D_j - \frac{1}{2}\left(\gamma^j D_j\right)^2 \tag{2.26}$$

We can rewrite this expression using the commutator relation for the covariant derivative

$$[D_\mu, D_\nu] = igF_{\mu\nu} \tag{2.27}$$

so that:

$$\begin{aligned}
O_{(1)1} =& -\frac{1}{2}\left\{-\gamma^j\gamma^0 D_j D_0 - \gamma^0\gamma^j D_0 D_j + \gamma^j\gamma^k D_j D_k\right\} \\
=& -\frac{1}{2}\left\{-\gamma^j\gamma^0 D_j D_0 + \gamma^j\gamma^0 D_0 D_j + \gamma^j\gamma^k D_j D_k + D_j D^j - D_j D^j\right\} \\
=& -\frac{1}{2}\left\{-\gamma^j\gamma^0 \left(D_j D_0 - D_0 D_j\right) + \gamma^j\gamma^k D_j D_k - \eta^{jk} D_j D_k\right\} - \frac{1}{2} D_j D^j \\
=& -\frac{1}{2}\left\{-\gamma^j\gamma^0 \left[D_j, D_0\right] + \frac{1}{2}\left(\gamma^j\gamma^k D_j D_k + \gamma^j\gamma^k D_j D_k - 2\eta^{jk} D_j D_k\right)\right\} \\
& -\frac{1}{2} D_j D^j \\
=& +\frac{ig}{2}\gamma^j\gamma^0 F_{j0} - \frac{1}{4}\left(\gamma^j\gamma^k D_j D_k - \left(2\eta^{jk} - \gamma^j\gamma^k\right) D_j D_k\right) - \frac{1}{2} D_j D^j \\
=& +\frac{ig}{2}\gamma^j\gamma^0 F_{j0} - \frac{1}{4}\left(\gamma^j\gamma^k D_j D_k - \gamma^k\gamma^j D_j D_k\right) - \frac{1}{2} D_j D^j \\
=& -\frac{1}{2} D_j D^j + \frac{ig}{2}\gamma^j\gamma^0 F_{j0} \\
& -\frac{1}{8}\left(\gamma^j\gamma^k D_j D_k - \gamma^j\gamma^k D_k D_j - \gamma^k\gamma^j D_j D_k + \gamma^k\gamma^j D_k D_j\right) \\
=& -\frac{1}{2} D_j D^j + \frac{ig}{2}\gamma^j\gamma^0 F_{j0} - \frac{1}{8}\left(\gamma^j\gamma^k - \gamma^k\gamma^j\right)\left(D_j D_k - D_k D_j\right) \\
=& -\frac{1}{2} D_j D^j + \frac{ig}{2}\gamma^j\gamma^0 F_{j0} - \frac{1}{8}\left[\gamma^j, \gamma^k\right]\left[D_j, D_k\right] \\
=& -\frac{1}{2} D_j D^j + \frac{ig}{2}\gamma^j\gamma^0 F_{j0} - \frac{ig}{8}\left[\gamma^j, \gamma^k\right] F_{jk}
\end{aligned} \tag{2.28}$$

This first order correction can be grouped into a commuting and an anti-commuting part with regard to γ^0 as $O_{(1)1} = O^C_{(1)1} + O^A_{(1)1}$ with:

$$O^C_{(1)1} = -\frac{1}{2} D_j D^j - \frac{ig}{8}\left[\gamma^j, \gamma^k\right] F_{jk} \tag{2.29}$$

$$O^A_{(1)1} = +\frac{ig}{2}\gamma^j\gamma^0 F_{j0} \tag{2.30}$$

To cancel the anti-commuting term of first order, we perform a second redefinition

$$\begin{aligned}\Psi_{(1)} &= \exp\left(\frac{1}{2m_Q^2}O^A_{(1)1}\right)\Psi_{(2)}\\ \overline{\Psi}_{(1)} &= \overline{\Psi}_{(2)}\exp\left(\frac{1}{2m_Q^2}O^A_{(1)1}\right)\end{aligned} \tag{2.31}$$

which results in the new Lagrangian:

$$\mathcal{L} = \overline{\Psi}_{(2)}\left(i\gamma^0 D_0 - m_Q\right)\Psi_{(2)} + \sum_{n=1}^{\infty}\frac{1}{m_Q^n}\overline{\Psi}_{(2)}O_{(2)n}\Psi_{(2)} \tag{2.32}$$

Note that we first have to include all terms up to $\mathcal{O}\left(1/m_Q^2\right)$ in the expansion in (2.24) to successfully eliminate all terms of $\mathcal{O}\left(1/m_Q\right)$. The relevant expression up to required order is calculated in Appendix B.1. Afterwards, one has to repeat the expansion using now the second redefinition (2.31) up to $\mathcal{O}\left(1/m_Q^2\right)$. Finally, we extract the expressions for $O_{(2)n}$ while we divide again into commuting and anti-commuting parts $O_{(2)n} = O^C_{(2)n} + O^A_{(2)n}$. This calculation can be found in Appendix B.2. In the end, we receive the following terms for $O_{(2)n}$:

$$\begin{aligned}O^C_{(2)1} &= O^C_{(1)1}\\ O^A_{(2)1} &= 0\\ O^C_{(2)2} &= -\frac{g}{8}\gamma^0\left(D_j^* F_{j0} - \frac{1}{2}\left[\gamma^j,\gamma^k\right]\{D_j, F_{k0}\}\right)\\ O^A_{(2)2} &= \frac{i}{3}\gamma^j\gamma^k\gamma^l D_j D_k D_l + \frac{g}{4}\gamma^j\left[D_0, F_{j,0}\right]\end{aligned} \tag{2.33}$$

We can continue eliminating anti-commuting terms till we reach the desired order in $\frac{1}{m_Q}$. So if we want to cancel the term $O^A_{(2)2}$, we have to perform another redefinition in the same way as before in (2.23) and (2.31):

$$\begin{aligned}\Psi_{(2)} &= \exp\left(\frac{1}{2m_Q^3}O^A_{(2)2}\right)\Psi_{(3)}\\ \overline{\Psi}_{(2)} &= \overline{\Psi}_{(3)}\exp\left(\frac{1}{2m_Q^3}O^A_{(2)2}\right)\end{aligned} \tag{2.34}$$

The Lagrangian reads

$$\mathcal{L} = \overline{\Psi}_{(3)} \left(i\gamma^0 D_0 - m_Q \right) \Psi_{(3)} + \sum_{n=1}^{\infty} \frac{1}{m_Q^n} \overline{\Psi}_{(3)} O_{(3)n} \Psi_{(3)} \tag{2.35}$$

with:

$$\begin{aligned} O^C_{(3)1} &= O^C_{(2)1} \\ O^A_{(3)1} &= 0 \\ O^C_{(3)2} &= O^C_{(2)2} \\ O^A_{(3)2} &= 0 \end{aligned} \tag{2.36}$$

At this stage, we stop after the last redefinition, so we have included all terms up to $\mathcal{O}\left(1/m_Q^2\right)$. Thus, we do not explicitly compute higher orders in $1/m_Q$, namely the term $O_{(3)3}$, but apply this redefinition especially to eliminate $O^A_{(2)2}$. However, further redefinitions can be used to cancel terms like $O^A_{(3)3}$ and to improve the Lagrangian by further orders of $1/m_Q$.
It is important to emphasise that all remaining terms commute with γ^0 and there are no additional time derivatives introduced.
In a final step, we can remove the quark mass term by redefining (see Appendix B.3):

$$\begin{aligned} \Psi_{(3)} &= \exp\left(-im_Q x^0 \gamma^0\right) \widetilde{\Psi} \\ \overline{\Psi}_{(3)} &= \overline{\widetilde{\Psi}} \exp\left(im_Q x^0 \gamma^0\right) \end{aligned} \tag{2.37}$$

The final Lagrangian is given by:

$$\begin{aligned} \mathcal{L} = \overline{\widetilde{\Psi}} \Bigg[& i\gamma^0 D_0 - \frac{1}{2m_Q} D_j D^j - \frac{ig}{8m_Q} \left[\gamma^j, \gamma^k\right] F_{jk} \\ & - \frac{g}{8m_Q^2} \gamma^0 \left(D_j^* F_{j0} - \frac{1}{2} \left[\gamma^j, \gamma^k\right] \{D_j, F_{k0}\} \right) \Bigg] \widetilde{\Psi} + \mathcal{O}\left(\frac{1}{m_Q^3}\right) \end{aligned} \tag{2.38}$$

For further simplification of (2.38), we use the relation

$$\left[\gamma^j, \gamma^k\right] = -2i\epsilon_{jkl}\Sigma^l \quad \text{with} \quad \Sigma^l = \begin{pmatrix} \sigma^l & 0 \\ 0 & \sigma^l \end{pmatrix} \tag{2.39}$$

insert the definition of the chromoelectric and chromomagnetic fields

$$E_j = F_{0j} \quad \text{and} \quad B_j = -\frac{1}{2}\epsilon_{jkl} F_{kl} \tag{2.40}$$

and obtain accordingly:

$$\begin{aligned}\mathcal{L} = \overline{\widetilde{\Psi}} \Bigg[& i\gamma^0 D_0 + \frac{\mathbf{D}^2}{2m_Q} + \frac{g}{2m_Q}\boldsymbol{\Sigma}\cdot\mathbf{B} \\ & + \frac{g}{8m_Q^2}\gamma^0 \left(\mathbf{D}^*\cdot\mathbf{E} + i\boldsymbol{\Sigma}\cdot(\mathbf{D}\times\mathbf{E} - \mathbf{E}\times\mathbf{D}) \right) \Bigg] \widetilde{\Psi} + \mathcal{O}\left(\frac{1}{m_Q^3}\right)\end{aligned} \tag{2.41}$$

Remembering the initial idea to decouple the Lagrangian into a particle and an anti-particle equation, we introduce the two components ψ and χ of the spinor $\widetilde{\Psi}$ explicitly:

$$\widetilde{\Psi} = \begin{pmatrix} \psi \\ \chi \end{pmatrix}, \qquad \overline{\widetilde{\Psi}} = \begin{pmatrix} \psi^\dagger, & -\chi^\dagger \end{pmatrix} \tag{2.42}$$

Inserting (2.42) in (2.41), we get the decoupled Lagrangian:

$$\begin{aligned}\mathcal{L} = & \psi^\dagger \left[iD_0 + \frac{\mathbf{D}^2}{2m_Q} + \frac{g}{2m_Q}\boldsymbol{\sigma}\cdot\mathbf{B} + \frac{g}{8m_Q^2}\left(\mathbf{D}^*\cdot\mathbf{E} + i\boldsymbol{\sigma}\cdot(\mathbf{D}\times\mathbf{E} - \mathbf{E}\times\mathbf{D}) \right) \right] \psi \\ & + \chi^\dagger \left[iD_0 - \frac{\mathbf{D}^2}{2m_Q} - \frac{g}{2m_Q}\boldsymbol{\sigma}\cdot\mathbf{B} + \frac{g}{8m_Q^2}\left(\mathbf{D}^*\cdot\mathbf{E} + i\boldsymbol{\sigma}\cdot(\mathbf{D}\times\mathbf{E} - \mathbf{E}\times\mathbf{D}) \right) \right] \chi \\ & + \mathcal{O}\left(\frac{1}{m_Q^3}\right)\end{aligned} \tag{2.43}$$

Here, $\mathbf{E}$ are the chromoelectric and $\mathbf{B}$ the chromomagnetic fields.
As expected, the Lagrangian has been decoupled into a particle and an anti-particle solution. If we compare (2.43) with the Pauli equation in (2.20), we see that the two equations coincide up to $\mathcal{O}(1/m_Q)$. We conclude that we made a reasonable choice for our ansatz and successfully determined the effective Lagrangian.

2.4 Power Counting

The effective Lagrangian derived in Sec. 2.3 is equivalent for systems containing heavy-light hadrons as well as heavy-heavy mesons. However, the expansion parameter and thus the order of the contributions varies (cf. [21, 28]).
For systems containing only one heavy quark, the energy scale is dominated by the gluon dynamics and thus controlled by Λ_{QCD}. Moreover, momentum exchange between the heavy quark and the light components is also of order Λ_{QCD}. Consequently, for the covariant derivatives, we find:

$$|\mathbf{D}| \sim |D_0| \sim \Lambda_{\mathrm{QCD}}. \tag{2.44}$$

The same is given for the gluon potential A_μ:

$$|g\mathbf{A}| \sim |gA_0| \sim \Lambda_{\mathrm{QCD}} \tag{2.45}$$

and:

$$|g\mathbf{E}| \sim |g\mathbf{B}| \sim \Lambda_{\mathrm{QCD}}^2. \tag{2.46}$$

One can show, that the contributions in the Lagrangian (2.43) represented by the formal expansion parameter $1/m_Q^n$ are of order:

$$\left(\frac{\Lambda_{\mathrm{QCD}}}{m_Q}\right)^n \tag{2.47}$$

So, (2.43) includes all terms up to $\mathcal{O}\left(\frac{\Lambda_{\mathrm{QCD}}}{m_Q}\right)^2$. In the static limit $m_Q \to \infty$, the Lagrangian reduces to

$$\mathcal{L} = \psi^\dagger i D_0 \psi \tag{2.48}$$

This Lagrangian is referred to as the *heavy quark effective theory (HQET)* Lagrangian.

Nevertheless, in this thesis we consider systems with more than one heavy quark and therefore we chose the framework of *NRQCD*. It can be applied for heavy-heavy systems as well as for light-heavy systems and is therefore more appropriate to be used for our purposes. As already discussed in Sec. 2.2, the order parameter is the spatial velocity v, so we will consider the physical quantities in powers of v.

The spatial momentum and the kinetic energy are given by:

$$|\mathbf{k}| \sim m_Q v, \qquad E_{kin} \sim m_Q v^2 \tag{2.49}$$

and thus the covariant derivative is also of order:

$$|\mathbf{D}| \sim m_Q v \tag{2.50}$$

For small distances, the quark-antiquark potential is similar to the Coulomb potential. Therefore, the kinetic and potential energy are also of the same order, so consequently:

$$|gA_0| \sim E_{kin} \sim m_Q v^2 \tag{2.51}$$

From the Schrödinger equation, we can conclude that:

$$|D_0| \sim \left|\frac{\mathbf{D}^2}{2m_Q}\right| \sim m_Q v^2 \tag{2.52}$$

Finally, using the Yang-Mills equations [30] gives evidence about the vector potentials:

$$|g\mathbf{E}| \sim m_Q^2 v^3, \qquad |g\mathbf{B}| \sim m_Q^2 v^4 \tag{2.53}$$

Referring to the Lagrangian in (2.43), we realise that the included contributions are up to order v^4. In other words, our formal expansion parameter $1/m_Q^n$ is replaced by $1/(v^2)^n$. However, there is one term of $\mathcal{O}(v^4)$ missing. To detect this term we consider the expansion of the kinetic energy:

$$E_{kin} = \left(m_Q^2 + \mathbf{k}^2\right)^{\frac{1}{2}} - m_Q = \frac{\mathbf{k}^2}{2m_Q} - \frac{\mathbf{k}^4}{8m_Q^3} + \frac{\mathbf{k}^6}{16m_Q^5} + \mathcal{O}\left(\frac{1}{m_Q^7}\right) \tag{2.54}$$

We remark that the term $\frac{\mathbf{D}^4}{8m_Q^3}$ is not included in (2.43), so we have to add it by hand. The final NRQCD Lagrangian for the particle solution takes on the following shape:

$$\mathcal{L}_{\text{NRQCD}} = \psi^\dagger \left[iD_0 + \frac{\mathbf{D}^2}{2m_Q} + \frac{g\boldsymbol{\sigma}\cdot\mathbf{B}}{2m_Q} + \frac{\mathbf{D}^4}{8m_Q^3} + \frac{g}{8m_Q^2}\left(\mathbf{D}^*\cdot\mathbf{E} + i\boldsymbol{\sigma}\cdot(\mathbf{D}\times\mathbf{E} - \mathbf{E}\times\mathbf{D})\right)\right]\psi + \mathcal{O}\left(v^6\right) \tag{2.55}$$

2.5 Lattice NRQCD

To continue, we have to put our effective theory on the lattice. Therefore we will first convert the continuum Lagrangian (2.55) given in Minkowski space-time to Euclidean space-time. In the next step, we deduce the Green function which makes it possible to evolve the heavy quark propagator.

2.5.1 Euclidean NRQCD Lagrangian

For transforming to Euclidean space-time, we use the identities

$$x_0^{(M)} = -ix_0^{(E)}, \quad D_0^{(M)} = iD_0^{(E)}, \quad E_i^{(M)} = -iE_i^{(E)} \tag{2.56}$$

whereas all other quantities remain the same. We use the relation between the actions in Minkowski and Euclidean space $iS^{(M)} = -S^{(E)}$, so we get:

$$
\begin{aligned}
iS^{(M)} &= i\int d^3x\, dx_0^{(M)} \mathcal{L}^{(M)}_{\text{NRQCD}} \\
&= i\int d^3x\, dx_0^{(M)} \psi^\dagger \Bigg[iD_0^{(M)} + \frac{\mathbf{D}^2}{2m_Q} + \frac{g\boldsymbol{\sigma}\cdot\mathbf{B}^{(M)}}{2m_Q} + \frac{\mathbf{D}^4}{8m_Q^3} \\
&\qquad + \frac{g}{8m_Q^2}\left(\mathbf{D}^*\cdot\mathbf{E}^{(M)} + i\boldsymbol{\sigma}\cdot\left(\mathbf{D}\times\mathbf{E}^{(M)} - \mathbf{E}^{(M)}\times\mathbf{D}\right)\right)\Bigg]\psi \\
&= i\int d^3x \left(-i dx_0^{(E)}\right)\psi^\dagger \Bigg[i\left(iD_0^{(E)}\right) + \frac{\mathbf{D}^2}{2m_Q} + \frac{g\boldsymbol{\sigma}\cdot\mathbf{B}^{(E)}}{2m_Q} + \frac{\mathbf{D}^4}{8m_Q^3} \\
&\qquad + \frac{g}{8m_Q^2}\left(-i\mathbf{D}^*\cdot\mathbf{E}^{(E)} + \boldsymbol{\sigma}\cdot\left(\mathbf{D}\times\mathbf{E}^{(E)} - \mathbf{E}^{(E)}\times\mathbf{D}\right)\right)\Bigg]\psi \\
&= -\int d^3x\ dx_0^{(E)}\psi^\dagger \Bigg[D_0^{(E)} - \frac{\mathbf{D}^2}{2m_Q} - \frac{g\boldsymbol{\sigma}\cdot\mathbf{B}^{(E)}}{2m_Q} - \frac{\mathbf{D}^4}{8m_Q^3} \\
&\qquad + \frac{ig}{8m_Q^2}\left(\mathbf{D}^*\cdot\mathbf{E}^{(E)} + i\boldsymbol{\sigma}\cdot\left(\mathbf{D}\times\mathbf{E}^{(E)} - \mathbf{E}^{(E)}\times\mathbf{D}\right)\right)\Bigg]\psi \\
&= -\int d^3x\, dx_0^{(E)} \mathcal{L}^{(E)}_{\text{NRQCD}} = -S^{(E)}
\end{aligned}
\tag{2.57}
$$

Consequently, the Euclidean Lagrangian is given by (note that we omit the index (E)):

$$
\mathcal{L}_{\text{NRQCD}} = \psi^\dagger \left[D_0 - \frac{\mathbf{D}^2}{2m_Q} - \frac{g\boldsymbol{\sigma}\cdot\mathbf{B}}{2m_Q} - \frac{\mathbf{D}^4}{8m_Q^3} + \frac{ig}{8m_Q^2}\left(\mathbf{D}^*\cdot\mathbf{E} + i\boldsymbol{\sigma}\cdot(\mathbf{D}\times\mathbf{E} - \mathbf{E}\times\mathbf{D})\right)\right]\psi \tag{2.58}
$$

2.5.2 Derivation of the Green Function

In this section we will sketch the derivation of the Green function, i.e. the quark propagator for the lowest order $\propto v^2$. For a more detailed discussion of the Green function and further improvements used, cf. [28, 30, 31].
The $\mathcal{O}(v^2)$ Lagrangian is given by:

$$
\mathcal{L} = \psi^\dagger \left[D_0 - \frac{\mathbf{D}^2}{2m_Q}\right]\psi + \mathcal{O}\left(v^4\right) \tag{2.59}
$$

For lattice calculations, we have to discretise our theory so we are moving to a four-dimensional space-time grid with a total extent of L_μ ($\mu = 0, 1, 2, 3$) and a finite number of lattice points x_μ for each direction with a lattice spacing of a. The quark fields are located at the nodes of the lattice whereas the gauge fields are represented by gauge links connecting the lattice points. Mathematically, they are expressed by a unitary matrix $U_\mu(x)$ which connects the lattice point x with the following point in μ-th direction.
In order to transform the Lagrangian (2.59) to a lattice version, the derivatives are replaced by forward, backward or centred differences:

$$\begin{aligned} a\Delta_\mu^{(+)}\psi(x) &= U_\mu(x)\psi(x+a\hat{\mu}) - \psi(x) \\ a\Delta_\mu^{(-)}\psi(x) &= \psi(x) - U_\mu^\dagger(x-a\hat{\mu})\psi(x-a\hat{\mu}) \\ \Delta_\mu^{\pm} &= \frac{1}{2}\left(\Delta_\mu^{(+)} + \Delta_\mu^{(-)}\right) \end{aligned} \tag{2.60}$$

The Laplacian operator on the lattice is defined as:

$$\mathbf{\Delta}^{(2)} = \sum_i \Delta_i^{(+)}\Delta_i^{(-)} = \sum_i \Delta_i^{(-)}\Delta_i^{(+)} \tag{2.61}$$

Consequently, the lattice version of (2.59) looks like:

$$\mathcal{L} = \psi^\dagger a\left[\Delta_0 - \frac{\mathbf{\Delta}^{(2)}}{2\hat{m}_Q}\right]\psi \tag{2.62}$$

with the mass transformed also to dimensionless lattice units $\hat{m}_Q = a \cdot m_Q$.

For the sake of briefness, we introduce the abbreviation

$$H_0 = -\frac{\mathbf{\Delta}^{(2)}}{2\hat{m}_Q} \tag{2.63}$$

In the next step, we will develop the evolution equation for the heavy quark propagator by determining the Green function.
The Green function is the inverse of the full Lagrangian kernel, so it is given by:

$$a\left(\Delta_0 + H_0\right) G_\psi(x, x') = \delta^4(x - x') \tag{2.64}$$

with $x = (\tau, \mathbf{x})$ and $x' = (\tau', \mathbf{x}')$. For the time evolution of the Green function, we have to use the retarded one with $\tau < \tau'$, so

$$a\left(\Delta_0 + H_0\right) G_\psi(\tau, \mathbf{x}, \tau', \mathbf{x}') = 0 \tag{2.65}$$

Inserting the discrete covariant forward derivative given in (2.60) and using the abbreviation $G_{\psi_\tau} \equiv G_\psi(\tau, \mathbf{x}, \tau', \mathbf{x}')$, we find:

$$\begin{aligned} U_0(x)G_{\psi_{\tau+1}} - G_{\psi_\tau} + aH_0G_{\psi_\tau} &= 0 \\ U_0(x)G_{\psi_{\tau+1}} &= \left(1 - aH_0\right)G_{\psi_\tau} \\ G_{\psi_{\tau+1}} &= U_0^\dagger(x)\left(1 - aH_0\right)G_{\psi_\tau} \end{aligned} \tag{2.66}$$

Since we are including only terms of $\mathcal{O}(a)$, we can rewrite $U_0^\dagger(x)\left(1 - aH_0\right)$ in a symmetric way using $U_0^\dagger(x) = \mathrm{e}^{-iaA_0} = 1 - iaA_0 + \mathcal{O}(a^2)$, thus:

$$\begin{aligned} & U_0^\dagger(x)\,(1-aH_0)+\mathcal{O}(a^2) \\ =& U_0^\dagger(x)-2U_0^\dagger(x)\frac{aH_0}{2}+\mathcal{O}(a^2) \\ =& -\frac{aH_0}{2}U_0^\dagger(x)+U_0^\dagger(x)-U_0^\dagger(x)\frac{aH_0}{2}+\mathcal{O}(a^2) \\ =& \left(1-\frac{aH_0}{2}\right)U_0^\dagger(x)\left(1-\frac{aH_0}{2}\right)+\mathcal{O}(a^2) \end{aligned} \tag{2.67}$$

Consequently, we find:

$$G_{\psi_{\tau+1}}=\left(1-\frac{aH_0}{2}\right)U_0^\dagger(x)\left(1-\frac{aH_0}{2}\right)G_{\psi_\tau} \tag{2.68}$$

Note that we are considering the limit $m_Q \to \infty$ in the expansion above, but we would like to perform the calculation with finite mass. However, (2.68) becomes unstable for small masses (cf. [31]). To solve this problem, one introduces a parameter n to provide stability:

$$G_{\psi_{\tau+1}}=\left(1-\frac{aH_0}{2n}\right)^n U_0^\dagger(x)\left(1-\frac{aH_0}{2n}\right)^n G_{\psi_\tau} \tag{2.69}$$

In this work though we are using an improved version of the Green function which is illustrated in (2.70). A more detailed discussion can also be found in [28, 30].

$$\begin{aligned} G_\psi(\tau,\mathbf{x},\tau',\mathbf{x}') = & \left(1-\frac{\delta H}{2}\right)\left(1-\frac{H_0}{2n}\right)^n U_0^\dagger(\tau-1,\mathbf{x}) \\ & \times\left(1-\frac{H_0}{2n}\right)^n\left(1-\frac{\delta H}{2}\right)G_\psi(\tau-1,\mathbf{x},\tau',\mathbf{x}') \end{aligned} \tag{2.70}$$

In this formulation, Symanzik improvement is applied to remove discretisation errors and we are working with tree-level values. H_0 contains the kinetic terms of leading order $\mathcal{O}\left(v^2\right)$ and is defined in the same way as introduced in (2.63) (we omit the hat indicating lattice units in the following):

$$H_0=-\frac{\boldsymbol{\Delta}^{(2)}}{2m_Q} \tag{2.71}$$

The term δH contains additional corrections like the already mentioned Symanzik improvement. We can distinguish between $\mathcal{O}(v^4)$ and $\mathcal{O}(v^6)$ corrections which are given by:

$$\delta H=\delta H_{v^4}+\delta H_{v^6} \tag{2.72}$$

$$\begin{aligned}\delta H_{v^4} =& - c_1 \frac{\left(\boldsymbol{\Delta}^{(2)}\right)^2}{8m_Q^3} + c_2 \frac{ig}{8m_Q^2}\left(\boldsymbol{\nabla}\cdot\tilde{\boldsymbol{E}} - \tilde{\boldsymbol{E}}\cdot\boldsymbol{\nabla}\right) - c_3 \frac{g}{8m_Q^2}\boldsymbol{\sigma}\left(\tilde{\boldsymbol{\nabla}}\times\tilde{\boldsymbol{E}} - \tilde{\boldsymbol{E}}\times\tilde{\boldsymbol{\nabla}}\right) \\ & - c_4 \frac{g}{2m_Q}\boldsymbol{\sigma}\cdot\tilde{\boldsymbol{B}} + c_5 \frac{\boldsymbol{\Delta}^{(4)}}{24m_Q} - c_6 \frac{\left(\boldsymbol{\Delta}^{(2)}\right)^2}{16n\, m_Q^2}\end{aligned} \tag{2.73}$$

$$\begin{aligned}\delta H_{v^6} =& - c_7 \frac{g}{8m_Q^3}\left\{\boldsymbol{\Delta}^{(2)}, \boldsymbol{\sigma}\cdot\tilde{\boldsymbol{B}}\right\} - c_8 \frac{3g}{64m_Q^4}\left\{\boldsymbol{\Delta}^{(2)}, \boldsymbol{\sigma}\left(\tilde{\boldsymbol{\nabla}}\times\tilde{\boldsymbol{E}} - \tilde{\boldsymbol{E}}\times\tilde{\boldsymbol{\nabla}}\right)\right\} \\ & - c_9 \frac{ig^2}{8m_Q^3}\boldsymbol{\sigma}\tilde{\boldsymbol{E}}\times\tilde{\boldsymbol{E}}\end{aligned} \tag{2.74}$$

The contributions with coefficients c_1 to c_4 are order v^4 corrections while c_3 and c_4 indicate the leading spin dependent terms. c_5 and c_6 belong to the temporal and spatial corrections for H_0. The corrections of $\mathcal{O}(v^6)$ with coefficients c_7 to c_9 include only spin dependent terms, i.e. the first correction for the spin. For this work, however, we set $c_7 = c_8 = c_9 = 0$. Since we are working at tree-level, all other coefficients c_i are equal to 1.

Additionally, the action is tadpole improved using the Landau gauge u_{0L}. For a more detailed discussion of the tadpole improvement, we refer to [32, 33].

Chapter 3

Lattice QCD Setup and Error Analysis

In this chapter, we present the lattice gauge configurations used as well as a discussion of errors occurring in lattice calculations.
Our computations are performed for different sets of gauge configurations which differ in lattice spacing, spatial and temporal extent, and pion mass. Lattice results depend on these parameters, so consequently for a detailed study, one has to estimate the influence of these values and extrapolate them to real world physics. The ensembles used are characterised in the following section.
As a consequence, the results extracted from lattice calculations must not be assumed as exact but are rather including errors caused by several different reasons. In this chapter, we will therefore also specify and discuss the different sources of errors and introduce the methods used in this thesis to estimate their numerical values.

In general, one distinguishes between statistical errors and systematic errors which together form the total error.
As the name suggests, the statistical error is caused by statistical variations due to the probability distribution used in lattice calculations. There are well-established methods to compute the value of this error. In Sec. 3.2 we describe the reason for statistical uncertainties in more detail and present how to compute them.
Systematic error sources are multiple. They arise as a consequence of incorrect or rather imprecise frameworks or measurement methods. For lattice calculations, one example is the utilization of a finite lattice spacing and hence the lattice discretization instead of a continuous space-time. We will discuss all occurring systematic errors in Sec. 3.3. In contrast to determining statistical errors, no standard method is available for systematic uncertainties. However, we present our method of choice applied in this thesis.

3.1 Lattice QCD Setup

There are several different sets of gauge link configurations available which have been used to perform computations. All of them are generated by the RBC and UKQCD collaboration using an Iwasaki gauge action and $N_f = 2 + 1$ domain-wall fermions. The first one is named ensemble C54 which comprises 1676 configurations. Information about this ensemble can be found in Table 3.1 or [18, 42].
The following ensembles are generated using all-mode-averaging (AMA) with 32 or 64 sloppy and 1 or 2 exact measurements per configuration. They differ in the number of lattice points, lattice spacing, and pion mass. Depending on the ensemble, there are different numbers of measurements available. We distinguish between the two coarse lattices C005 and C01, the fine lattices F004 and F006, and finally the coarse lattice C00078 at almost physical pion mass. More details about these ensembles are included in Table 3.1 or [45].

For all cases, the light quark propagators are computed using point-to-all propagators (cf. [41]). That means, for each measurement, there is one fixed point source with a determined location which is the starting point for the light quark propagator connected to all other points. The heavy quark propagators are treated in the framework of NRQCD (cf. Sec. 2) with tadpole improved action (for more details, cf. [28, 42]). For all quark propagators, Gaussian smearing is enabled.

The all-mode-averaging is applied for each configuration n independently by evaluating:

$$O^{(n)}_{\mathrm{AMA}} = O^{(n)}_{\mathrm{ex}} - O^{(n)}_{\mathrm{sl},i=1} + \frac{1}{32}\sum_{i=1}^{32} O^{(n)}_{\mathrm{sl},i} \tag{3.1}$$

where O describes an observable, e.g. the correlation function $C(t)$ for a sloppy ($O^{(n)}_{\mathrm{sl},i}$) or exact ($O^{(n)}_{\mathrm{ex}}$) measurement. Here, n is the current configuration number, with $n = 1, \ldots, N_{\mathrm{meas,ex}}$ while i labels the sloppy measurements for the given configuration. $O^{(n)}_{\mathrm{sl},i=1}$ names the first sloppy observable, which has equal source location as the exact measurement $O^{(n)}_{\mathrm{ex}}$. $O^{(n)}_{\mathrm{AMA}}$ is the final value for the n-th configuration.

Ens.	$N_s^3 \times N_t$	a [fm]	$am^{(sea)}_{u;d}$	$am^{(sea)}_{s}$	$am^{(val)}_{u;d}$	m_π [MeV]	N_{meas}
C54	$24^3 \times 64$	0.1119(17)	0.005	0.04	0.005	336(5)	1676
C005	$24^3 \times 64$	0.1106(3)	0.005	0.04	0.005	340(1)	9952 sl, 311 ex
C01	$24^3 \times 64$	0.1106(3)	0.01	0.04	0.01	431(1)	9056 sl, 283 ex
F004	$32^3 \times 64$	0.0828(3)	0.004	0.03	0.004	303(1)	8032 sl, 251 ex
F006	$32^3 \times 64$	0.0828(3)	0.006	0.03	0.006	360(1)	14144 sl, 442 ex
C00078	$48^3 \times 96$	0.1141(3)	0.00078	0.0362	0.00078	139(1)	2560 sl, 80 ex

Table 3.1: Gauge link ensembles C54, C005, C01, F004, F006, and C00078. Each ensemble, except for C54, uses all-mode-averaging with 32 or 64 sloppy and 1 or 2 exact measurements per configuration. N_s/N_t: spatial/temporal lattice extent in units of a, a: lattice spacing, $am^{(sea)}_{u;d}$: light sea quark mass, $am^{(sea)}_{s}$: strange sea quark mass, $am^{(val)}_{u;d}$: light valence quark mass, m_π: pion mass, N_{meas}: number of measurements taken on different gauge link configurations and/or point source locations, “sl“: sloppy, “ex“: exact.

3.2 Statistical Errors

3.2.1 Sources of Statistical Errors

Statistical uncertainties arise as a consequence of observables which are generated by probability distributions. In the case of lattice calculations, path integrals describing physical observables are evaluated via Monte Carlo simulations. Therefore, every generated configuration is based on the associated probability distribution and hence statistical discrepancies appear. To reach a sensible result, a large number of such configurations is necessary while the statistical fluctuations are expressed by the computed statistical error.

3.2.2 Jackknife Method

In this thesis, our final results and the associated statistical errors based on the available configurations are computed using the Jackknife method.
We call the number of samples - which is equal to the number of configurations - N. For each sample, the observable of interest x_i is computed independently where $i = 1, \ldots, N$ denotes the number of the sample. For uncorrelated data, we construct N reduced samples by removing the i-th entry of the original data and computing the average $\tilde{x}_i$ for each reduced sample:

$$\tilde{x}_i = \frac{1}{N-1} \sum_{k \neq i}^{N} x_k \tag{3.2}$$

We also compute the average of the original sample defined by:

$$\bar{x} = \frac{1}{N} \sum_{k}^{N} x_k \tag{3.3}$$

The Jackknife error is then computed via:

$$\sigma_{\bar{x}}^2 \equiv \frac{N-1}{N} \sum_{i=1}^{N} (\tilde{x}_i - \bar{x})^2 \tag{3.4}$$

Finally, the statistical error is given by the square root of the variance, so we call it $\sigma_{\bar{x}}$.

If the data are correlated, it is possible to take this into account by using a binning method. If the number of data points assembled in one bin is N_{bin}, then the total number of data is reduced to N/N_{bin}, while additional data which do not completely fill one bin are discarded. The data set is now composed of the averages X_i with $i = 1, \ldots, N/N_{\text{bin}}$ of every bin. The Jackknife error is computed in the same way as explained for uncorrelated data but using now the binned averages X_i instead of the raw data x_i.

3.3 Systematic Errors

3.3.1 Sources of Systematic Errors

For a successful and meaningful lattice computation it is essential to consider all possible systematic errors which might affect the results. In the following paragraph we will therefore discuss occurring systematic uncertainties on the lattice. An enormous advantage of lattice QCD as a first principle approach is that all occurring errors can be controlled and systematically decreased.

First, we are introducing a four-dimensional space-time grid with a finite lattice spacing a instead of a continuous space-time. However, real world physics is only valid for a zero lattice spacing a which is not feasible. Therefore, it is obvious that assuming a discrete space-time with a lattice spacing $a \neq 0$ causes uncertainties, the so-called *discretization errors*. Since each lattice QCD result is depending on the lattice spacing a, one aims to quantify these errors and extrapolate the results to the physical point. This can be done by applying the continuum limit $a \to 0$. Technically, one performs calculations with various lattice spacings while keeping all additional parameters constant. Finally, using these results, one can extrapolate them to the physical point at $a = 0$.
Further systematic errors are caused by the *finite volume* of the space-time grid. If this lattice is chosen too small, particles cannot be accommodated inside or particle interactions are strongly affected. Such results are not reliable and cannot represent the real world physics in an infinite volume. Therefore, one has to ensure that the lattice extent is sufficiently large. For this purpose, one repeats the calculation for different physical volumes with fixed lattice spacing. Comparing the computed results, one can estimate the influence of finite volumes. The lattices used in this work are comparatively large, so we neglect finite volume effects.
Another systematic error appears as a consequence of *unphysical heavy quark masses*. Lattice calculations become the more expansive the lighter the quark masses are. Therefore it is numerically cheaper and more efficient to perform calculations using heavier quark masses. However, we have to extract reliable physical values so we extrapolate our results to the physical mass in a similar way as done for discretization errors. Instead of using different lattice spacings, we choose several (unphysical) quark masses and extrapolate the results to the physical point.
For completeness, we also mention systematic errors due to *quenching*. This refers to the fact that the spontaneous creation and annihilation of quark pairs (so-called sea quarks) from the vacuum is neglected in our theory. However, the occurring errors are usually much smaller compared to statistical errors and therefore will not be discussed in this thesis.
Finally, there are also systematic errors which arise during the data analysis. Our data are fitted to a certain functional relation, however, the fitting range is generally chosen only eye-guided and thus determined very subjectively. In the following paragraph we discuss how to roughly estimate an associated systematic error.

3.3.2 Estimating Systematic Errors

Having generated the raw data in the numerical simulation, we apply the generalized eigenvalue problem (GEP) and evaluate our data using a χ^2 minimizing plateau fit. More details about the GEP will be given in Sec. 6.3. However, the fit range $[t_{min}, t_{max}]$ for the least-χ^2 fit has to be chosen manually, thus the actual choice influences the obtained results. In order to estimate the incorporated systematic error we perform a large number N of fits with

- $T_{min} \leq t_{min} \leq T_{max} - 1$
- $t_{min} < t_{max} \leq T_{max}$

T_{min} and T_{max} are the lower/upper boundary for possible fit regions while they are specified in such a way that fits are feasible as well as sensible.

For each fit, we get a result x_i with an associated statistical error Δx_i and χ^2_i determining the quality of the fit. The index $i = 1, \ldots, N$ denotes the different fits performed.
In the next step, we construct a distribution using the results x_i weighted by $\mathrm{e}^{\left(-\chi^2_i/\mathrm{d.o.f.}\right)}$. The central value is finally determined by the median $x_{i=\mathrm{Med}}$ of this distribution while the final statistical error is given by the associated statistical error $\Delta x_{i=\mathrm{Med}}$. The lower/upper systematic error is constructed using the difference between the 16th/84th percentiles and the median. We chose the 16th/84th percentiles, since this represents 1σ corresponding to a Gaussian distribution. As our constructed distribution will not be symmetric in general, the systematic error will consequently be asymmetric, too. For a more detailed discussion of this method, cf. [34].

Chapter 4

Investigation of Bottomonium States by Means of NRQCD

This chapter focuses on the investigation of the well-known bottomonium states $\eta_B(1S)$ and $\Upsilon(1S)$. It provides a first test of the non-relativistic QCD concepts and allows us to study the implementation of heavy quark propagators for well-established states. Furthermore, it enables us to set the scale for the lattice configuration used, since the heavy quark masses are shifted to unphysical values as a consequence of applying NRQCD. We will follow the standard method in lattice QCD for hadron spectroscopy: After determining the analytic form of the correlation function and computing its value numerically, we will extract the bottomonium masses by solving the generalized eigenvalue problem (GEP).
We use the two creation operators

$$\begin{aligned} \mathcal{O}_{\eta_B}(t) &= \sum_{\mathbf{x}} \bar{b}(\mathbf{x},t)\gamma_5 b(\mathbf{x},t) \\ \mathcal{O}_{\Upsilon}(t) &= \sum_{\mathbf{x}} \bar{b}(\mathbf{x},t)\gamma_j b(\mathbf{x},t) \end{aligned} \tag{4.1}$$

which generates the $\eta_B(1S)$ and $\Upsilon(1S)$ states with their associated quantum numbers.

The two discussed bottomonium states are both $b\bar{b}$ pairs. We can distinguish between them by their quantum numbers and especially their angular momenta. Whereas the η_B has quantum numbers $J^{PC} = 0^{-+}$ and is accordingly a pseudo scalar meson, the Υ is characterized as a vector meson with $J^{PC} = 1^{--}$. Nevertheless, their masses are quite similar at approximately 9 GeV. More precisely, they have been measured with $m_{\eta_B} = 9399.0(2.3)$ MeV and $m_{\Upsilon} = 9460.30(26)$ MeV (cf. [1]). We aim to achieve agreement with these experimental data by performing calculations in the framework of NRQCD.

Our discussion starts by proving that the chosen operators generate the correct quantum numbers and will continue afterwards by deriving the correlation functions.

4.1 $b\bar{b}$ Quantum Numbers

The two $b\bar{b}$ creation operators are specified in (4.1) and can be generalized via $\mathcal{O}_i$ with $i \in \{\eta_B, \Upsilon\}$. A bottomonium state is generated if the creation operator $\mathcal{O}_i$ is acting on the vacuum state $|\Omega\rangle$:

$$|\Phi_i\rangle = \mathcal{O}_i|\Omega\rangle \tag{4.2}$$

In the next step, we will apply the quantum number operators given in Appendix A.2 to the two bottomonium states and extract their associated quantum numbers for parity, charge conjugation, and angular momentum. We formulate the calculations in Euclidean representation and omit the space-time arguments for the sake of simplicity.

4.1.1 The $\eta_B(1S)$ State

Applying the creation operator $\mathcal{O}_{\eta_B}$ to the vacuum yields the particle state $|\Phi_{\eta_B}\rangle = \bar{b}\gamma_5 b|\Omega\rangle$. Subsequently we will compute its quantum numbers explicitly.

Parity

First of all, we determine the parity of the η_B state. It is defined as the eigenvalue of the parity operator (A.1) acting on the particle state.

$$\begin{aligned}\mathcal{P}|\Phi_{\eta_B}\rangle &= \mathcal{P}(\bar{b}\gamma_5 b)|\Omega\rangle = \mathcal{P}(b^\dagger)\gamma_0\gamma_5\mathcal{P}(b)|\Omega\rangle = (\gamma_0\ b)^\dagger\gamma_0\gamma_5\gamma_0\ b|\Omega\rangle \\ &= b^\dagger\gamma_0\gamma_0\gamma_5\gamma_0\ b|\Omega\rangle = b^\dagger\gamma_5\gamma_0\ b|\Omega\rangle = -b^\dagger\gamma_0\gamma_5\ b|\Omega\rangle = -1\cdot|\Phi_{\eta_B}\rangle\end{aligned} \tag{4.3}$$

Conveniently, the parity is negative ($P = -$).

Charge Conjugation

We proceed with the charge conjugation whose transformation behaviour is given in (A.2). Applying it to $|\Phi_{\eta_B}\rangle$ yields:

$$\begin{aligned}\mathcal{C}|\Phi_{\eta_B}\rangle &= \mathcal{C}(\bar{b}\gamma_5 b)\ |\Omega\rangle = \mathcal{C}(\bar{b})\gamma_5\mathcal{C}(b)\ |\Omega\rangle = -b^T\mathcal{C}\gamma_5\mathcal{C}^{-1}\bar{b}^T\ |\Omega\rangle \\ &= -b^T\gamma_2\gamma_0\gamma_5\gamma_0\gamma_2\bar{b}^T\ |\Omega\rangle = -b^T\gamma_2\gamma_0\gamma_0\gamma_2\gamma_5\bar{b}^T\ |\Omega\rangle = -b^T\gamma_5\bar{b}^T\ |\Omega\rangle \\ &= -b^T\gamma_5^T\bar{b}^T\ |\Omega\rangle = \bar{b}\gamma_5 b\ |\Omega\rangle = +1\cdot|\Phi_{\eta_B}\rangle\end{aligned} \tag{4.4}$$

Therefore the charge conjugation is positive ($C = +$).

Angular momentum

The last quantum number to be calculated is the angular momentum. We will restrain the computation to the z-component while the other directions are completely analogous. The rotation operator for small angular is applied, i.e. we use the rotation operator's

expansion including terms up to order $\mathcal{O}(\alpha)$ given in (A.3). Concerning the η_B state, we get:

$$\begin{aligned}
\mathcal{R}_3(\alpha)|\Phi_{\eta_B}\rangle =& \mathcal{R}_3(\alpha)(\bar{b}\gamma_5 b)\ |\Omega\rangle \\
=& \left[\left(1+\frac{\alpha}{4}\left[\gamma_1,\gamma_2\right]\right)\ b\right]^\dagger \gamma_0\gamma_5 \left(1+\frac{\alpha}{4}\left[\gamma_1,\gamma_2\right]\right)\ b\ |\Omega\rangle + \mathcal{O}(\alpha^2) \\
=& b^\dagger \left(1+\frac{\alpha}{4}\left(\gamma_2^\dagger\gamma_1^\dagger - \gamma_1^\dagger\gamma_2^\dagger\right)\right)\gamma_0\gamma_5 \left(1+\frac{\alpha}{4}\left(\gamma_1\gamma_2-\gamma_2\gamma_1\right)\right)\ b\ |\Omega\rangle + \mathcal{O}(\alpha^2) \\
=& b^\dagger\gamma_0\gamma_5 \left\{1+\frac{\alpha}{4}\left[(\gamma_2\gamma_1-\gamma_1\gamma_2)+(\gamma_1\gamma_2-\gamma_2\gamma_1)\right]\right\}\ b|\Omega\rangle + \mathcal{O}(\alpha^2) \\
=& \bar{b}\gamma_5 b\ |\Omega\rangle + \mathcal{O}(\alpha^2) = |\Phi_{\eta_B}\rangle + \mathcal{O}(\alpha^2)
\end{aligned} \tag{4.5}$$

Comparing to $\mathcal{R}_3(\alpha)|\Psi\rangle = [1+i\alpha J_3]\,|\Psi\rangle + \mathcal{O}(\alpha^2)$, it is obvious that $J_3 = 0$. It can be easily shown that the analogous calculation for $\mathcal{R}_{1,2}(\alpha)$ yields also $J_{1,2} = 0$. Therefore, the total angular momentum is $J = 0$ and the supposed quantum numbers $J^{PC} = 0^{-+}$ are verified.

4.1.2 The $\Upsilon(1S)$ State

We proceed with the same calculation for $|\Phi_\Upsilon\rangle = \bar{b}\gamma_j b|\Omega\rangle$ which is generated by applying $\mathcal{O}_\Upsilon$ - given in (4.1) - to the vacuum. The quantum numbers are computed analogously to the previous section.

Parity

$$\begin{aligned}
\mathcal{P}|\Phi_\Upsilon\rangle &= \mathcal{P}(\bar{b}\gamma_j b)|\Omega\rangle = \mathcal{P}(b^\dagger)\gamma_0\gamma_j\mathcal{P}(b)|\Omega\rangle = (\gamma_0\ b)^\dagger\gamma_0\gamma_j\gamma_0\ b|\Omega\rangle \\
&= b^\dagger\gamma_0\gamma_0\gamma_j\gamma_0\ b|\Omega\rangle = b^\dagger\gamma_j\gamma_0\ b|\Omega\rangle = -b^\dagger\gamma_0\gamma_j\ b|\Omega\rangle = -1\cdot|\Phi_{\eta_B}\rangle
\end{aligned} \tag{4.6}$$

Consequently, we find a negative parity ($P = -$).

Charge Conjugation

$$\begin{aligned}
\mathcal{C}|\Phi_\Upsilon\rangle &= \mathcal{C}(\bar{b}\gamma_j b)\ |\Omega\rangle = \mathcal{C}(\bar{b})\gamma_j\mathcal{C}(b)\ |\Omega\rangle = -b^T\mathcal{C}\gamma_j\mathcal{C}^{-1}\bar{b}^T\ |\Omega\rangle \\
&= -b^T\left(-\gamma_j^T\right)\bar{b}^T\ |\Omega\rangle = b^T\gamma_j^T\bar{b}^T\ |\Omega\rangle = -\bar{b}\gamma_j b\ |\Omega\rangle = -1\cdot|\Phi_\Upsilon\rangle
\end{aligned} \tag{4.7}$$

with:

$$\mathcal{C}\gamma_j\mathcal{C}^{-1} = \gamma_2\gamma_0\gamma_j\gamma_0\gamma_2 = \begin{cases} -\gamma_2 & ,j=2 \\ +\gamma_j & ,j\neq 2 \end{cases} = \begin{cases} -\gamma_2^T & ,j=2 \\ -\gamma_j^T & ,j\neq 2 \end{cases} = -\gamma_j^T \tag{4.8}$$

So the charge conjugation is negative ($C = -$).

Angular momentum

$$\begin{aligned}\mathcal{R}_3(\alpha)|\Phi_\Upsilon\rangle =&\mathcal{R}_3(\alpha)(\bar{b}\gamma_j b)\ |\Omega\rangle \\ =&\left[\left(1+\frac{\alpha}{4}\left[\gamma_1,\gamma_2\right]\right)\ b\right]^\dagger \gamma_0\gamma_j\left(1+\frac{\alpha}{4}\left[\gamma_1,\gamma_2\right]\right)\ b\ |\Omega\rangle+\mathcal{O}(\alpha^2) \\ =&b^\dagger\left(1-\frac{\alpha}{4}\left[\gamma_1,\gamma_2\right]\right)\gamma_0\gamma_j\left(1+\frac{\alpha}{4}\left[\gamma_1,\gamma_2\right]\right)\ b\ |\Omega\rangle+\mathcal{O}(\alpha^2)\end{aligned} \tag{4.9}$$

We have to evaluate this expression for all three components $j = 1, 2, 3$ to determine the transformation behaviour of the 3-dimensional spinor. The detailed calculation is performed in Appendix C.1 and yields $J = 1$. Finally, the quantum numbers of Υ are given by $J^{PC} = 1^{--}$.

4.2 Correlation Functions

Besides the operators given in (4.1) the associated daggered operators are required to compute the correlation functions $C_i(t)$:

$$\begin{aligned}\mathcal{O}^\dagger_{\eta_B}(t) &= -\sum_{\mathbf{x}}\bar{b}(\mathbf{x},t)\gamma_5 b(\mathbf{x},t) \\ \mathcal{O}^\dagger_{\Upsilon}(t) &= -\sum_{\mathbf{x}}\bar{b}(\mathbf{x},t)\gamma_j b(\mathbf{x},t)\end{aligned} \tag{4.10}$$

In the following calculation the space-time arguments are omitted after the first line to enhance readability. Moreover, the arguments $(\mathbf{x}, t)$ are included in the unprimed indices while the arguments $(\mathbf{y}, 0)$ are expressed by the primed ones. The correlation functions for the two bottomonium states are consequently given by:

Correlation Function for $\eta_B(1S)$ State

$$\begin{aligned}C_{\eta_B}(t) &= \left\langle \mathcal{O}_{\eta_B}(t)\mathcal{O}^\dagger_{\eta_B}(0)\right\rangle = -\sum_{\mathbf{x},\mathbf{y}}\left\langle \bar{b}(\mathbf{x},t)\gamma_5 b(\mathbf{x},t)\,\bar{b}(\mathbf{y},0)\gamma_5 b(\mathbf{y},0)\right\rangle \\ &= -\sum_{\mathbf{x},\mathbf{y}}\left\langle \bar{b}^a_A\gamma_{5AB}b^a_B\,\bar{b}^{a'}_{A'}\gamma_{5A'B'}b^{a'}_{B'}\right\rangle = -\sum_{\mathbf{x},\mathbf{y}}\gamma_{5AB}\gamma_{5A'B'}\left\langle \bar{b}^a_A b^a_B\,\bar{b}^{a'}_{A'}b^{a'}_{B'}\right\rangle \\ &= \sum_{\mathbf{x},\mathbf{y}}\left\langle B^{a'a}_{B'A}\gamma_{5AB}\,B^{aa'}_{BA'}\gamma_{5A'B'}\right\rangle = \sum_{\mathbf{x},\mathbf{y}}\left\langle \mathrm{Tr}\left[B(x,y)\gamma_5\,B(y,x)\gamma_5\right]\right\rangle \\ &= \sum_{\mathbf{x},\mathbf{y}}\left\langle \mathrm{Tr}\left[B(x,y)\,B(x,y)^\dagger\right]\right\rangle\end{aligned} \tag{4.11}$$

Correlation Function for $\Upsilon(1S)$ State

$$\begin{aligned}C_{\Upsilon}(t) &= \left\langle \mathcal{O}_{\Upsilon}(t)\mathcal{O}^\dagger_{\Upsilon}(0)\right\rangle = -\sum_{\mathbf{x},\mathbf{y}}\left\langle \bar{b}(\mathbf{x},t)\gamma_j b(\mathbf{x},t)\,\bar{b}(\mathbf{y},0)\gamma_j b(\mathbf{y},0)\right\rangle \\ &= -\sum_{\mathbf{x},\mathbf{y}}\gamma_{jAB}\gamma_{jA'B'}\left\langle \bar{b}^a_A b^a_B\,\bar{b}^{a'}_{A'}b^{a\prime}_{B\prime}\right\rangle = \sum_{\mathbf{x},\mathbf{y}}\left\langle B^{a'a}_{B'A}\gamma_{jAB}\,B^{aa'}_{BA'}\gamma_{jA'B'}\right\rangle\end{aligned} \tag{4.12}$$

$$= \sum_{\mathbf{x},\mathbf{y}} \left\langle \mathrm{Tr}\left[B(x,y)\gamma_j\gamma_5 B(x,y)^\dagger \gamma_5\gamma_j \right] \right\rangle$$
$$= \sum_{\mathbf{x},\mathbf{y}} \left\langle \mathrm{Tr}\left[\gamma_5\gamma_j B(x,y) \left[B(x,y)\gamma_5\gamma_j\right]^\dagger \right] \right\rangle$$

$B^{ab}_{AB} \equiv b^a_A \bar{b}^b_B$ is the heavy quark propagator. We apply the γ_5-hermiticity for the quark propagators: $B(y,x) = \gamma_5 \left[B(x,y)\right]^\dagger \gamma_5 \equiv \gamma_5 B(x,y)^\dagger \gamma_5$.

4.3 Numerical Results

Our calculations are performed for ensemble C54 presented in Table 3.1.

The correlation function is explicitly given by:

$$C_i(t) = \left\langle \mathcal{O}_i(t)\mathcal{O}_i^\dagger(0) \right\rangle = \sum_n \langle \Omega|\mathcal{O}_i(0)|n\rangle \left\langle n|\mathcal{O}_i^\dagger(0)|\Omega\right\rangle \mathrm{e}^{-E_n^{(i)}t} \tag{4.13}$$

$E_n^{(i)}$ denotes the n-th energy eigenvalue while $E_0^{(i)}$ corresponds to the ground state energy. For sufficiently large times t we can approximate the sum by omitting all contributions with $n \geq 1$ so that only the ground state energy level remains. To extract now the ground state energy, we compute the so-called effective mass $aE^{(i)}_{\mathrm{eff}}(t)$ which is given by:

$$aE^{(i)}_{\mathrm{eff}}(t) = \ln\left(\frac{\mathcal{C}_i(t)}{\mathcal{C}_i(t+a)}\right) \tag{4.14}$$

For large times t, it reaches a plateau which can be identified with the ground state energy, so $aE^{(i)}_{\mathrm{eff}}(t) \xrightarrow{t\to\infty} aE_0^{(i)}$. The results for the two bottomonium states are presented in Fig. 4.1.

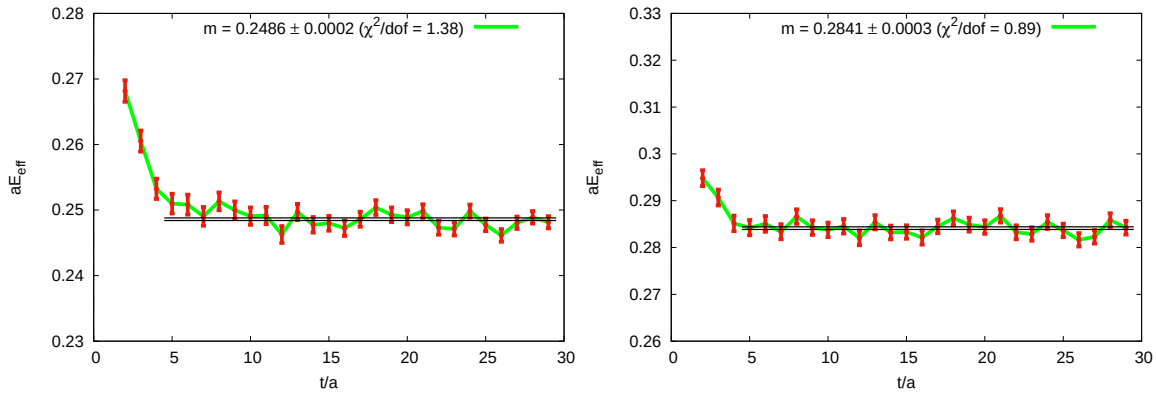

Figure 4.1: Effective masses for bottomonium states. **(left):** η_B meson. **(right):** Υ meson. Results are extracted by a plateau fit in the region $5 \leq t \leq 30$.

Extracting the effective masses from Fig. 4.1 and converting them to physical units using the lattice spacing from Table 3.1 and the convention for natural units $1\ \mathrm{fm}^{-1} = 197.3\ \mathrm{MeV}$, we find:

$$\begin{aligned} m_{\eta_B} &= 0.2486(2) \cdot \frac{1}{0.1119(17)\text{ fm}} = 438.33\text{ MeV} \pm 7.01\text{ MeV} \\ m_{\Upsilon} &= 0.2841(3) \cdot \frac{1}{0.1119(17)\text{ fm}} = 500.92\text{ MeV} \pm 8.14\text{ MeV} \end{aligned} \tag{4.15}$$

Note that in the NRQCD framework the heavy quark masses are shifted and therefore these results do not represent the physical bottomonium masses. However, the mass differences are unaffected and thus the mass splitting between the calculated bottomonium masses has to coincide with the experimental energy splitting. Taking advantage of this fact, we consider the numerically determined energy splitting and compare it to the experimental one in order to prove the validity of our results.

The mass difference for our calculated effective masses is given by:

$$\Delta m = m_{\Upsilon} - m_{\eta_B} = 62.59\text{ MeV} \pm 15.15\text{ MeV} \tag{4.16}$$

while the physical mass splitting can be computed using the data from [1]:

$$\Delta m_{\text{phys}} = m_{\Upsilon,\text{phys}} - m_{\eta_B,\text{phys}} = 61.30\text{ MeV} \pm 2.56\text{ MeV} \tag{4.17}$$

Accordingly, we can state good agreement for our numerical results with the experimental data.

We will conclude by setting the scale for ensemble C54. Therefore, we choose one hadron, in this case the η_B meson, and identify its mass m_{η_B} with the associated physical mass $m_{\eta_B,\text{phys}} = 9399.0$ MeV$\pm$2.3 MeV. In the next step, we do not extract absolute values from our lattice calculations but the relative differences compared to the mass m_{η_B}. Finally, this mass difference is added to the specified mass $m_{\eta_B,\text{phys}}$ to receive the physical mass of the investigated hadron.
So for instance, the real mass $m_{\Upsilon,\text{real}}$ is computed by adding the difference Δm in (4.16) to $m_{\eta_B,\text{phys}}$:

$$m_{\Upsilon,\text{real}} = m_{\eta_B,\text{phys}} + \Delta m = 9461.59\text{ MeV} \pm 17.45\text{ MeV} \tag{4.18}$$

This is consistent with the experimental results for the Υ mass of $m_{\Upsilon,\text{phys}} = 9460.30$ MeV $\pm$ 0.26 MeV.

4.4 Summary

In this chapter, we successfully determined the energy splitting between the two bottomonium states $\eta_B(1S)$ and $\Upsilon(1S)$ by means of NRQCD and proved agreement with the experimental results. Moreover, we illustrated how to set the scale in the framework of NRQCD using the bottomonium states exemplarily.

Chapter 5

Investigation of $\bar{b}\bar{b}bb$ by Means of NRQCD

In this chapter, we concentrate on a four-quark system consisting of four bottom quarks. The $\bar{b}\bar{b}bb$ system has recently been intensely discussed in high-energy physics and there have arisen conflicting views if a bound state exists or not (e.g. cf. [36, 37, 38]). This system enables us to focus only on heavy quarks and depicts an ideal approach for discussing four-quark systems with lattice NRQCD. We restrict ourselves to the $J^{PC} = 1^{+-}$ channel and use a simplified operator basis containing two creation operators. Here, we search for a $\bar{b}\bar{b}bb$ tetraquark with a mass below the lowest non-interacting bottomonium pair threshold. However, we do not claim to discuss the system in detail. For a more elaborate lattice QCD investigation, we refer to [36].
In our investigation, we include the two bottomonium states η_B and Υ presented in Chapter 4 to generate the four-quark system. We distinguish between a mesonic molecule and a scattering state. The creation operators are obtained by combining $\mathcal{O}_{\eta_B}$ and $\mathcal{O}_\Upsilon$ from (4.1). The quantum numbers can be derived in the same way as done in Sec. 4.1 or easily extracted from the quantum numbers of η_B and Υ.

Mesonic Molecule:

The mesonic molecule is gained by an equal spatial location for both bottomonium mesons. Mathematically, this means that we project the total momentum to zero. The operator reads:

$$\mathcal{O}_{[\eta_B\Upsilon](0)}(t) = \sum_{\mathbf{x}} \bar{b}(\mathbf{x},t)\gamma_5 b(\mathbf{x},t)\,\bar{b}(\mathbf{x},t)\gamma_j b(\mathbf{x},t) \tag{5.1}$$

Scattering State:

For the scattering state, the mesons are spatially separated, so we distinguish the space-time indices for the η_B and the Υ meson. This case coincides with projecting the momenta separately to zero for each meson. The operator is given by:

$$\mathcal{O}_{\eta_B(0)\Upsilon(0)}(t) = \sum_{\mathbf{x},\mathbf{y}} \bar{b}(\mathbf{x},t)\gamma_5 b(\mathbf{x},t)\,\bar{b}(\mathbf{y},t)\gamma_j b(\mathbf{y},t) \tag{5.2}$$

A detailed discussion of the two possible momentum projections and the associated operator shapes will be given in Sec. 6.1.2.

5.1 Correlation Matrix

Instead of single correlation functions as in the previous chapter (cf. Chapter 4) we have got a set of two creation operators which can be used both as sink and source operators. Consequently, we get a 2×2 correlation matrix with $\mathcal{O}_i, \mathcal{O}_j \in \{\mathcal{O}_{[\eta_B \Upsilon](0)}, \mathcal{O}_{\eta_B(0)\Upsilon(0)}\}$ in contrast to a single correlation function:

$$C_{ij}(t) = \langle \mathcal{O}_i(t)\, \mathcal{O}_j^\dagger(0) \rangle \tag{5.3}$$

sink \ source	$\mathcal{O}^\dagger_{[\eta_B \Upsilon](0)}$	$\mathcal{O}^\dagger_{\eta_B(0)\Upsilon(0)}$
$\mathcal{O}_{[\eta_B \Upsilon](0)}$	c.	n.c.
$\mathcal{O}_{\eta_B(0)\Upsilon(0)}$	c.	n.c.

Table 5.1: The correlation matrix for $\bar{b}\bar{b}bb$. Elements labelled with c. are computed in this chapter by numerical calculation while elements labelled n.c. are not computed due to numerical efficiency.

Due to the numerical efficiency, we restrict ourselves to the mesonic operator $\mathcal{O}^\dagger_{[\eta_B \Upsilon](0)}$ at the source and compute the two associated correlation matrix elements. We do not consider the scattering state operator $\mathcal{O}^\dagger_{\eta_B(0)\Upsilon(0)}$ at the source since calculations would become numerically extremely expansive as a consequence of the spatial separated source locations. Additionally, we keep the source position fixed.

The two included correlation functions are given by:

$$\begin{aligned} C_{11}(t) &\equiv \left\langle \mathcal{O}_{[\eta_B \Upsilon](0)}(t)\, \mathcal{O}^\dagger_{[\eta_B \Upsilon](0)}(0) \right\rangle \\ &= \sum_{\mathbf{x}} \left\langle \bar{b}(\mathbf{x},t)\gamma_5 b(\mathbf{x},t)\, \bar{b}(\mathbf{x},t)\gamma_j b(\mathbf{x},t)\, \bar{b}(\mathbf{y},0)\gamma_5 b(\mathbf{y},0)\, \bar{b}(\mathbf{y},0)\gamma_j b(\mathbf{y},0) \right\rangle \end{aligned} \tag{5.4}$$

$$\begin{aligned} C_{21}(t) &\equiv \left\langle \mathcal{O}_{\eta_B(0)\Upsilon(0)}(t)\, \mathcal{O}^\dagger_{[\eta_B \Upsilon](0)}(0) \right\rangle \\ &= \sum_{\mathbf{x},\mathbf{y}} \left\langle \bar{b}(\mathbf{x},t)\gamma_5 b(\mathbf{x},t)\, \bar{b}(\mathbf{y},t)\gamma_j b(\mathbf{y},t)\, \bar{b}(\mathbf{z},0)\gamma_5 b(\mathbf{z},0)\, \bar{b}(\mathbf{z},0)\gamma_j b(\mathbf{z},0) \right\rangle \end{aligned} \tag{5.5}$$

We will perform the calculation for these correlation functions in detail to illustrate the proceeding which is equivalent to the approach for the heavy-light tetraquark discussed in Chapter 6.

Both correlation matrix elements presented can be evaluated together if we first compute $C_{21}(t)$ and finally identify $y = x$ and omit the sum over $\mathbf{y}$ to gain $C_{11}(t)$.

For our computation, we start with the latter term in (5.5):

$$\begin{aligned}
&\sum_{\mathbf{x},\mathbf{y}} \Big\langle \bar{b}(\mathbf{x},t)\gamma_5 b(\mathbf{x},t)\, \bar{b}(\mathbf{y},t)\gamma_j b(\mathbf{y},t)\, \bar{b}(\mathbf{z},0)\gamma_5 b(\mathbf{z},0)\, \bar{b}(\mathbf{z},0)\gamma_j b(\mathbf{z},0) \Big\rangle \\
=&\sum_{\mathbf{x},\mathbf{y}} \gamma_{5AB}\gamma_{jCD}\gamma_{5A'B'}\gamma_{jC'D'} \Big\langle \underbrace{\bar{b}^a_A b^a_B \bar{b}^b_C b^b_D \bar{b}^{a'}_{A'} b^{a'}_{B'} \bar{b}^{b'}_{C'} b^{b'}_{D'}}_{(*)} \Big\rangle
\end{aligned} \tag{5.6}$$

while we write the Dirac and colour indices explicitly. Furthermore, we improve readability by including the space-time arguments in the colour indices via the identification:

$$(\mathbf{x},t) \leftrightarrow a, \quad (\mathbf{y},t) \leftrightarrow b, \quad (\mathbf{z},0) \leftrightarrow a', b' \tag{5.7}$$

We continue with the expression $(*)$ which can be reformed in four different ways to heavy quark propagators:

$$\begin{aligned}
(*)_{(1)} \quad &= -b^a_B \bar{b}^b_C b^b_D \bar{b}^{a'}_{A'} b^{a'}_{B'} \bar{b}^a_A \bar{b}^{b'}_{C'} b^{b'}_{D'} = -\bar{b}^b_C b^b_D b^a_B \bar{b}^{a'}_{A'} b^{a'}_{B'} \bar{b}^a_A \bar{b}^{b'}_{C'} b^{b'}_{D'} \\
&= +b^a_B \bar{b}^{a'}_{A'} b^{a'}_{B'} \bar{b}^a_A b^b_D \bar{b}^{b'}_{C'} b^{b'}_{D'} \bar{b}^b_C = B^{aa'}_{BA'} B^{a'a}_{B'A} B^{bb'}_{DC'} B^{b'b}_{D'C}
\end{aligned} \tag{5.8}$$

$$\begin{aligned}
(*)_{(2)} \quad &= -b^a_B \bar{b}^b_C b^b_D \bar{b}^{a'}_{A'} b^{a'}_{B'} \bar{b}^a_A \bar{b}^{b'}_{C'} b^{b'}_{D'} = +\bar{b}^b_C b^b_D \bar{b}^{a'}_{A'} b^{a'}_{B'} \bar{b}^a_A b^a_B \bar{b}^{b'}_{C'} b^{b'}_{D'} \\
&= -B^{ba'}_{DA'} B^{a'a}_{B'A} B^{ab'}_{BC'} B^{b'b}_{D'C}
\end{aligned} \tag{5.9}$$

$$\begin{aligned}
(*)_{(3)} \quad &= -b^a_B \bar{b}^b_C b^b_D \bar{b}^{a'}_{A'} b^{a'}_{B'} \bar{b}^{b'}_{C'} b^{b'}_{D'} \bar{b}^a_A = -\bar{b}^b_C b^b_D b^a_B \bar{b}^{a'}_{A'} b^{a'}_{B'} \bar{b}^{b'}_{C'} b^{b'}_{D'} \bar{b}^a_A \\
&= -b^a_B \bar{b}^{a'}_{A'} b^{a'}_{B'} \bar{b}^b_C b^b_D \bar{b}^{b'}_{C'} b^{b'}_{D'} \bar{b}^a_A = -B^{aa'}_{BA'} B^{a'b}_{B'C} B^{bb'}_{DC'} B^{b'a}_{D'A}
\end{aligned} \tag{5.10}$$

$$\begin{aligned}
(*)_{(4)} \quad &= -b^a_B \bar{b}^b_C b^b_D \bar{b}^{a'}_{A'} b^{a'}_{B'} \bar{b}^{b'}_{C'} b^{b'}_{D'} \bar{b}^a_A = +b^b_D \bar{b}^{a'}_{A'} b^{a'}_{B'} \bar{b}^b_C b^a_B \bar{b}^{b'}_{C'} b^{b'}_{D'} \bar{b}^a_A \\
&= B^{ba'}_{DA'} B^{a'b}_{B'C} B^{ab'}_{BC'} B^{b'a}_{D'A}
\end{aligned} \tag{5.11}$$

Combining the four terms (5.8) to (5.11) and inserting them in (5.6) yields the final form of the correlation function:

$$\begin{aligned}
= \sum_{\mathbf{x},\mathbf{y}} \gamma_{5AB}\gamma_{jCD}\gamma_{5A'B'}\gamma_{jC'D'} \Big\langle & B^{aa'}_{BA'} B^{a'a}_{B'A} B^{bb'}_{DC'} B^{b'b}_{D'C} - B^{ba'}_{DA'} B^{a'a}_{B'A} B^{ab'}_{BC'} B^{b'b}_{D'C} \\
& - B^{aa'}_{BA'} B^{a'b}_{B'C} B^{bb'}_{DC'} B^{b'a}_{D'A} + B^{ba'}_{DA'} B^{a'b}_{B'C} B^{ab'}_{BC'} B^{b'a}_{D'A} \Big\rangle
\end{aligned} \tag{5.12}$$

$$\begin{aligned}
= \sum_{\mathbf{x},\mathbf{y}} \langle & \mathrm{Tr}\left[B(x,z)\gamma_5 B(z,x)\gamma_5\right] \mathrm{Tr}\left[B(y,z)\gamma_j B(z,y)\gamma_j\right] \\
& - \mathrm{Tr}\left[B(y,z)\gamma_5 B(z,x)\gamma_5 B(x,z)\gamma_j B(z,y)\gamma_j\right] \\
& - \mathrm{Tr}\left[B(x,z)\gamma_5 B(z,y)\gamma_j B(y,z)\gamma_j B(z,x)\gamma_5\right] \\
& + \mathrm{Tr}\left[B(y,z)\gamma_5 B(z,y)\gamma_j\right] \mathrm{Tr}\left[B(x,z)\gamma_j B(z,x)\gamma_5\right] \rangle
\end{aligned} \tag{5.13}$$

$$
\begin{aligned}
= \sum_{\mathbf{x},\mathbf{y}} \Big\langle & \operatorname{Tr}\left[B(x,z)B(x,z)^\dagger\right] \operatorname{Tr}\left[B(y,z)\gamma_j\gamma_5 B(y,z)^\dagger\gamma_5\gamma_j\right] \\
& - \operatorname{Tr}\left[B(y,z)B(x,z)^\dagger B(x,z)\gamma_j\gamma_5 B(y,z)^\dagger\gamma_5\gamma_j\right] \\
& - \operatorname{Tr}\left[B(x,z)B(y,z)^\dagger\gamma_5\gamma_j B(y,z)\gamma_j\gamma_5 B(x,z)^\dagger\right] \\
& + \operatorname{Tr}\left[B(y,z)B(y,z)^\dagger\gamma_5\gamma_j\right] \operatorname{Tr}\left[B(x,z)\gamma_j\gamma_5 B(x,z)^\dagger\right]\Big\rangle
\end{aligned}
\tag{5.14}
$$

Here $B^{ab}_{AB} \equiv b^a_A \bar{b}^b_B$ is the bottom quark propagator and in the last step, we apply the γ_5-hermiticity $B(x,y) = \gamma_5 \left[B(y,x)\right]^\dagger \gamma_5$. We will use $B(y,x)^\dagger \equiv \left[B(y,x)\right]^\dagger$ to increase readability. Note that this is not equivalent to $B^\dagger(x,y) = \left[B(y,x)\right]^\dagger$. We also remark the use of four-dimensional arguments, e.g. $x = (\mathbf{x}, t)$.

We receive $C_{11}(t)$ by setting $y = x$ and omitting the summation over $\mathbf{y}$:

$$
\begin{aligned}
C_{11}(t) = \sum_{\mathbf{x}} \Big\langle & \operatorname{Tr}\left[B(x,z)B(x,z)^\dagger\right] \operatorname{Tr}\left[B(x,z)\gamma_j\gamma_5 B(x,z)^\dagger\gamma_5\gamma_j\right] \\
& - \operatorname{Tr}\left[B(x,z)B(x,z)^\dagger B(x,z)\gamma_j\gamma_5 B(x,z)^\dagger\gamma_5\gamma_j\right] \\
& - \operatorname{Tr}\left[B(x,z)B(x,z)^\dagger\gamma_5\gamma_j B(x,z)\gamma_j\gamma_5 B(x,z)^\dagger\right] \\
& + \operatorname{Tr}\left[B(x,z)B(x,z)^\dagger\gamma_5\gamma_j\right] \operatorname{Tr}\left[B(x,z)\gamma_j\gamma_5 B(x,z)^\dagger\right]\Big\rangle
\end{aligned}
\tag{5.15}
$$

Since the double sum in $C_{21}(t)$ increases the time for numerical calculation extremely, one gets rid of this problem by factorizing the sums. If necessary, traces and sums are interchanged. The expectation value is reached by averaging over several configurations, so the angled brackets are omitted and we get the factorized formula for the correlation function:

$$
\begin{aligned}
C_{21}(t) = & \left(\sum_{\mathbf{x}} \operatorname{Tr}\left[B(x,z)B(x,z)^\dagger\right]\right)\left(\sum_{\mathbf{y}} \operatorname{Tr}\left[B(y,z)\gamma_j\gamma_5 B(y,z)^\dagger\gamma_5\gamma_j\right]\right) \\
& - \operatorname{Tr}\left[\left(\sum_{\mathbf{x}} B(x,z)^\dagger B(x,z)\right)\gamma_j\gamma_5\left(\sum_{\mathbf{y}} B(y,z)^\dagger\gamma_5\gamma_j B(y,z)\right)\right] \\
& - \operatorname{Tr}\left[\left(\sum_{\mathbf{x}} B(x,z)^\dagger B(x,z)\right)\left(\sum_{\mathbf{y}} B(y,z)^\dagger\gamma_5\gamma_j B(y,z)\right)\gamma_j\gamma_5\right] \\
& + \left(\sum_{\mathbf{x}} \operatorname{Tr}\left[B(x,z)B(x,z)^\dagger\gamma_5\gamma_j\right]\right)\left(\sum_{\mathbf{y}} \operatorname{Tr}\left[B(y,z)\gamma_j\gamma_5 B(y,z)^\dagger\right]\right)
\end{aligned}
\tag{5.16}
$$

5.2 Numerical Results

For calculation, we are using the gauge link configurations of ensemble C54 presented in Table 3.1. We compute the effective masses for the two presented correlation matrix elements from Table 5.1 and compare the results to the $\eta_B\Upsilon$ threshold. For a bound $\bar{b}\bar{b}bb$ state, the effective mass has to be lower than the threshold energy which is obtained by the sum of $aE_{\eta_B} + aE_\Upsilon$ computed in Chapter 4. We display the effective masses $aE_{\text{eff}}(t)$ in Fig. 5.1.

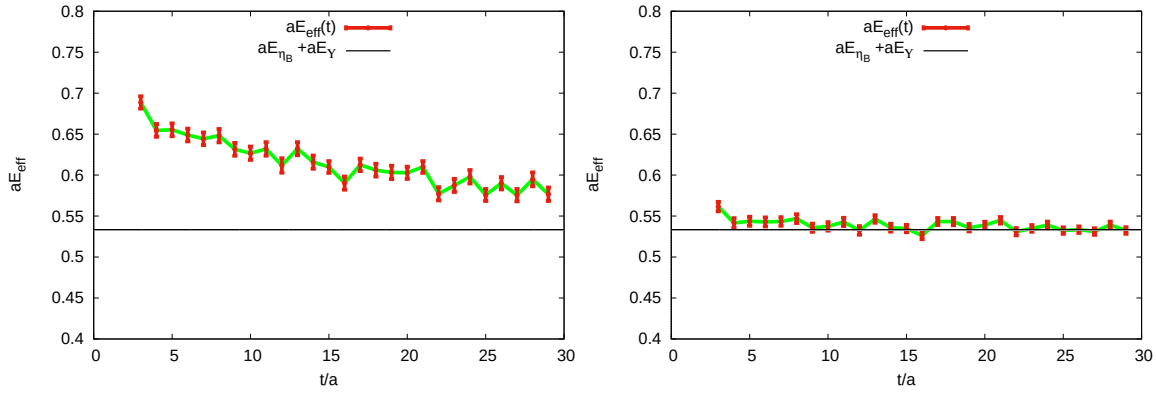

Figure 5.1: Effective masses for the $\bar{b}\bar{b}bb$ system. **(left):** Correlation matrix element C_{11}. **(right):** Correlation matrix element C_{21}.

As already mentioned above we are interested in a possible bound state, so we have to compare the results of Fig. 5.1 with the $\eta_B\Upsilon$ threshold. Fig. 5.2 illustrates the effective masses for both correlation functions as well as the threshold energy. It is obvious that the lowest energy level decreases only till it reaches the threshold but it does not sink below. This gives evidence that no bound state can be formed: The energetically most convenient state is realised by two independent mesons.
Furthermore, the numerical results are presented in Table 5.2. They support the visual conclusion: Within errors, the mass difference between the $\bar{b}\bar{b}bb$ energy and the threshold is close to zero. If we take into account that systematic uncertainties due to the chosen fit ranges can slightly affect the determined effective masses, we deduce thus that no bound state is formed.

$aE_{\eta_B} + aE_\Upsilon$	0.5334(7)
$aE_{C_{21}}$	0.5364(9)
ΔE [MeV]	5.3(2.8)

Table 5.2: Threshold energy and effective mass for C_{21} as well as energy difference to threshold in MeV for the $\bar{b}\bar{b}bb$ system.

We can extract additional information from Fig. 5.2: The effective mass for the correlation function including a scattering state decreases faster and reaches the threshold prior to the correlation function with the two mesonic operators. This effect can be investigated in more detail by considering the general correlation function:

$$C_{ij}(t) = \Big\langle \Omega | \mathcal{O}_i(t) \mathcal{O}_j^\dagger(0) | \Omega \Big\rangle = \sum_n \underbrace{\Big\langle \Omega | \mathcal{O}_i(0) | n \Big\rangle}_{Z_i^{(n)}} \underbrace{\Big\langle n | \mathcal{O}_j^\dagger(0) | \Omega \Big\rangle}_{Z_j^{*(n)}} \mathrm{e}^{-E_n t} \tag{5.17}$$

with the abbreviations $Z_i^{(n)}$ and $Z_j^{*(n)}$. If we take all contributions into account, the effective mass is given by:

$$aE_{\text{eff}}(t) = \ln\left(\frac{C_{ij}(t)}{C_{ij}(t+a)}\right) = \ln\left(\frac{\sum_n Z_i^{(n)} Z_j^{*(n)} \mathrm{e}^{-E_n t}}{\sum_n Z_i^{(n)} Z_j^{*(n)} \mathrm{e}^{-E_n (t+a)}}\right) \tag{5.18}$$

Approximating the correlation functions, we include only the ground state for the denominator and ground state plus first excited state for the nominator:

$$\begin{aligned} aE_{\text{eff}}(t) =& \ln\left(\frac{C_{ij}(t)}{C_{ij}(t+a)}\right) \simeq \ln\left(\frac{Z_i^{(0)} Z_j^{*(0)} \mathrm{e}^{-E_0 t} + Z_i^{(1)} Z_j^{*(1)} \mathrm{e}^{-E_1 t}}{Z_i^{(0)} Z_j^{*(0)} \mathrm{e}^{-E_0 (t+a)}}\right) \\ =& \ln\left(\mathrm{e}^{aE_0}\right) + \ln\left(\frac{Z_i^{(0)} Z_j^{*(0)} \mathrm{e}^{-E_0 t} + Z_i^{(1)} Z_j^{*(1)} \mathrm{e}^{-E_1 t}}{Z_i^{(0)} Z_j^{*(0)} \mathrm{e}^{-E_0 t}}\right) \\ =& aE_0 + \ln\left(1 + \frac{Z_i^{(1)} Z_j^{*(1)}}{Z_i^{(0)} Z_j^{*(0)}} \mathrm{e}^{-(E_1 - E_0) t}\right) \\ \simeq& aE_0 + \frac{Z_i^{(1)} Z_j^{*(1)}}{Z_i^{(0)} Z_j^{*(0)}} \mathrm{e}^{-(E_1 - E_0) t} \end{aligned} \tag{5.19}$$

E_0 describes the ground state energy while the additional term is the first correction due to higher state contributions. If the considered operator has a large overlap with the ground state, i.e. the additional contributions $Z_i^{(1)}, Z_j^{*(1)}$ are small compared to the ground state, the plateau value of $E_{\text{eff}}(t)$ will be reached faster.
Applying this to our case, the plateau is reached earlier when including the scattering state, so the overlap with the ground state must be larger. In other words, the scattering state describes the four-quark system better than a mesonic molecule. This confirms our numerical result, consequently, there is no evidence for a bound $\bar{b}\bar{b}bb$ tetraquark state. The same results have been obtained by the detailed study of this system in [36].

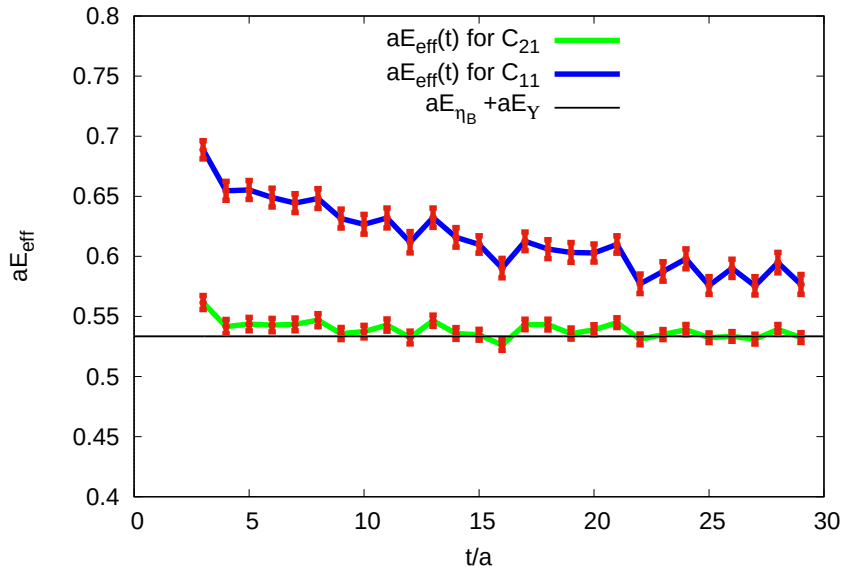

Figure 5.2: Effective masses for both components of $\bar{b}\bar{b}bb$ as well as the threshold energy $aE_{\eta_B} + aE_\Upsilon$.

5.3 Summary

In this chapter, we discussed the $\bar{b}\bar{b}bb$ tetraquark system using NRQCD and searched for the existence or non-existence of a bound state. We studied only the $J^{PC} = 1^{+-}$ channel which is constructed using the two bottomonium states η_B and Υ. Our calculations do not reveal any evidence of a $\bar{b}\bar{b}bb$ bound state in this channel and predict rather a η_B and Υ pair as energetically favourable. This is in accordance with a further $\bar{b}\bar{b}bb$ lattice QCD study (cf. [36]).

Chapter 6

Investigation of $\bar{b}\bar{b}ud$ by Means of NRQCD

In this chapter, we will investigate a tetraquark system containing two heavy antiquarks $\bar{b}$ and two light quarks u and d. Referring to it, we will be talking about the $\bar{b}\bar{b}ud$ system. We aim to determine if a bound state exists and - if so - compute its binding energy.
There are several reasons why we choose the $\bar{b}\bar{b}ud$ system for our investigation: First and foremost it is theoretically known that two heavy (anti-)quarks Q and two rather light (anti-)quarks q favour forming a tetraquark. Additionally, a $\bar{Q}\bar{Q}qq$ system containing two heavy antiquarks is technically less complicated to study than, for example, a system consisting of a heavy quark and heavy antiquark $\bar{Q}Q\bar{q}q$. The first one cannot decay in heavy quarkonium $\bar{Q}Q$ and a light meson $\bar{q}q$ while the latter can do so. We also recognize that no quark-antiquark annihilation is possible. Therefore we focus on the $\bar{b}\bar{b}ud$ system which has only one remaining decay channel:

$$\bar{b}\bar{b}ud \rightarrow B^{(*)} + B^{(*)} \tag{6.1}$$

where $B^{(*)}$ indicates either a B or B^* meson.
So the system can only decompose into two B mesons. For the quantum numbers $I(J^P) = 0(1^+)$ studied in this work, two possible realisations exist: either two B^* mesons or one B^* meson and one B meson.
In order to get evidence about a possible bound state we will compute the mass of the $\bar{b}\bar{b}ud$ system and compare it to the added masses of a B and a B^* meson. For the existence of a bound state, the required condition is:

$$m_{\bar{b}\bar{b}ud} < m_{B^*} + m_B \tag{6.2}$$

We can choose various approaches to study the $\bar{b}\bar{b}ud$ system applying different approximations.
On a first level, one can assume static bottom quarks, i.e. we are using an infinite b-quark mass. The associated theory is known as the Born-Oppenheimer approximation. In this static limit, evidence was found for a bound state with a binding energy of $E_{\bar{b}\bar{b}ud} \simeq -90$ MeV in the $I(J^P) = 0(1^+)$ channel (cf. [16, 17]). For more details about the computation in the Born-Oppenheimer approximation, we also refer to [14, 15].

Assigning the bottom quarks an infinite mass introduces inaccuracies which causes discrepancies from probable experimental results. However, it is crucial to perform the theoretical calculations as precisely as possible. Therefore, the next logical level means considering dynamical bottom quarks with a finite mass. This is achievable, treating the heavy quarks non-relativistically in the framework of NRQCD. Recent studies also predict a stable tetraquark state when applying NRQCD methods (cf. [23, 24]).
In this work, we will study the $\bar{b}\bar{b}ud$ system in the framework of non-relativistic QCD (cf. Chapter 2), that means we are using finite b-quark masses. We will employ several different creation operator structures which generate four-quark systems with the appropriated quantum numbers. Afterwards we determine the $\bar{b}\bar{b}ud$ energy spectrum in order to gain insights about possible bound states in the $I(J^P) = 0(1^+)$ channel.

6.1 Creation Operators for the $\bar{b}\bar{b}ud$ System

The $\bar{b}\bar{b}ud$ system can be realised in various ways. Even if the quark content is specified, there are several quark structures which can generate this four-quark system and have to be taken into account. Additionally, some of these structures can be represented in different momentum projections. In the following section we will specify all operators that can create a $\bar{b}\bar{b}ud$ tetraquark molecule with quantum numbers $I(J^P) = 0(1^+)$.

6.1.1 Quark Structure

First, we focus on the different quark structures, independently of the possible momentum projections. Consequently, the space-time indices are omitted in this notation. Moreover, we do not write the Dirac indices explicitly at this level. There exist three different structures in the $I(J^P) = 0(1^+)$ channel. The calculation of the quantum numbers in detail can be found in Appendix C.2.

Mesonic Molecule BB^*

The first possible structure consists of a scalar B meson and a vector B^* meson. The creation operator is given by:

$$\mathcal{O}_{BB^*} = \bar{b}^a \Gamma_1 d^a \, \bar{b}^b \Gamma_2 u^b - \bar{b}^a \Gamma_1 u^a \, \bar{b}^b \Gamma_2 d^b \tag{6.3}$$

With the Gamma matrices $\Gamma_1 = \gamma_5$ and $\Gamma_2 = \gamma_j$, this realises quantum numbers $I(J^P) = 0(1^+)$.

Mesonic Molecule B^*B^*

As a second structure, we introduce two B^* mesons. The creation operator reads:

$$\mathcal{O}_{B^*B^*} = \bar{b}^a \Gamma_1 d^a \, \bar{b}^b \Gamma_2 u^b - \bar{b}^a \Gamma_1 u^a \, \bar{b}^b \Gamma_2 d^b \tag{6.4}$$

With ϵ_{ijk} ($\Gamma_1 = \gamma_j, \quad \Gamma_2 = \gamma_k$), the required quantum numbers are fulfilled.

Diquark-antidiquark Dd

The last structure considered in this work is a diquark-antidiquark structure with the diquark ud and the antidiquark $\bar{b}\bar{b}$. This creation operator reads:

$$\mathcal{O}_{Dd} = \epsilon^{abc} \bar{b}^b \Gamma_1 \left[\bar{b}^c\right]^T \epsilon^{ade} \left(\left[d^d\right]^T \Gamma_2 u^e - \left[u^d\right]^T \Gamma_2 d^e \right) \tag{6.5}$$

where we choose $\Gamma_1 = \gamma_j \mathcal{C}$ and $\Gamma_2 = \mathcal{C}\gamma_5$ to gain the expected quantum numbers. $\mathcal{C}$ denotes the charge conjugation matrix. The T describes transposing in Dirac space.

Whereas the operators for the mesonic structures are quite evident, we emphasise the different structure for the diquark-antidiquark operator. Obviously, there are two differences: First, summing over the colour indices, epsilon tensors are included. Second, the charge conjugation matrix $\mathcal{C}$ appears in the definition of the Gamma matrices. These modifications are necessary to preserve gauge invariance as well as invariance under Lorentz transformations.

We consider first gauge transformations which are given by:

$$\begin{aligned} \psi(x) &\to \psi'(x) = \Omega(x)\psi(x) \\ \bar{\psi}(x) &\to \bar{\psi}'(x) = \bar{\psi}(x)\Omega^{\dagger}(x) \end{aligned} \tag{6.6}$$

where $\Omega(x)$ is a SU(3) matrix and $\psi \in \{u, d, b\}$. An essential relation for SU(3) matrices is given by (cf. chapter 3.1 in [27]):

$$\epsilon^{ace}\Omega^{ab}\Omega^{cd}\Omega^{ef} = \epsilon^{bdf} \tag{6.7}$$

with small letters indicating colour indices.
We study now the behaviour of the diquark-antidiquark operator under gauge transformations. To increase readability, we use only the first term of (6.5):

$$\epsilon^{abc}\,\bar{b}^b\Gamma_1\left[\bar{b}^c\right]^T\,\epsilon^{ade}\,\left[d^d\right]^T\Gamma_2 u^e \longrightarrow \epsilon^{abc}\,\bar{b}^f\Omega^{\dagger fb}\Gamma_1\left[\bar{b}^g\Omega^{\dagger gc}\right]^T\,\epsilon^{ade}\,\left[\Omega^{dh}d^h\right]^T\Gamma_2\Omega^{ei}u^i \tag{6.8}$$

Using (6.7), we can express:

$$\epsilon^{ade}\,\Omega^{dh}\,\Omega^{ei} = \epsilon^{hij}\,\Omega^{\dagger ja}; \qquad \epsilon^{abc}\,\Omega^{\dagger fb}\,\Omega^{\dagger gc} = \epsilon^{kfg}\,\Omega^{ak} \tag{6.9}$$

This yields:

$$\begin{aligned} &\epsilon^{abc}\,\Omega^{\dagger fb}\,\Omega^{\dagger gc}\,\bar{b}^f\Gamma_1\left[\bar{b}^g\right]^T\,\epsilon^{ade}\,\Omega^{dh}\,\Omega^{ei}\,\left[d^h\right]^T\Gamma_2 u^i \\ =&\,\epsilon^{kfg}\,\Omega^{ak}\,\bar{b}^f\Gamma_1\left[\bar{b}^g\right]^T\,\epsilon^{hij}\,\Omega^{\dagger ja}\,\left[d^h\right]^T\Gamma_2 u^i \\ =&\,\epsilon^{kfg}\,\bar{b}^f\Gamma_1\left[\bar{b}^g\right]^T\,\epsilon^{khi}\,\left[d^h\right]^T\Gamma_2 u^i \\ =&\,\epsilon^{abc}\,\bar{b}^b\Gamma_1\left[\bar{b}^c\right]^T\,\epsilon^{ade}\,\left[d^d\right]^T\Gamma_2 u^e \end{aligned} \tag{6.10}$$

Finally, we receive the same operator as in (6.5), thus including the epsilon tensors in the summation over the colour indices ensures our operator to be gauge invariant.

To include Lorentz transformations, we first discuss charge conjugation. Applying it, we define the transformation as:

$$\psi \xrightarrow{\mathcal{C}} \psi' = \mathcal{C}\bar{\psi}^T \tag{6.11}$$

and consequently:

$$\bar{\psi} \xrightarrow{\mathcal{C}} \bar{\psi}' = \psi^T \gamma_0^* \mathcal{C}^\dagger \gamma_0 \tag{6.12}$$

Since we expect $\psi \xrightarrow{\mathcal{C}\mathcal{C}} \psi' = \psi$, we get:

$$\psi \xrightarrow{\mathcal{C}} \mathcal{C}\bar{\psi}^T \xrightarrow{\mathcal{C}} \mathcal{C}\left(\psi^T \gamma_0^* \mathcal{C}^\dagger \gamma_0\right)^T = \mathcal{C}\gamma_0^T \mathcal{C}^* \gamma_0^\dagger \psi \tag{6.13}$$

That means:

$$\mathcal{C}\gamma_0^T \mathcal{C}^* \gamma_0^\dagger = 1 \quad \text{or} \quad \gamma_0^* \mathcal{C}^\dagger \gamma_0 \mathcal{C}^T = 1 \tag{6.14}$$

Additionally, we expect the Dirac Lagrangian $\bar{\psi}\left(\gamma_\mu \partial^\mu + m\right)\psi$ to be invariant under charge conjugation.

$$\begin{aligned} &\psi^T \gamma_0^* \mathcal{C}^\dagger \gamma_0 \left(\gamma_\mu \partial^\mu + m\right) \mathcal{C}\bar{\psi}^T \\ =&\psi^T \left(\gamma_0^* \mathcal{C}^\dagger \gamma_0 \gamma_\mu \mathcal{C} \partial^\mu + \gamma_0^* \mathcal{C}^\dagger \gamma_0 \mathcal{C} m\right) \bar{\psi}^T \end{aligned} \tag{6.15}$$

It is consequently required that:

$$\gamma_0^* \mathcal{C}^\dagger \gamma_0 \mathcal{C} = -1 \quad \text{and} \quad \gamma_0^* \mathcal{C}^\dagger \gamma_0 \gamma_\mu \mathcal{C} = \gamma_\mu^T \tag{6.16}$$

Comparing (6.14) and (6.16), we find $\mathcal{C} = -\mathcal{C}^T$ as well as:

$$\mathcal{C}^{-1} \gamma_\mu \mathcal{C} = -\gamma_\mu^T \tag{6.17}$$

Now we consider the Lorentz transformation for a spinor while the well-known transformation behaviour of a space time argument is $x^\mu \to x^{\mu\prime} = \Lambda^\mu_{\ \nu} x^\nu$.

$$\psi(x) \to \psi'(x') = S(\Lambda)\psi(x) \quad ; \qquad \bar{\psi}(x) \to \bar{\psi}'(x') = \bar{\psi}(x) S^{-1}(\Lambda) \tag{6.18}$$

For an infinitesimal Lorentz transformation $\Lambda^\nu_{\ \mu} = \delta^\nu_\mu + \omega^\nu_\mu$, one can easily prove that:

$$S(\Lambda) = 1 - \frac{i}{4}\sigma_{\alpha\beta}\omega^{\alpha\beta} \qquad \text{with: } \sigma_{\alpha\beta} = \frac{i}{2}\left[\gamma_\alpha, \gamma_\beta\right] \tag{6.19}$$

and consequently, the finite transformation is given by:

$$S(\Lambda) = \exp\left(-\frac{i}{4}\sigma_{\alpha\beta}\omega^{\alpha\beta}\right) \tag{6.20}$$

Obviously, $S(\Lambda)$ is unitary, so $S^{-1}(\Lambda) = S^\dagger(\Lambda)$.

Having established all prerequisites, we return to the diquark-antidiquark operator and prove that the given structure is Lorentz invariant. Note that for the mesonic structures Lorentz invariance is given by construction:

$$\bar{\psi}_{(1)}(x)\Gamma_i\psi_{(2)}(x) \to \bar{\psi}'_{(1)}(x)\Gamma_i\psi'_{(2)}(x) = \bar{\psi}_{(1)}(x)S^{-1}(\Lambda)\Gamma_i S(\Lambda)\psi_{(2)}(x) = \bar{\psi}_{(1)}(x)\Gamma_i\psi_{(2)}(x) \tag{6.21}$$

with $\psi_{(1)}, \psi_{(2)} \in \{u, d, b\}$.

Considering the diquark-antidiquark operator, we claim Lorentz invariance for the terms

$$\bar{\psi}_{(1)}(x)\Gamma_i\bar{\psi}^T_{(2)}(x); \qquad \psi^T_{(1)}(x)\Gamma_i\psi_{(2)}(x) \tag{6.22}$$

This will be reached including the charge conjugation matrix $\mathcal{C}$. We state that $\mathcal{C}\bar{\psi}^T$ transforms in the same way as ψ and $\psi^T\mathcal{C}$ in the same way as $\bar{\psi}$. It can be proved easily using (6.17) and (6.20):

$$\begin{aligned}
\psi^T\mathcal{C} \to [S\psi]^T\mathcal{C} &= \psi^T\left[\exp\left(-\frac{i}{4}\sigma_{\alpha\beta}\omega^{\alpha\beta}\right)\right]^T\mathcal{C} \\
&= \psi^T\exp\left(-\frac{i}{4}\sigma_{\alpha\beta}\frac{i}{2}\left[\gamma_\alpha,\gamma_\beta\right]^T\right)\mathcal{C} \\
&= \psi^T\exp\left(-\frac{i}{4}\sigma_{\alpha\beta}\frac{i}{2}\left(\gamma^T_\beta\gamma^T_\alpha - \gamma^T_\alpha\gamma^T_\beta\right)\right)\mathcal{C} \\
&= \psi^T\mathcal{C}\exp\left(-\frac{i}{4}\sigma_{\alpha\beta}\frac{i}{2}\left(\gamma_\beta\gamma_\alpha - \gamma_\alpha\gamma_\beta\right)\right) \\
&= \psi^T\mathcal{C}\exp\left(\frac{i}{4}\sigma_{\alpha\beta}\omega^{\alpha\beta}\right) = \psi^T\mathcal{C}S^{-1}
\end{aligned} \tag{6.23}$$

$$\begin{aligned}
\mathcal{C}\bar{\psi}^T \to \mathcal{C}\left[\bar{\psi}S^{-1}\right]^T &= \mathcal{C}\left[\exp\left(\frac{i}{4}\sigma_{\alpha\beta}\omega^{\alpha\beta}\right)\right]^T\bar{\psi}^T \\
&= \mathcal{C}\exp\left(\frac{i}{4}\sigma_{\alpha\beta}\frac{i}{2}\left(\gamma^T_\beta\gamma^T_\alpha - \gamma^T_\alpha\gamma^T_\beta\right)\right)\bar{\psi}^T \\
&= \exp\left(-\frac{i}{4}\sigma_{\alpha\beta}\omega^{\alpha\beta}\right)\mathcal{C}\bar{\psi}^T = \; S\mathcal{C}\bar{\psi}^T
\end{aligned} \tag{6.24}$$

In (6.24) we insert $\mathcal{C}\mathcal{C}^{-1}$ in the second line and use $\mathcal{C}\gamma^T_\mu\mathcal{C}^{-1} = -\gamma_\mu$. For (6.23), we also insert $\mathcal{C}\mathcal{C}^{-1}$ but apply additionally the relation between the gamma matrices and their transposed version (see Appendix A.1). Afterwards, we use (6.17) in the third step.

To sum up, the transformation behaviour is given by:

$$\psi^T(x)\mathcal{C} \to \psi^T(x)\mathcal{C}S^{-1}(\Lambda) \quad ; \qquad \mathcal{C}\bar{\psi}^T(x) \to S(\Lambda)\mathcal{C}\bar{\psi}^T(x) \tag{6.25}$$

Consequently, we have to include the charge conjugation matrix $\mathcal{C}$ in the gamma matrices to conserve Lorentz invariance for the diquark operator, i.e. we use $\Gamma_1 = \gamma_j\mathcal{C}$ and $\Gamma_2 = \mathcal{C}\gamma_5$.

6.1.2 Momentum Projection

Additionally, we consider two different momentum projections which appear for the quark structures (cf. [21]). To be more precise, only for the structures including B mesons are two projections available. First, we can project the total momentum of the system to zero. Second, we also have to include the momentum projection for each B meson separately to zero. Note that for the diquark-antidiquark system only the total momentum projection to zero can be applied because a single diquark/antidiquark cannot exist due to quark confinement.

First, we consider the creation operator for a B meson which is given by:

$$\mathcal{O}_{B(\mathbf{p})}(t) = \frac{1}{\sqrt{V_s}} \sum_{\mathbf{x}\in V_s} \bar{b}(\mathbf{x},t)\Gamma_1 u(\mathbf{x},t)\mathrm{e}^{-i\mathbf{x}\mathbf{p}} \tag{6.26}$$

Due to the lattice discretisation the momenta are discrete and given by $p_j = \frac{2\pi}{aL_j} n_j$ with L_j being the lattice extent in the j-th direction, i.e. the number of lattice points in this direction and $n_j = 0, 1, \ldots, L_j - 1$. In general, the lattice extent is the same for all spatial directions. Therefore we use $L = L_1 = L_2 = L_3$ instead of the L_j's. V_s describes the spatial volume defined by $V_s = L^3$.

Projecting the operator to zero, i.e. $\mathbf{p} = 0$, leads to :

$$\mathcal{O}_{B(0)}(t) = \frac{1}{\sqrt{V_s}} \sum_{\mathbf{x}\in V_s} \bar{b}(\mathbf{x},t)\Gamma_1 u(\mathbf{x},t) \tag{6.27}$$

Note that the sum over the spatial extent is required to describe the bottom quark dynamically in contrast to a static limit where the bottom quark's position is fixed and thus requiring no sum.

Continuing the discussion for a four-quark system consisting of two B mesons, the creation operator in the most general form concerning momentum projection is given by:

$$\mathcal{O}_{B(\mathbf{p})B(\mathbf{q})}(t) = \frac{1}{\sqrt{V_s}} \sum_{\mathbf{x}\in V_s} \bar{b}(\mathbf{x},t)\Gamma_1 u(\mathbf{x},t)\mathrm{e}^{-i\mathbf{x}\mathbf{p}} \frac{1}{\sqrt{V_s}} \sum_{\mathbf{y}\in V_s} \bar{b}(\mathbf{y},t)\Gamma_2 u(\mathbf{y},t)\mathrm{e}^{-i\mathbf{y}\mathbf{q}} \tag{6.28}$$

We must now distinguish the two cases mentioned above: In the first instance, we take the total momentum projection to zero into account, i.e. the added momenta of the system are zero $\mathbf{p} + \mathbf{q} = 0$, with $\mathbf{p}$ and $\mathbf{q}$ being the particular momenta of the B mesons. The operator (6.28) reduces to:

$$\mathcal{O}_{[BB](0)}(t) = \frac{1}{\sqrt{V_s}} \sum_{\mathbf{x}\in V_s} \bar{b}(\mathbf{x},t)\Gamma_1 u(\mathbf{x},t) \frac{1}{\sqrt{V_s}} \sum_{\mathbf{y}\in V_s} \bar{b}(\mathbf{y},t)\Gamma_2 u(\mathbf{y},t)\mathrm{e}^{-i(\mathbf{x}-\mathbf{y})\mathbf{p}} \tag{6.29}$$

Since we describe a mesonic molecule, both B mesons have to be located at the same spatial position $\mathbf{x} = \mathbf{y}$, so the final operator for projecting to total zero momentum is:

$$\mathcal{O}_{[BB](0)}(t) = \frac{1}{\sqrt{V_s}} \sum_{\mathbf{x}\in V_s} \bar{b}(\mathbf{x},t)\Gamma_1 u(\mathbf{x},t)\bar{b}(\mathbf{x},t)\Gamma_2 u(\mathbf{x},t) \tag{6.30}$$

If we project each momentum separately to zero, i.e. $\mathbf{p} = \mathbf{q} = 0$ in (6.28), this operator is given by:

$$\mathcal{O}_{B(0)B(0)}(t) = \frac{1}{\sqrt{V_s}} \sum_{\mathbf{x}\in V_s} \bar{b}(\mathbf{x},t)\Gamma_1 u(\mathbf{x},t) \frac{1}{\sqrt{V_s}} \sum_{\mathbf{y}\in V_s} \bar{b}(\mathbf{y},t)\Gamma_2 u(\mathbf{y},t) \tag{6.31}$$

Note that in this case the sums over $\mathbf{x}$ and $\mathbf{y}$ are executed independently and these results are multiplied. In contrast to the mesonic molecule in the first case, now we are talking about a mesonic scattering state.

6.1.3 Listing of All Creation Operators for $\bar{b}\bar{b}ud$

Taking all different creation operator structures discussed in the previous sections into account, we get five different creation operators that generate a $\bar{b}\bar{b}ud$ four-quark system in the $I(J^P) = 0(1^+)$ channel. These are:

- First, a system consisting of a B meson and a B^* meson with the two different momentum projections:
  - $B(0)B^*(0)$: mesonic scattering state - the momenta are separately projected to zero momentum.
  - $[BB^*](0)$: mesonic molecule - the total momentum of the whole four-quark system is projected to zero.

  The associated operators are called $\mathcal{O}_{B(0)B^*(0)}$ and $\mathcal{O}_{[BB^*](0)}$.

- Additionally, a system including two B^* mesons. There the same momentum projections as above are available:
  - $B^*(0)B^*(0)$: mesonic scattering state - the momenta are separately projected to zero momentum.
  - $[B^*B^*](0)$: mesonic molecule - the total momentum of the whole four-quark system is projected to zero.

  As above the operators are labelled as $\mathcal{O}_{B^*(0)B^*(0)}$ and $\mathcal{O}_{[B^*B^*](0)}$.

- Finally, the diquark-antidiquark operator. Due to quark confinement there exists only one reasonable momentum projection which realises a diquark molecule:
  - $[Dd](0)$: the total momentum of the whole four-quark system is projected to zero.

  This operator is called $\mathcal{O}_{[Dd](0)}$.

6.2 Correlation Matrix

For investigating the $\bar{b}\bar{b}ud$ tetraquark molecule all operators mentioned in the previous section have to be taken into account for numerical calculations. Therefore it is not sufficient to describe the system only by a single correlation function but rather by a complete correlation matrix while each element contains one specific correlation function. These correlation functions are generally given by:

$$C_{ij}(t_{\text{sink}} - t_{\text{source}}) = \langle \Omega | \mathcal{O}_i(t_{\text{sink}}) \mathcal{O}_j^\dagger(t_{\text{source}}) | \Omega \rangle \equiv \langle \mathcal{O}_i(t_{\text{sink}}) \mathcal{O}_j^\dagger(t_{\text{source}}) \rangle \tag{6.32}$$

with $\mathcal{O}_i, \mathcal{O}_j \in \left\{ \mathcal{O}_{B(0)B^*(0)}, \mathcal{O}_{[BB^*](0)}, \mathcal{O}_{B^*(0)B^*(0)}, \mathcal{O}_{[B^*B^*](0)}, \mathcal{O}_{[Dd](0)} \right\}$ and the vacuum state $|\Omega\rangle$.
In a descriptive representation, one assumes the correlation function to create a particle from the vacuum at the source position possessing the structure of the applied creation operator $\mathcal{O}_j^\dagger(t_{\text{source}})$. Afterwards, the particle moves on the lattice to the sink position where it is annihilated by the operator $\mathcal{O}_i(t_{\text{sink}})$.

6.2.1 Hermiticity of the Correlation Matrix

It can be easily proven that the correlation matrix is always hermitian regardless of the operator basis. This is a very useful property for numerical calculation. In the following, we start with the correlation function

$$\begin{aligned} C_{ij}(t_{\text{sink}} - t_{\text{source}}) =& \langle \Omega | \mathcal{O}_i(t_{\text{sink}}) \mathcal{O}_j^\dagger(t_{\text{source}}) | \Omega \rangle \\ =& \sum_n \langle \Omega | \mathcal{O}_i(0) | n \rangle \langle n | \mathcal{O}_j^\dagger(0) | \Omega \rangle \mathrm{e}^{-E_n(t_{\text{sink}} - t_{\text{source}})} \end{aligned} \tag{6.33}$$

Calculating the complex conjugated correlation matrix elements $C_{ij}^*(t_{\text{sink}} - t_{\text{source}}) = C_{ij}^\dagger(t_{\text{sink}} - t_{\text{source}})$ yields:

$$\begin{aligned} & C_{ij}^\dagger(t_{\text{sink}} - t_{\text{source}}) \\ =& \sum_n \left[\langle \Omega | \mathcal{O}_i | n \rangle \langle n | \mathcal{O}_j^\dagger | \Omega \rangle \mathrm{e}^{-E_n(t_{\text{sink}} - t_{\text{source}})} \right]^\dagger \\ =& \sum_n \langle \Omega | \mathcal{O}_i | n \rangle^\dagger \langle n | \mathcal{O}_j^\dagger | \Omega \rangle^\dagger \mathrm{e}^{-E_n(t_{\text{sink}} - t_{\text{source}})} \\ =& \sum_n \langle n | \mathcal{O}_i^\dagger | \Omega \rangle \langle \Omega | \mathcal{O}_j | n \rangle \mathrm{e}^{-E_n(t_{\text{sink}} - t_{\text{source}})} \\ =& \sum_n \langle \Omega | \mathcal{O}_j | n \rangle \langle n | \mathcal{O}_i^\dagger | \Omega \rangle \mathrm{e}^{-E_n(t_{\text{sink}} - t_{\text{source}})} \\ =& C_{ji}(t_{\text{sink}} - t_{\text{source}}) \end{aligned} \tag{6.34}$$

Finally, we have shown that $C_{ij}^\dagger(t) = C_{ji}(t)$ with $t = t_{\text{sink}} - t_{\text{source}}$, consequently the matrix is hermitian.

6.2.2 Correlation Matrix Elements

For our numerical calculations, we are using point-to-all propagators for the light quarks. That means, the propagators for a specific configuration are not computed from each space-time position to every other but rather from only one chosen source location to all others. Consequently, the source position of our propagator is fixed. For more details on different techniques to compute quark propagators, cf. e.g. [41]. However, if we consider zero momentum projection for each meson separately, we have to evaluate the operator at two different spatial positions (cf. (6.31)). Since our source position is fixed though, we are not able to compute correlation matrix elements with such source operators. In other words, we cannot project separately the momentum to zero at the source. Therefore, there appear several elements in the correlation matrix which are not computable. In fact, only a 5×3 submatrix is accessible in our approach. We present the complete correlation matrix in Table 6.1.

sink \ source	$\mathcal{O}^\dagger_{[BB^*](0)}$		$\mathcal{O}^\dagger_{[B^*B^*](0)}$		$\mathcal{O}^\dagger_{[Dd](0)}$		$\mathcal{O}^\dagger_{B(0)B^*(0)}$	$\mathcal{O}^\dagger_{B^*(0)B^*(0)}$
$\mathcal{O}_{[BB^*](0)}$	c.	I	c.	I	c.	IV	n.c.	n.c.
$\mathcal{O}_{[B^*B^*](0)}$	c.	I	c.	I	c.	IV	n.c.	n.c.
$\mathcal{O}_{[Dd](0)}$	c.	III	c.	III	c.	II	n.c.	n.c.
$\mathcal{O}_{B(0)B^*(0)}$	c.	I	c.	I	c.	IV	n.c.	n.c.
$\mathcal{O}_{B^*(0)B^*(0)}$	c.	I	c.	I	c.	IV	n.c.	n.c.

Table 6.1: The correlation matrix for $\bar{b}\bar{b}ud$. Elements labelled with c. can be computed directly by numerical calculation while elements labelled n.c. are not computable. The Roman numerals indicate the type of the correlation function.

Besides the differentiation between computable and non-computable elements, we have classified four types of correlation functions which differ in the chosen sink and source operators. We start this examination by naming the five operators described in Sec. 6.1.3 including space-time arguments explicitly.

$$\mathcal{O}_{[BB^*](0)}(t) = \sum_{\mathbf{x}} \bar{b}^a \Gamma_1 d^a(\mathbf{x},t)\, \bar{b}^b \Gamma_2 u^b(\mathbf{x},t) - \bar{b}^a \Gamma_1 u^a(\mathbf{x},t)\, \bar{b}^b \Gamma_2 d^b(\mathbf{x},t) \tag{6.35}$$

with $\Gamma_1 = \gamma_5, \quad \Gamma_2 = \gamma_j$.

$$\mathcal{O}_{[B^*B^*](0)}(t) = \sum_{\mathbf{x}} \bar{b}^a \Gamma_1 d^a(\mathbf{x},t)\, \bar{b}^b \Gamma_2 u^b(\mathbf{x},t) - \bar{b}^a \Gamma_1 u^a(\mathbf{x},t)\, \bar{b}^b \Gamma_2 d^b(\mathbf{x},t) \tag{6.36}$$

with ϵ_{ijk} $(\Gamma_1 = \gamma_j, \quad \Gamma_2 = \gamma_k)$.

$$\mathcal{O}_{B(0)B^*(0)}(t) = \sum_{\mathbf{x},\mathbf{y}} \bar{b}^a \Gamma_1 d^a(\mathbf{x},t)\, \bar{b}^b \Gamma_2 u^b(\mathbf{y},t) - \bar{b}^a \Gamma_1 u^a(\mathbf{x},t)\, \bar{b}^b \Gamma_2 d^b(\mathbf{y},t) \tag{6.37}$$

with $\Gamma_1 = \gamma_5, \quad \Gamma_2 = \gamma_j$.

$$\mathcal{O}_{B^*(0)B^*(0)}(t) = \sum_{\mathbf{x},\mathbf{y}} \bar{b}^a \Gamma_1 d^a(\mathbf{x},t)\, \bar{b}^b \Gamma_2 u^b(\mathbf{y},t) - \bar{b}^a \Gamma_1 u^a(\mathbf{x},t)\, \bar{b}^b \Gamma_2 d^b(\mathbf{y},t) \tag{6.38}$$

with ϵ_{ijk} ($\Gamma_1 = \gamma_j, \quad \Gamma_2 = \gamma_k$).

$$\mathcal{O}_{[Dd](0)}(t) = \sum_{\mathbf{x}} \epsilon^{abc} \bar{b}^b \Gamma_1 \left[\bar{b}^c\right]^T (\mathbf{x}, t) \epsilon^{ade} \left(\left[d^d\right]^T \Gamma_2 u^e(\mathbf{x}, t) - \left[u^d\right]^T \Gamma_2 d^e(\mathbf{x}, t) \right) \tag{6.39}$$

with $\Gamma_1 = \gamma_j \mathcal{C}, \quad \Gamma_2 = \mathcal{C}\gamma_5$.

We have introduced colour indices explicitly while suppressing Dirac indices. The exponential T in $\mathcal{O}_{[Dd](0)}$ denotes "transposed in Dirac space". For the sake of briefness, we will omit the T in the calculations but keep in mind that is is necessary to maintain the correct structure for Dirac space.
The operators (6.35) to (6.38) differ only by the Γ's and the space-time arguments. We can generalize these operators via:

$$\mathcal{O}_{BB}(t) = \sum_{\mathbf{x},\mathbf{y}} \bar{b}^a \Gamma_1 d^a(\mathbf{x}, t)\, \bar{b}^b \Gamma_2 u^b(\mathbf{y}, t) - \bar{b}^a \Gamma_1 u^a(\mathbf{x}, t)\, \bar{b}^b \Gamma_2 d^b(\mathbf{y}, t) \tag{6.40}$$

while replacing the Γ's at the end and setting $\mathbf{x} = \mathbf{y}$ when considering total zero momentum projection. Using the operators (6.39) and (6.40), we define the four general types of correlation functions:

- Type I: $\left\langle \mathcal{O}_{BB}(t) \mathcal{O}^\dagger_{BB}(0) \right\rangle =$

$$\begin{aligned} =& \sum_{\mathbf{x},\mathbf{y}} \Big\langle \left[\bar{b}^a \Gamma_1 d^a(\mathbf{x}, t)\, \bar{b}^b \Gamma_2 u^b(\mathbf{y}, t) - \bar{b}^a \Gamma_1 u^a(\mathbf{x}, t)\, \bar{b}^b \Gamma_2 d^b(\mathbf{y}, t) \right] \\ & \times \left[\bar{d}^{a'} \Gamma_1' b^{a'}(\mathbf{z}, 0)\, \bar{u}^{b'} \Gamma_2' b^{b'}(\mathbf{z}, 0) - \bar{u}^{a'} \Gamma_1' b^{a'}(\mathbf{z}, 0)\, \bar{d}^{b'} \Gamma_2' b^{b'}(\mathbf{z}, 0) \right] \Big\rangle \end{aligned} \tag{6.41}$$

- Type II: $\left\langle \mathcal{O}_{[Dd](0)}(t) \mathcal{O}^\dagger_{[Dd](0)}(0) \right\rangle =$

$$\begin{aligned} =& \sum_{\mathbf{x}} \Big\langle \left[\epsilon^{abc} \bar{b}^b \Gamma_1 \bar{b}^c(\mathbf{x}, t) \epsilon^{ade} \left(d^d \Gamma_2 u^e(\mathbf{x}, t) - u^d \Gamma_2 d^e(\mathbf{x}, t) \right) \right] \\ & \times \left[\epsilon^{a'd'e'} \left(\bar{u}^{d'} \Gamma_2' \bar{d}^{e'}(\mathbf{z}, 0) - \bar{d}^{d'} \Gamma_2' \bar{u}^{e'}(\mathbf{z}, 0) \right) \epsilon^{a'b'c'} b^{b'} \Gamma_1' b^{c'}(\mathbf{z}, 0) \right] \Big\rangle \end{aligned} \tag{6.42}$$

- Type III: $\left\langle \mathcal{O}_{[Dd](0)}(t) \mathcal{O}^\dagger_{BB}(0) \right\rangle =$

$$\begin{aligned} =& \sum_{\mathbf{x}} \Big\langle \left[\epsilon^{abc} \bar{b}^b \Gamma_1 \bar{b}^c(\mathbf{x}, t) \epsilon^{ade} \left(d^d \Gamma_2 u^e(\mathbf{x}, t) - u^d \Gamma_2 d^e(\mathbf{x}, t) \right) \right] \\ & \times \left[\bar{d}^{a'} \Gamma_1' b^{a'}(\mathbf{z}, 0)\, \bar{u}^{b'} \Gamma_2' b^{b'}(\mathbf{z}, 0) - \bar{u}^{a'} \Gamma_1' b^{a'}(\mathbf{z}, 0)\, \bar{d}^{b'} \Gamma_2' b^{b'}(\mathbf{z}, 0) \right] \Big\rangle \end{aligned} \tag{6.43}$$

- Type IV: $\left\langle \mathcal{O}_{BB}(t) \mathcal{O}^\dagger_{[Dd](0)}(0) \right\rangle =$

$$\begin{aligned} =& \sum_{\mathbf{x},\mathbf{y}} \Big\langle \left[\bar{b}^a \Gamma_1 d^a(\mathbf{x}, t)\, \bar{b}^b \Gamma_2 u^b(\mathbf{y}, t) - \bar{b}^a \Gamma_1 u^a(\mathbf{x}, t)\, \bar{b}^b \Gamma_2 d^b(\mathbf{y}, t) \right] \\ & \times \left[\epsilon^{a'd'e'} \left(\bar{u}^{d'} \Gamma_2' \bar{d}^{e'}(\mathbf{z}, 0) - \bar{d}^{d'} \Gamma_2' \bar{u}^{e'}(\mathbf{z}, 0) \right) \epsilon^{a'b'c'} b^{b'} \Gamma_1' b^{c'}(\mathbf{z}, 0) \right] \Big\rangle \end{aligned} \tag{6.44}$$

Note that $\Gamma_i' \equiv \gamma_0 \Gamma_i^\dagger \gamma_0$ with $i = 1, 2$.
Evaluation has been performed for all four correlation function types separately. We have proceeded in the same way as presented in Sec. 5.1. Inserting finally the appropriated Γ-matrices and identifying $\mathbf{y} = \mathbf{x}$ for total momentum projection to zero yields all 15 correlation matrix elements. In Appendix D.1 we illustrate exemplarily the computation for type I correlation functions.

6.2.3 Symmetries

In this section, we will investigate the symmetries - namely hermiticity and time reversal - of the correlation matrix explicitly. Afterwards, we depict how to use the symmetries to improve the statistical quality of the raw data.

Hermiticity

The correlation matrix is defined as a hermitian matrix (proof see Sec. 6.2.1), so:

- The diagonal elements are real: $C_{ii} = C_{ii}^*$
- The off-diagonal elements are complex conjugated to each other: $C_{ij} = C_{ji}^*$

We will prove these two conditions explicitly for the given correlation matrix in the following paragraph.

Before, we note an indispensable relation for the complex conjugated quark spinors:

$$[q(t)]^\dagger = q^\dagger(-t) \tag{6.45}$$

This relation can be proven easily by applying the time evolution of the quark field in Euclidean time with the hermitian Hamiltonian operator H:

$$q(t) = \mathrm{e}^{tH} q(0) \mathrm{e}^{-tH} \tag{6.46}$$

Thus, daggering the quark field yields:

$$[q(t)]^\dagger = \left[\mathrm{e}^{tH} q(0) \mathrm{e}^{-tH}\right]^\dagger = \mathrm{e}^{-tH} q(0)^\dagger \mathrm{e}^{tH} = q^\dagger(-t) \tag{6.47}$$

Consequently, the same relation is valid for the daggered quark field:

$$\left[q^\dagger(t)\right]^\dagger = q(-t) \tag{6.48}$$

In the next step, we will prove hermiticity explicitly for the correlation matrix elements $C_{11}(t)$ and $C_{12}(t)$. For this purpose, we apply complex conjugation to the type I correlation function given in (6.41). Prior to this we can simplify computations using the generalized form $\bar{q}\Gamma_i q'(\mathbf{x},t)$ for the operator's components. With $q, q' \in \{b,u,d\}$ and $\Gamma_i \in \{\Gamma_1, \Gamma_2, \Gamma_1', \Gamma_2'\}$ all appearing mesonic structures of correlation matrix elements can be constructed. For the diquark-antidiquark operator, the generalization is analogous. Applying complex conjugation to this expression using (6.45) and (6.48), we find:

$$\begin{aligned}\Big[\bar{q}\Gamma_i q'(\mathbf{x},t)\Big]^\dagger &= \Big[\bar{q}(\mathbf{x},t)\Gamma_i q'(\mathbf{x},t)\Big]^\dagger = \Big[q'(\mathbf{x},t)\Big]^\dagger \Gamma_i^\dagger \gamma_0 \Big[q^\dagger(\mathbf{x},t)\Big]^\dagger \\ &= q'^\dagger(\mathbf{x},-t)\gamma_0\Gamma_i^\dagger q(\mathbf{x},-t) = \bar{q'}(\mathbf{x},-t)\Gamma_i^\dagger q(\mathbf{x},-t) \quad = \bar{q'}\Gamma_i^\dagger q(\mathbf{x},-t)\end{aligned} \tag{6.49}$$

Now we use (6.49) to determine the complex conjugation for the type I correlation function $C_{ij}(t)$. Note that in (6.41) we have fixed the source position to $\mathbf{z}$ and thus omitted the sums over the source locations due to the use of point sources. However, now we consider the most general form of the correlation function. Therefore we introduce an additional spatial coordinate $\mathbf{u}$ and sum over all spatial positions. The complex conjugated correlation function $C_{ij}^*(t)$ is given by:

$$\begin{aligned} & C_{ij}^*(t) = C_{ij}^\dagger(t) \\ = & \sum_{\mathbf{x},\mathbf{y},\mathbf{z},\mathbf{u}} \Big[\Big[\bar{b}\Gamma_1 d(\mathbf{x},t)\,\bar{b}\Gamma_2 u(\mathbf{y},t) - \bar{b}\Gamma_1 u(\mathbf{x},t)\,\bar{b}\Gamma_2 d(\mathbf{y},t)\Big] \\ & \quad \times \Big[\bar{d}\Gamma_1' b(\mathbf{z},0)\,\bar{u}\Gamma_2' b(\mathbf{u},0) - \bar{u}\Gamma_1' b(\mathbf{z},0)\,\bar{d}\Gamma_2' b(\mathbf{u},0)\Big]\Big]^\dagger \end{aligned} \tag{6.50}$$

$$\begin{aligned} = & \sum_{\mathbf{x},\mathbf{y},\mathbf{z},\mathbf{u}} \Big[\bar{b}\Gamma_2'^\dagger u(\mathbf{u},0)\,\bar{b}\Gamma_1'^\dagger d(\mathbf{z},0) - \bar{b}\Gamma_2'^\dagger d(\mathbf{u},0)\,\bar{b}\Gamma_1'^\dagger u(\mathbf{z},0)\Big] \\ & \quad \times \Big[\bar{u}\Gamma_2^\dagger b(\mathbf{y},-t)\,\bar{d}\Gamma_1^\dagger b(\mathbf{x},-t) - \bar{d}\Gamma_2^\dagger b(\mathbf{y},-t)\,\bar{u}\Gamma_1^\dagger b(\mathbf{x},-t)\Big] \end{aligned} \tag{6.51}$$

Note that $\{\Gamma_i, \gamma_0\} = \{\Gamma_i', \gamma_0\} = 0$.
We can now shift the time argument by $+\,t$ due to time translation symmetry and rename the spatial arguments $\mathbf{x} \leftrightarrow \mathbf{z}$ and $\mathbf{y} \leftrightarrow \mathbf{u}$ to get:

$$\begin{aligned} = & \sum_{\mathbf{x},\mathbf{y},\mathbf{z},\mathbf{u}} \Big[\bar{b}\Gamma_1'^\dagger d(\mathbf{x},t)\,\bar{b}\Gamma_2'^\dagger u(\mathbf{y},t) - \bar{b}\Gamma_1'^\dagger u(\mathbf{x},t)\,\bar{b}\Gamma_2'^\dagger d(\mathbf{y},t)\Big] \\ & \quad \times \Big[\bar{d}\Gamma_1^\dagger b(\mathbf{z},0)\,\bar{u}\Gamma_2^\dagger b(\mathbf{u},0) - \bar{u}\Gamma_1^\dagger b(\mathbf{z},0)\,\bar{d}\Gamma_2^\dagger b(\mathbf{u},0)\Big] \end{aligned} \tag{6.52}$$

While the generic form of the correlation function is identical to the undaggered version, we have to consider the Γ's for a final statement about the behaviour under complex conjugation. For $C_{11}(t)$ (where $\mathbf{y} = \mathbf{x}$ and $\mathbf{u} = \mathbf{z}$ is valid) we can insert $\Gamma_1 = -\Gamma_1' = \gamma_5$ and $\Gamma_2 = -\Gamma_2' = \gamma_j$ and obtain:

$$\begin{aligned} C_{11}^*(t) = & \sum_{\mathbf{x},\mathbf{y},\mathbf{z},\mathbf{u}} \Big[\bar{b}\gamma_5 d(\mathbf{x},t)\,\bar{b}\gamma_j u(\mathbf{y},t) - \bar{b}\gamma_5 u(\mathbf{x},t)\,\bar{b}\gamma_j d(\mathbf{y},t)\Big] \\ & \quad \times \Big[\bar{d}\gamma_5 b(\mathbf{z},0)\,\bar{u}\gamma_j b(\mathbf{u},0) - \bar{u}\gamma_5 b(\mathbf{z},0)\,\bar{d}\gamma_j b(\mathbf{u},0)\Big] \end{aligned} \tag{6.53}$$

This is identical to $C_{11}(t)$, so $C_{11}^*(t) = C_{11}(t)$ is proven.

For $C_{12}(t)$ we insert $\Gamma_1 = \gamma_5$, $\Gamma_2 = \gamma_i$ and $\epsilon_{ijk}\,(\Gamma'_1 = -\gamma_j, \Gamma'_2 = -\gamma_k)$ and obtain:

$$\begin{aligned} C^*_{12}(t) = \epsilon_{ijk} \sum_{\mathbf{x},\mathbf{y},\mathbf{z},\mathbf{u}} &\Big[\bar{b}\gamma_j d(\mathbf{x},t)\,\bar{b}\gamma_k u(\mathbf{y},t) - \bar{b}\gamma_j u(\mathbf{x},t)\,\bar{b}\gamma_k d(\mathbf{y},t)\Big] \\ &\times \Big[\bar{d}\gamma_5 b(\mathbf{z},0)\,\bar{u}\gamma_i b(\mathbf{u},0) - \bar{u}\gamma_5 b(\mathbf{z},0)\,\bar{d}\gamma_i b(\mathbf{u},0)\Big] \end{aligned} \tag{6.54}$$

This is identical to $C_{21}(t)$ with $\epsilon_{ijk}\,(\Gamma_1 = \gamma_j, \Gamma_2 = \gamma_k)$, $\Gamma'_1 = -\gamma_5$, $\Gamma'_2 = -\gamma_i$. So we find $C^*_{12}(t) = C_{21}(t)$.

We leave it to the readers to repeat this calculation for all other elements and to convince themselves of the explicit hermiticity of the correlation matrix.

Time Reversal

In this paragraph, we investigate the behaviour of the correlation matrix elements with respect to time reversal. We expect the correlation functions to be symmetric or anti-symmetric, so $\mathcal{T}\,[C_{jk}(t)] = \pm C_{jk}(-t)$. If we know the specific relation, we can use this to improve our statistics: The correlation function will be computed for negative as well as positive times. Using the T-symmetry properties, we can average these two values to increase the quality of the data.
The time reversal operator $\mathcal{T}$ is expressed by gamma-matrices as:

$$\begin{aligned} \Psi(t) &\xrightarrow{\mathcal{T}} \gamma_5\gamma_0\Psi(-t) \\ \overline{\Psi}(t) &\xrightarrow{\mathcal{T}} \overline{\Psi}(-t)\gamma_0\gamma_5 \end{aligned} \tag{6.55}$$

The correlation functions considered in this work can be constructed using only six different structures:

- $\bar{q}(t)\gamma_5 q'(t)$
- $\bar{q}(t)\gamma_j q'(t)$
- $\bar{q}(t)\gamma_j\mathcal{C}\bar{q'}(t)^T$
- $q(t)^T\gamma_0\,(\gamma_j\mathcal{C})^\dagger\,\gamma_0 q'(t)$
- $q(t)^T\mathcal{C}\gamma_5 q'(t)$
- $\bar{q}(t)\mathcal{C}\gamma_5\bar{q'}(t)^T$

with $q, q' \in \{b, u, d\}$. Note that we are omitting the spatial arguments in this paragraph because we are only focusing on the temporal dependency.

We will investigate the behaviour of these six structures under T-symmetry and combine them to extract the time reversal sign for each correlation matrix element. We chose this approach in order to simplify the derivation of time reversal significantly.

Computing the time reversal for these structures, we find:

$$\begin{aligned} \mathcal{T}\,[\bar{q}(t)\gamma_5 q'(t)] =& \bar{q}(-t)\gamma_0\gamma_5\gamma_5\gamma_5\gamma_0 q'(-t) = +\bar{q}(-t)\gamma_0\gamma_5\gamma_0 q'(-t) \\ =& -\bar{q}(-t)\gamma_5\gamma_0\gamma_0 q'(-t) = -\bar{q}(-t)\gamma_5 q'(-t) \end{aligned} \tag{6.56}$$

$$\begin{aligned}\mathcal{T}\left[\bar{q}(t)\gamma_j q'(t)\right] =& \bar{q}(-t)\gamma_0\gamma_5\gamma_j\gamma_5\gamma_0 q'(-t) = \bar{q}(-t)\gamma_j\gamma_0\gamma_5\gamma_5\gamma_0 q'(-t)\\ =& +\bar{q}(-t)\gamma_j q'(-t)\end{aligned} \tag{6.57}$$

$$\begin{aligned}\mathcal{T}\left[\bar{q}(t)\gamma_j\mathcal{C}\bar{q'}(t)^T\right] =& \bar{q}(-t)\gamma_0\gamma_5\gamma_j\mathcal{C}\gamma_5\gamma_0\bar{q'}(-t)^T = -\bar{q}(-t)\gamma_j\mathcal{C}\gamma_0\gamma_5\gamma_5\gamma_0\bar{q'}(-t)^T\\ =& -\bar{q}(-t)\gamma_j\mathcal{C}\bar{q'}(-t)^T\end{aligned} \tag{6.58}$$

$$\begin{aligned}\mathcal{T}\left[q(t)^T\gamma_0\left(\gamma_j\mathcal{C}\right)^\dagger\gamma_0 q'(t)\right] =& q(-t)^T\gamma_0\gamma_5\gamma_0\left(\gamma_j\mathcal{C}\right)^\dagger\gamma_0\gamma_5\gamma_0 q'(-t)\\ =& q(-t)^T\gamma_0\gamma_5\left(\gamma_j\mathcal{C}\right)^\dagger\gamma_5\gamma_0 q'(-t) = -q(-t)^T\gamma_0\left(\gamma_j\mathcal{C}\right)^\dagger\gamma_5\gamma_5\gamma_0 q'(-t)\\ =& -q(-t)^T\gamma_0\left(\gamma_j\mathcal{C}\right)^\dagger\gamma_0 b(-t)\end{aligned} \tag{6.59}$$

$$\begin{aligned}\mathcal{T}\left[q(t)^T\mathcal{C}\gamma_5 q'(t)\right] =& q(-t)^T\gamma_0\gamma_5\mathcal{C}\gamma_5\gamma_5\gamma_0 q'(-t) = q(-t)^T\mathcal{C}\gamma_5\gamma_0\gamma_0 q'(-t)\\ =& +q(-t)^T\mathcal{C}\gamma_5 q'(-t)\end{aligned} \tag{6.60}$$

$$\mathcal{T}\left[\bar{q}(t)\mathcal{C}\gamma_5\bar{q'}(t)^T\right] = +\bar{q}(-t)\mathcal{C}\gamma_5\bar{q'}(-t)^T \tag{6.61}$$

We obviously get the T-symmetry for a specific correlation matrix element by inserting the appropriated combination of the structures computed in (6.56) to (6.61). For instance, $C_{11}(t)$ is expressed by:

$$\begin{aligned}\mathcal{T}\left[C_{11}(t)\right] = \mathcal{T}\Big\{&\left[\bar{b}\gamma_5 d(t)\,\bar{b}\gamma_j u(t) - \bar{b}\gamma_5 u(t)\,\bar{b}\gamma_j d(t)\right]\\ &\times\ \left[\bar{d}\gamma_5 b(0)\,\bar{u}\gamma_j b(0) - \bar{u}\gamma_5 b(0)\,\bar{d}\gamma_j b(0)\right]\Big\} = +C_{11}(-t)\end{aligned} \tag{6.62}$$

Calculations for all other matrix elements can be found in Appendix D.2, the results are summarized in Table 6.2.

Correlation function	$C_{11}(t)$	$C_{12}(t)$	$C_{13}(t)$	$C_{21}(t)$	$C_{22}(t)$	$C_{23}(t)$	$C_{31}(t)$	$C_{32}(t)$
$\mathcal{T}$ sign	+	−	+	−	+	−	+	−

Correlation function	$C_{33}(t)$	$C_{41}(t)$	$C_{42}(t)$	$C_{43}(t)$	$C_{51}(t)$	$C_{52}(t)$	$C_{53}(t)$
$\mathcal{T}$ sign	+	+	−	+	−	+	−

Table 6.2: Transformation behaviour for the correlation matrix elements under time reversal $\mathcal{T}$.

Improving Numerical Data

With regard to numerical simulations, we can utilise the proven symmetries to increase the quality of the data.

Time symmetry
Knowing the behaviour under T-symmetry for an arbitrary $C_{ij}(t)$ with $\mathcal{T}\left[C_{ij}(t)\right] = \pm C_{ij}(-t)$, we can improve the statistics by averaging the value of the correlation function for each time slice and configuration:

$$C_{ij}^{\mathrm{av}}(t) = \frac{1}{2}\left[C_{ij}(t) \pm C_{ij}(-t)\right] \tag{6.63}$$

hermiticity
Furthermore, the hermiticity of the correlation matrix provides additional symmetries, which should be used to enhance the quality of the data.
We can set the imaginary part of all diagonal elements to zero, since we have verified that $C_{ii}(t) \in \mathbb{R}$. All discrepancies from zero are caused by numerical fluctuations, so the raw data are improved by neglecting these contributions:

$$\mathrm{Im}\left[C_{ii}(t)\right] = 0 \tag{6.64}$$

For the off-diagonal elements, applying the relation $C_{ij}(t) = C_{ji}^{*}(t)$ can be used to average the associated matrix elements:

$$\mathrm{Re}\left[C_{ij}(t)\right] = \frac{1}{2}\left[\mathrm{Re}\left[C_{ij}(t)\right] + \mathrm{Re}\left[C_{ji}(t)\right]\right] = \mathrm{Re}\left[C_{ji}(t)\right] \tag{6.65}$$

$$\mathrm{Im}\left[C_{ij}(t)\right] = \frac{1}{2}\left[\mathrm{Im}\left[C_{ij}(t)\right] - \mathrm{Im}\left[C_{ji}(t)\right]\right] = -\mathrm{Im}\left[C_{ji}(t)\right] \tag{6.66}$$

This also ensures that the correlation matrix is hermitian which might have been violated by numerical inaccuracies before.

6.3 Analysis of the $\bar{b}\bar{b}ud$ System

Investigating the $\bar{b}\bar{b}ud$ four-quark system, we aim to find a bound state in the $I(J^P) = 0(1^+)$ channel with its associated binding energy $E_{\bar{b}\bar{b}ud}$. Thus we determine the energy spectrum of this system. Comparing the lowest energy level with the added binding energy of a B and a B^* meson, we get evidence about a possibly stable tetraquark state. In other words, if $E_{\bar{b}\bar{b}ud}$ is below the BB^* threshold, i.e. $E_{\bar{b}\bar{b}ud} < E_B + E_{B^*}$, a bound state is depicted.

Therefore, we will compute the correlation matrix described in Sec. 6.2.2 as well as the correlation functions for the B and the B^* meson. These correlation functions are given by:

$$C_B(t) = \sum_{\mathbf{x}} \left\langle \bar{b}\Gamma_1 u(x,t)\bar{u}\Gamma_1' b(y,0) \right\rangle \tag{6.67}$$

with $\Gamma_1 = \gamma_5$ and $\Gamma_1' = -\gamma_5$.

$$C_{B^*}(t) = \sum_{\mathbf{x}} \left\langle \bar{b}\Gamma_2 u(x,t)\bar{u}\Gamma_2' b(y,0) \right\rangle \tag{6.68}$$

with $\Gamma_2 = \gamma_j$ and $\Gamma_2' = -\gamma_j$.

In the next step, we are eager to extract the energy eigenvalues from the correlation functions. In the following, we present two possible approaches to isolate the ground state energy as well as contributions from higher excitations. Both are starting with the analytical expression of the correlation function from (6.33):

$$C_{ij}(t) = \sum_n \langle \Omega | \mathcal{O}_i(0) | n \rangle \langle n | \mathcal{O}_j^\dagger(0) | \Omega \rangle \mathrm{e}^{-E_n t} \tag{6.69}$$

with $t = t_{\text{sink}} - t_{\text{source}}$.

First of all, we can use a *correlated least-χ^2-fit* to extract the amplitudes and exponentials from (6.69) while including terms up to a chosen order of n. This enables us to treat all possible non-quadratic submatrices of Table 6.1 as well as the whole 5×3 matrix. More information about least-χ^2-fits and the routine used can be found in [28, 43].

As a second analysis tool, we use the *generalized eigenvalue problem (GEP)* to calculate the effective masses. In this thesis we will primarily apply this method.
To illustrate the proceeding, we will start with a single correlation function. Considering only the first order from (6.69), the correlation functions looks like:

$$C(t) = \langle \Omega | \mathcal{O}(0) | 0 \rangle \langle 0 | \mathcal{O}^\dagger(0) | \Omega \rangle \mathrm{e}^{-E_0 t} \tag{6.70}$$

We can easily extract the so-called effective mass from (6.70) using the fraction of the correlation function for two successive time slices via:

$$aE_{\text{eff}}(t) = \ln\left(\frac{C(t)}{C(t+a)}\right) \tag{6.71}$$

For large times t, $aE_{\text{eff}}(t)$ becomes a constant in time, so the ground state energy is determined by $aE_0 = aE_{\text{eff}}(t)|_{t\to\infty}$.

Working instead with a $N \times N$ correlation matrix, we have to solve the GEP

$$C(t)\vec{v}_n(t) = \lambda_n(t)C(t_0)\vec{v}_n(t), \qquad \text{with } 1 \leq n \leq N \tag{6.72}$$

where $\vec{v}_n(t)$ are the eigenvectors of the matrix and $\lambda_n(t)$ are the eigenvalues which decay exponentially, i.e. $\lambda_n(t) \propto \mathrm{e}^{-E_n t}$. The N effective masses are calculated by:

$$aE^n_{\text{eff}}(t) = \ln\left(\frac{\lambda_n(t)}{\lambda_n(t+a)}\right) \tag{6.73}$$

For further information and a detailed explanation of the GEP, we refer to [39, 40]. We will use the GEP to evaluate the upper left 3×3 matrix from Table 6.1, omitting the scattering operators. Moreover, we will also investigate all three 2×2 submatrices as well as the three diagonal elements C_{ii}.

A recent study on the $\bar{b}\bar{b}ud$ system in the static approximation including heavy spin effects (cf. [20]) gave evidence about the composition of a $\bar{b}\bar{b}ud$ bound state: The BB^* as well as the B^*B^* contribute in the same way. Therefore, we expect a lower ground state energy for the combined 2×2 correlation matrix consisting of BB^* and B^*B^* compared to the single correlation functions. Additionally, we include the diquark-antidiquark operator which provides a third possible operator structure. We hope to discover a deeper binding by considering also the diquark-antidiquark component and get new evidence about the tetraquark composition. We also aim to consider the scattering operators and study their influence on the effective energy.

Moreover, we perform calculations for two different heavy quark masses m_Q. Naturally, we start with the physical bottom quark mass $m_Q = m_b$ and conclude with an unphysical heavy bottom quark mass of $m_Q = 5m_b$. We are using ensemble C54 from Table 3.1 to realise this investigation. Previous studies ([15, 24]) forecast an increasing binding energy while increasing the bottom quark mass. For this reason, we have decided to investigate an unphysical heavy bottom quark mass: We expect a much stronger binding, so it should be easier to identify the ground state below threshold and consequently the tetraquark state. For the static approximation, in [21] it has been shown that increasing the bottom mass actually increases the binding energy.

Finally, we repeat the calculations for physical bottom mass $m_Q = m_b$ using the all-mode-averaging ensembles C005, C01, F004, F006, and C00078 from Table 3.1. These configurations enable us to extrapolate our results to the physical pion mass so that we receive a physically valuable result.

6.4 Evaluation of Numerical Results

This section is structured as follows: We first discuss the influence of the different operator structures for ensemble C005. In principle, this analysis will be done using the GEP. Nevertheless, we will finally also include the operators $\mathcal{O}_{B(0)B^*(0)}$ and $\mathcal{O}_{B^*(0)B^*(0)}$ which are only accessible using exponential fits and investigate their significance for mass extractions.
In the second paragraph, we present our results for the unphysical heavy bottom quark mass $m_Q = 5m_b$ and compare it to $m_Q = m_b$.
We conclude with an extrapolation to the physical pion mass in order to extract the ground state energy $E_{\bar{b}\bar{b}ud}$ at the physical point using all available AMA ensembles listed in Table 3.1.

6.4.1 Results for Operator Structures

In this section, we are focusing only on the ensemble C005 listed in 3.1. We present the numerical results, especially the effective masses computed for these gauge configurations and discuss possible qualitative statements about the operator structures used.

Note that the computed masses do not coincide directly with the physical particle mass but are shifted due to the use of NRQCD. For this reason, we have to set the scale to extract physical values. In Chapter 4, we have presented how to set the scale exemplarily for the two bottomonium states η_B and Υ. We showed that the energy difference is unaffected in NRQCD in contrast to the absolute value of the mass. Having computed the mass in lattice units for a particle with known physical mass and determining the energy difference to the investigated tetraquark system, one can consequently extract the physical mass.
For our purpose, the appropriated particles are the B and B^* mesons with the physical masses $m_{B,phys} = 5279.62(15)$ MeV and $m_{B^*,phys} = 5324.65(25)$ MeV (cf. [1]).
These two B mesons are the decay products of a $\bar{b}\bar{b}ud$ state and therefore determine the energy threshold for the tetraquark. Since we are interested in revealing bound states, it is sufficient to compute the relative mass difference to this energy threshold.
Hence, all results in physical units presented in this section are differences to the BB^* threshold discussed above.

BB^* Threshold Energy

Initially, we consider the effective mass for the B and B^* meson. This enables us to determine the BB^* threshold which is necessary to distinguish between a bound or scattering tetraquark state. The energy is extracted by inserting (6.67) and (6.68) respectively into (6.71) and fitting a plateau to the associated effective mass. The corresponding graphics can be found in Figure 6.1.

Consequently, the BB^* threshold can easily be determined by extracting the data from the fits and adding $aE_B + aE_{B^*}$ (cf. Table 6.3).

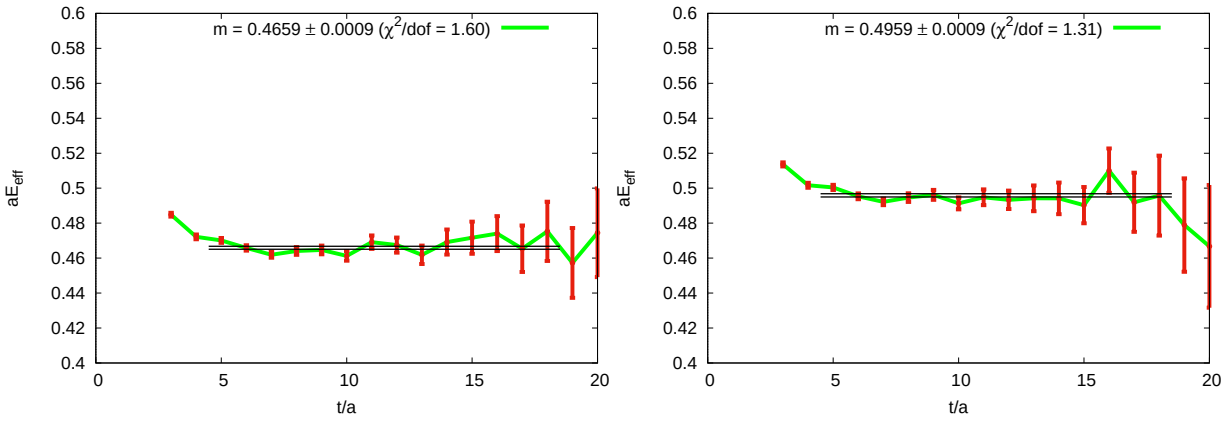

Figure 6.1: The effective mass $aE_{\text{eff}}(t)$ for the B and the B^* meson in units of the lattice spacing a as a function of the temporal lattice extent t/a for $m_Q = m_b$. Constant fit for $5 \leq t \leq 18$. **(left):** B meson. **(right):** B^* meson.

aE_B	0.4659(9)
aE_{B^*}	0.4959(9)
$aE_B + aE_{B^*}$	0.9618(18)

Table 6.3: Threshold energy $aE_B + aE_{B^*}$ in lattice units for $m_Q = m_b$.

Mesonic Operator Basis

Discussing the $\bar{b}\bar{b}ud$ system, in the first instance, we are including only the mesonic operator structures presented in Sec. 6.1.3 while we are adopting the same labelling as introduced there. Thus, we consider only the 3×3 submatrix of the correlation matrix depicted in Table 6.1. Since this matrix is quadratic, we are able to evaluate it using the GEP and to extract the effective masses.

We start with the three diagonal elements $C_{ii}(t)$ of the correlation matrix. Each is treated independently of the others, while the associated effective masses are labelled by $aE_{\text{eff},i}(t)$ with $i \in \{BB^*, B^*B^*, Dd\}$. The effective mass plots are illustrated in Fig. 6.2. Besides, the horizontal black line identifies the BB^* threshold energy given in Table 6.3.

Considering the extracted ground state energy $aE_{\text{eff},BB^*}(t)$ in Fig. 6.2 (top left), the effective mass seems to be at the same level or slightly below threshold. However, the statistical uncertainties do not allow any well-established statements. Next, regarding $aE_{\text{eff},B^*B^*}(t)$ in Fig. 6.2 (top right), its asymptotic value is located clearly above threshold. Consequently, both operators do not seem to generate a bound state at all. This coincides with our expectations, since a bound $\bar{b}\bar{b}ud$ system is assumed to be a composition of both structures with approximately the same weight.
Examining the third single correlation function built of the diquark-antidiquark operator seems to be a promising approach to discover a bound four-quark system. Looking at the associated graphic in Fig. 6.2 (bottom), $aE_{\text{eff},Dd}(t)$ appears to sink below threshold. So, there is a first indication for a bound state in the $\bar{b}\bar{b}ud$ system. We have to confirm this result including several correlation matrix elements simultaneously in our analysis. Nevertheless, at this juncture the diquark-antidiquark operator seems to be important to create a bound state.

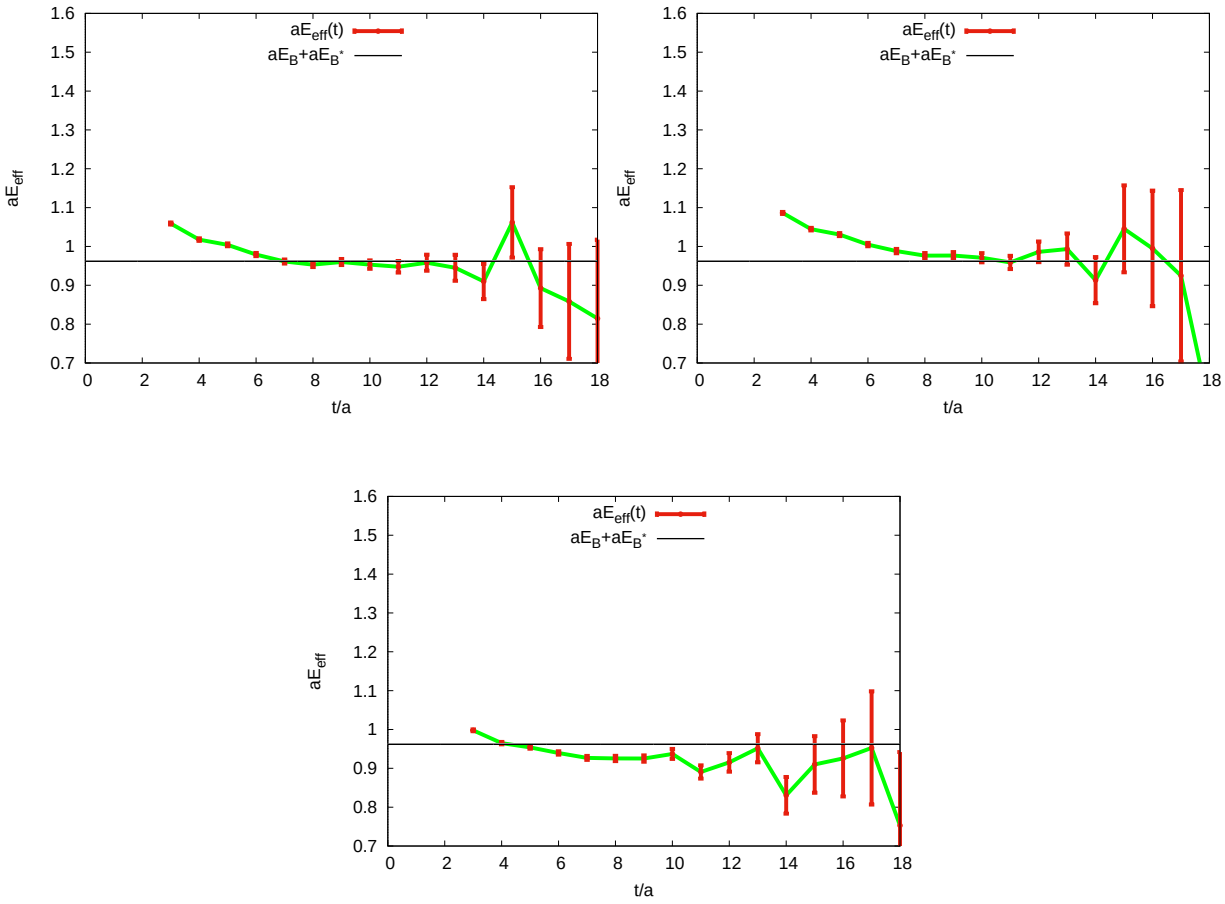

Figure 6.2: The effective masses $aE_{\text{eff}}(t)$ for the diagonal elements $\mathcal{C}_{ii}(t)$ of the correlation matrix 6.1. **(top left):** Effective mass for $\mathcal{O}_{[BB^*](0)}$.**(top right):** Effective mass for $\mathcal{O}_{[B^*B^*](0)}$.**(bottom):** Effective mass for $\mathcal{O}_{[Dd](0)}$.

We continue our investigation including two operators at the same time, i.e. we evaluate the GEP for the three 2×2 submatrices while we lable the associated effective masses $aE^{(n)}_{\text{eff},i}(t)$ with $i \in \{BB^* - B^*B^*, BB^* - Dd, B^*B^* - Dd\}$. The effective mass plots are illustrated in Fig. 6.3.

First, we take a close look at Fig. 6.3 (top left) which illustrates the operator set $\mathcal{O}_{[BB^*](0)}$, $\mathcal{O}_{[B^*B^*](0)}$. As expected, we recognize that the ground state energy is lowered compared to Fig. 6.2 (top left) and Fig. 6.2 (top right) and seems to be clearly below threshold. Therefore, a combination of a mesonic BB^* system with a mesonic B^*B^* system is a promising structure for a bound tetraquark state. To continue, we consider the diquark-antidiquark structure $\mathcal{O}_{[Dd](0)}$ combined with either $\mathcal{O}_{[BB^*](0)}$ (cf. Fig. 6.3 (top right)) or $\mathcal{O}_{[B^*B^*](0)}$ (cf. Fig. 6.3 (bottom)). For both cases, we recognize that the ground state is located clearly below the BB^* threshold. Comparing these two plots to Fig. 6.2 (bottom), the lowest energy level does not seem to change significantly. This supports the importance of the diquark-antidiquark operator $\mathcal{O}_{[Dd](0)}$ for the formation of a bound state.

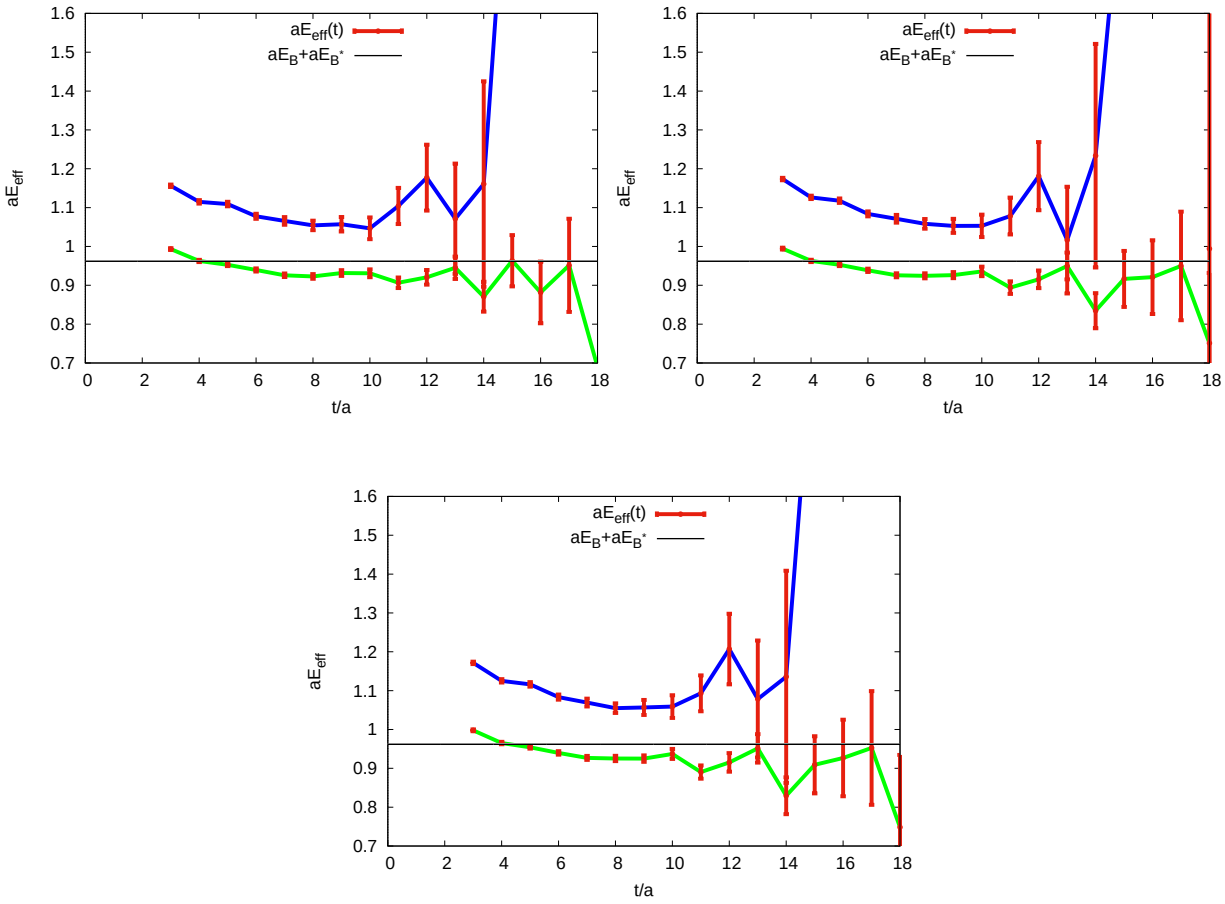

Figure 6.3: The effective masses $aE_{\text{eff}}(t)$ for the 2×2 submatrices of the correlation matrix 6.1. **(top left):** Effective masses for $\mathcal{O}_{[BB^*](0)}$ and $\mathcal{O}_{[B^*B^*](0)}$. **(top right):** Effective masses for $\mathcal{O}_{[BB^*](0)}$ and $\mathcal{O}_{[Dd](0)}$. **(bottom):** Effective masses for $\mathcal{O}_{[B^*B^*](0)}$ and $\mathcal{O}_{[Dd](0)}$.

We conclude the GEP analysis taking all three operators $\mathcal{O}_{[BB^*](0)}$, $\mathcal{O}_{[B^*B^*](0)}$ and $\mathcal{O}_{[Dd](0)}$ into account simultaneously, so we examine the whole 3×3 matrix. The associated effective mass plot can be found in Fig. 6.4. We can clearly identify the ground state below threshold as well as two excited states above threshold. However, we remark that a plateau fit for the second excited state does not yield reliable results due to the rapidly growing error bars.

In conclusion, in our GEP analysis we find clear evidence for a bound $\bar{b}\bar{b}ud$ tetraquark state in the $I(J^P) = 0(1^+)$ channel.

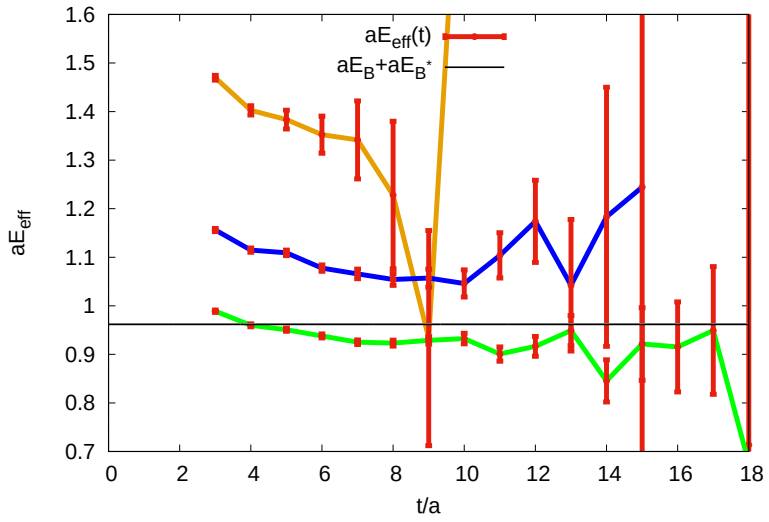

Figure 6.4: The effective mass $aE_{\text{eff}}(t)$ for the 3×3 correlation matrix 6.1 including $\mathcal{O}_{[BB^*](0)}$, $\mathcal{O}_{[B^*B^*](0)}$ and $\mathcal{O}_{[Dd](0)}$.

In the next step we perform a detailed statistical and systematic error analysis applying the methods discussed in Chapter 3 with $T_{\text{min}} = 6$ and $T_{\text{max}} = 18$. The associated total error is:

$$\sigma_{\text{total}} = \sqrt{\sigma_{\text{stat}}^2 + \sigma_{\text{syst}}^2} \tag{6.74}$$

We present the resulting energy levels relative to the BB^* threshold in Table 6.4 while we are using the abbreviations

$$\mathcal{O}_1 \equiv \mathcal{O}_{[BB^*](0)}, \qquad \mathcal{O}_2 \equiv \mathcal{O}_{[B^*B^*](0)}, \qquad \mathcal{O}_3 \equiv \mathcal{O}_{[Dd](0)} \tag{6.75}$$

to increase the readability of the table.

operator basis	ΔE_0 [MeV]	ΔE_1 [MeV]
$(\mathcal{O}_1) \times (\mathcal{O}_1)$	$-8.9\,^{+22.3}_{-21.5}$	
$(\mathcal{O}_2) \times (\mathcal{O}_2)$	$26.7\,^{+27.5}_{-22.2}$	
$(\mathcal{O}_3) \times (\mathcal{O}_3)$	$-65.5\,^{+26.8}_{-46.3}$	
$(\mathcal{O}_1, \mathcal{O}_2) \times (\mathcal{O}_1, \mathcal{O}_2)$	$-61.3\,^{+21.8}_{-29.0}$	$184.6\,^{+116.5}_{-38.4}$
$(\mathcal{O}_1, \mathcal{O}_3) \times (\mathcal{O}_1, \mathcal{O}_3)$	$-64.3\,^{+22.9}_{-43.3}$	$186.1\,^{+68.9}_{-25.9}$
$(\mathcal{O}_2, \mathcal{O}_3) \times (\mathcal{O}_2, \mathcal{O}_3)$	$-65.7\,^{+26.9}_{-46.7}$	$189.6\,^{+104.9}_{-40.3}$
$(\mathcal{O}_1, \mathcal{O}_2, \mathcal{O}_3) \times (\mathcal{O}_1, \mathcal{O}_2, \mathcal{O}_3)$	$-62.8\,^{+21.5}_{-36.3}$	$183.4\,^{+111.7}_{-38.7}$

Table 6.4: Energy differences relative to $E_B + E_{B^*}$ in MeV for the listed operator bases. Results are computed using the GEP and extracting the effective masses via plateau fits in the region $T_{\text{min}} = 6$ and $T_{\text{max}} = 18$. The presented uncertainties are the total errors (6.74).

We recognize that the lowest energy level yields a binding energy of $E_{\bar{b}\bar{b}ud} \equiv \Delta E_0 \simeq -60$ MeV and is within the error bars located below threshold. This energy level is already reached including only the diquark-antidiquark operator $\mathcal{O}_{[Dd](0)}$. Moreover, it is detected for all three 2×2 submatrices as well as for the complete 3×3 matrix. A possible interpretation might be that the diquark-antidiquark structure has good overlap with the ground state. Thus, if $\mathcal{O}_{[Dd](0)}$ is included in the operator basis, we assume that the ground state is matched. Additionally, the combination of $\mathcal{O}_{[BB^*](0)}$ and $\mathcal{O}_{[B^*B^*](0)}$ also yields the lowest energy state, so we also suppose good overlap using these two operators. However, each operator separately does not possess adequate overlap with the ground state.

So finally, taking the detailed error analysis into account, there is clear evidence for a bound state in the $\bar{b}\bar{b}ud$ tetraquark system.

Scattering + Mesonic Operator Basis

Referring to the correlation matrix in Table 6.1, we did not consider the matrix elements including scattering operators at the sink, since we cannot evaluate the 5×3 matrix using the GEP. Nevertheless we would like to investigate the impact of the scattering operators $\mathcal{O}_{B(0)B^*(0)}$ and $\mathcal{O}_{B^*(0)B^*(0)}$ on the extracted masses. For this purpose, we proceed as described in Sec. 6.3: The computed data are directly fitted to the analytic expression of the correlation functions. This is realised using the *QMBF* tool provided by Stefan Meinel (cf. [43]).

We apply a correlated fit of our data to (6.69) using the first two energy states, i.e. $n = 1$. Our fit results can be found in Table 6.5 while the energies are again given relative to the BB^* threshold. Note that only statistical errors are included at this juncture. We are adapting the same conventions as presented in 6.75, extended to:

$$\mathcal{O}_4 \equiv \mathcal{O}_{B(0)B^*(0)}, \qquad \mathcal{O}_5 \equiv \mathcal{O}_{B^*(0)B^*(0)} \tag{6.76}$$

In addition to the results for the complete 5×3 matrix, we have also performed fits for the 3×3 matrix in order to improve comparability with the results of the GEP.

operator basis	Fit range	χ^2/d.o.f.	ΔE_0 [MeV]	ΔE_1 [MeV]
$(\mathcal{O}_1, \mathcal{O}_2, \mathcal{O}_3) \times (\mathcal{O}_1, \mathcal{O}_2, \mathcal{O}_3)$	$11 \ldots 24$	1.75	$-48.9(19.6)$	36.2(33.4)
$(\mathcal{O}_1, \mathcal{O}_2, \mathcal{O}_3) \times (\mathcal{O}_1, \mathcal{O}_2, \mathcal{O}_3)$	$14 \ldots 24$	1.44	$-97.1(53.4)$	125.3(133.9)
$(\mathcal{O}_1, \mathcal{O}_2, \mathcal{O}_3, \mathcal{O}_4, \mathcal{O}_5) \times (\mathcal{O}_1, \mathcal{O}_2, \mathcal{O}_3)$	$11 \ldots 24$	1.25	$-101.0(16.2)$	$-8.6(26.6)$

Table 6.5: Energy differences relative to $E_B + E_{B^*}$ in MeV for the listed operator bases. Results are computed using exponential fitting. The presented uncertainties are the statistical errors.

If we first consider the 5×3 matrix, we notice that both energy values are considerably lower than the results generated by the GEP. At first glance, this is irritating since we are adding scattering operators which should not provide a stronger binding of a bound state. However, from a more general perspective the 5×3 operator basis seems to have a better

overlap with the four-quark system. In other words, including the scattering operators is more suitable to describe the whole tetraquark system. This can be explained as follows: The two additional scattering operators have a very good overlap with the first excited state. This is comprehensible, since this state is slightly above threshold, and consequently it is assumed to be a scattering state. Hence, this state is almost completely generated using the scattering operators, and its contributions to the lowest determined energy level are removed.
In contrast, if we do not include these scattering operators, the extracted ground state will have an admixture of this first excited state for small time values so the determined energy will be increased. Consequently, considering larger t regions, we should also get a significantly lower energy using the GEP. However, due to the large errors (cf. Fig. 6.2 to 6.4) it is not possible to perform fits in this region.

Certainly, we plan to support this assumption, so we consider the exponential fits for the 3×3 matrix using two different fit ranges (cf. Table 6.5). Performing the fit for the lower value $t_{\text{min}} = 11$, we extract a ground state energy of about -50 MeV which is within the errors comparable to the -60 MeV computed with the GEP. Applying $t_{\text{min}} = 14$ as lower fit boundary, we observe a drastic decline to approximately -100 MeV. This value, however, coincides well with the ground state energy extracted from the 5×3 matrix.
We assume that for $t_{\text{min}} = 14$ we get less contamination from the first excited state because the exponential is decreasing faster and so we get a purer ground state energy.

We can conclude that the results obtained from the GEP do not contradict those from exponential fitting. Nevertheless, the scattering operators increase the overlap with the four-quark system so that the effective mass plateaus are reached for smaller time values. Since we cannot include the scattering operators in the GEP, the results generated by exponential fitting seems to be more substantiated. Therefore, we state a bound tetraquark state with $E_{\bar{b}\bar{b}ud} \simeq -101.0(16.2)$. Moreover, we found the first excited state which is located at the level of threshold. Thus, this state might be a scattering state which supports our assumption that the scattering operators $\mathcal{O}_{B(0)B^*(0)}$ and $\mathcal{O}_{B^*(0)B^*(0)}$ possess good overlap with the first excitation.

Summary

In this subsection, we have investigated the $\bar{b}\bar{b}ud$ tetraquark system in the $I(J^P) = 0(1^+)$ channel for a specific ensemble in the framework of NRQCD while paying special attention to the different operator structures. Considering only mesonic creation operators, we have predicted a bound state with a binding energy of $E_{\bar{b}\bar{b}ud} \simeq -60$ MeV. We have illustrated the great importance of the diquark-antidiquark operator $\mathcal{O}_{[Dd](0)}$ for creating a bound state, and we have shown that an equal weighted combination of $\mathcal{O}_{[BB^*](0)}$ and $\mathcal{O}_{[B^*B^*](0)}$ is also a good candidate for a bound four-quark system. Furthermore, we have depicted the great significance of the scattering operators $\mathcal{O}_{B(0)B^*(0)}$ and $\mathcal{O}_{B^*(0)B^*(0)}$. They seem to have an excellent overlap with the first excited state so that the ground state can be determined with less admixtures. Including all operators we have found a bound state with $E_{\bar{b}\bar{b}ud} \simeq -100$ MeV whereas the first excited state is located at threshold level.

6.4.2 Computation for Unphysical Bottom Quark Mass $m_Q = 5m_b$

This section focuses on the unphysical heavy bottom quark mass $m_Q = 5m_b$. Even if this case cannot be found in real world physics, it is of huge conceptional interest.
Our calculations are performed using ensemble C54 presented in Table 3.1. We expect a significantly deeper bound state compared to $m_Q = m_b$. We start again with determining the B and B^* meson masses. The effective mass plots can be found in Fig. 6.5 whereas the extracted masses as well as the computed threshold energy $aE_B + aE_{B^*}$ are listed in Table 6.6.

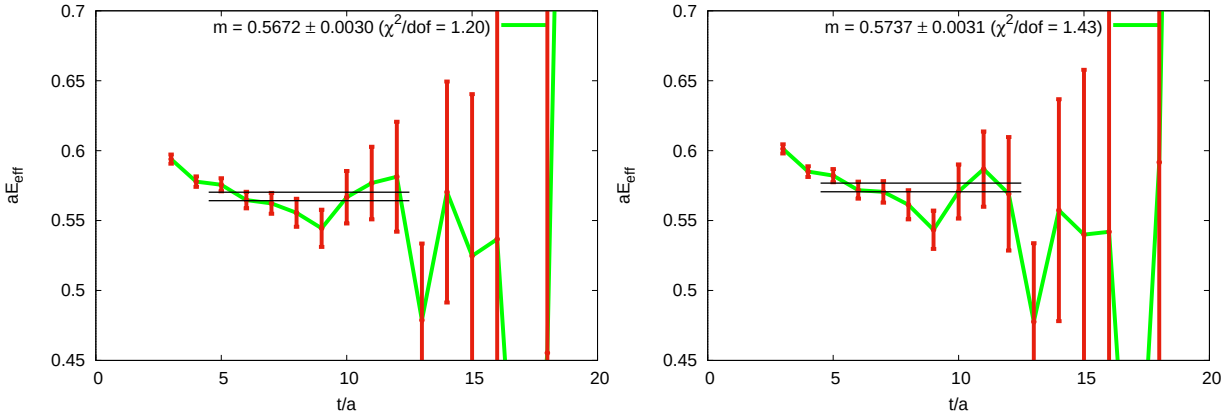

Figure 6.5: The effective mass $aE_{\text{eff}}(t)$ for the B and the B^* meson in units of the lattice spacing a as a function of the temporal lattice extent t/a for $m_Q = m_b$. Linear fit for $5 \leq t \leq 12$. **(left):** B meson for $m_Q = 5m_b$. **(right):** B^* meson for $m_Q = 5m_b$.

aE_B	0.5672(30)
aE_{B^*}	0.5737(31)
$aE_B + aE_{B^*}$	1.1409(61)

Table 6.6: Threshold energy $aE_B + aE_{B^*}$ in lattice units for $m_Q = 5m_b$.

We have repeated the GEP analysis for all available quadratic matrices and have extracted the associated effective masses. The results are presented in Table 6.7. Referring to the ground state energy, we identify an energy of $E_{\bar{b}\bar{b}ud,5m_b} \simeq -200$ MeV which is a drastically lower value compared to $m_Q = m_b$ where we found $E_{\bar{b}\bar{b}ud} \simeq -60$ MeV. We can detect the same behaviour for the first excited state which decreases from $E^{(1)}_{\bar{b}\bar{b}ud} \simeq 180$ MeV to $E^{(1)}_{\bar{b}\bar{b}ud,5m_b} \simeq 90$ MeV. It is notable that we do not create a second bound state while increasing the bottom quark mass. Nevertheless we detect a much deeper binding so consequently we can definitely speak about a bound state in this case.

Finally, in Fig. 6.6 (right) we present the effective mass plot for the complete 3×3 matrix. Note that we depict only the two lowest energy levels to keep the plot clearly arranged. One has to emphasise that the ensemble C54 provides substantially less measurements than C005, so consequently the statistical fluctuations are larger. To ensure good comparability, we repeated the calculation for the physical bottom mass $m_Q = m_b$ using ensemble C54. The effective mass plot extracted from the 3×3 matrix is illustrated in

Fig. 6.6 (left).
Comparing these two figures, we can graphically reveal the dropping energy levels. Especially the ground level is depicted to be clearly lower while the first excited state has also slightly decreased. It is also notable that the uncertainties for $m_Q = 5m_b$ grow faster and therefore no substantiated statements are possible for large t.

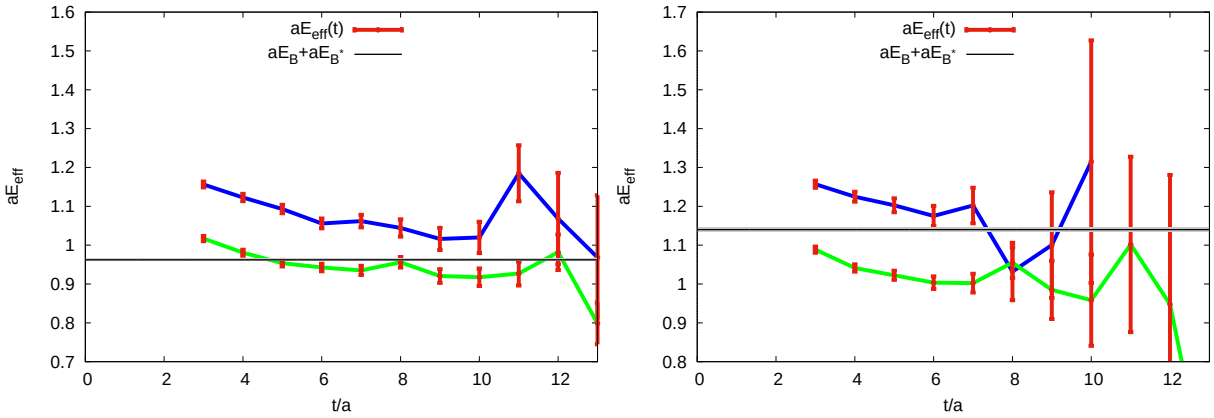

Figure 6.6: The effective mass $aE_{\text{eff}}(t)$ for the 3×3 correlation matrix 6.1 with $\mathcal{O}_{[BB^*](0)}$, $\mathcal{O}_{[B^*B^*](0)}$ and $\mathcal{O}_{[Dd](0)}$. **(left:)** for $m_Q = m_b$. **(right:)** for $m_Q = 5m_b$.

operator basis	ΔE_0 [MeV]	ΔE_1 [MeV]
$(\mathcal{O}_1) \times (\mathcal{O}_1)$	$-108.7\,^{+71.0}_{-92.7}$	
$(\mathcal{O}_2) \times (\mathcal{O}_2)$	$-99.4\,^{+71.9}_{-100.8}$	
$(\mathcal{O}_3) \times (\mathcal{O}_3)$	$-199.4\,^{+117.8}_{-48.0}$	
$(\mathcal{O}_1, \mathcal{O}_2) \times (\mathcal{O}_1, \mathcal{O}_2)$	$-200.6\,^{+75.1}_{-70.2}$	$90.0\,^{+98.4}_{-249.0}$
$(\mathcal{O}_1, \mathcal{O}_3) \times (\mathcal{O}_1, \mathcal{O}_3)$	$-199.0\,^{+109.8}_{-47.7}$	$75.4\,^{+263.0}_{-307.9}$
$(\mathcal{O}_2, \mathcal{O}_3) \times (\mathcal{O}_2, \mathcal{O}_3)$	$-198.9\,^{+111.9}_{-47.7}$	$89.4\,^{+261.5}_{-324.8}$
$(\mathcal{O}_1, \mathcal{O}_2, \mathcal{O}_3) \times (\mathcal{O}_1, \mathcal{O}_2, \mathcal{O}_3)$	$-205.1\,^{+77.6}_{-68.7}$	$90.0\,^{+98.4}_{-249.2}$

Table 6.7: Energy differences relative to $E_B + E_{B^*}$ in MeV for the listed operator bases with $m_Q = 5m_b$. Results are computed using the GEP and extracting the effective masses via plateau fits in the region $T_{\text{min}} = 3$ and $T_{\text{max}} = 12$. The presented uncertainties are the total errors (6.74).

6.4.3 Chiral Extrapolation

In the last section, we aim to extract the real physical result. Due to numerical efficiency, lattice calculations are generally performed for unphysically heavy pion masses. Four out of five available ensembles have pion masses between 303 MeV and 431 MeV while there is only one ensemble with the quite small pion mass of 139 MeV but a rather small number of available measurements and consequently low statistics (cf. Table 3.1). Therefore our results have to be extrapolated to the physical point via a chiral extrapolation.
The correlation matrix has been computed for the three lattices with coarse lattice spacing C01, C005, C00078 as well as for F004 and F006 which possess a finer lattice spacing. The effective masses are extracted from the 3×3 correlation matrices including only the mesonic operators applying the GEP. We assume that discretisation errors are negligible compared to the statistical uncertainties. Thus, we treat the fine and the coarse lattice in the same way and ignore possible effects caused by the differing lattice spacings. Moreover, we do not include any finite volume effects at this stage.

Performing the extrapolation, we fit the extracted ground state energy differences ΔE_0 as a function of the the pion mass m_π for all five ensembles to:

$$\Delta E_0(m_\pi) = \Delta E_{0,\text{phys}} + \lambda \left(m_\pi^2 - m_{\pi,\text{phys}}^2 \right) \tag{6.77}$$

Here, the physical pion mass is $m_{\pi,\text{phys}} = 135$ MeV. $\Delta E_{0,\text{phys}}$ and λ are the fit parameters while $\Delta E_{0,\text{phys}}$ denotes the binding energy at the physical point where $m_\pi = m_{\pi,\text{phys}}$.
The fit has $\chi^2/\text{d.o.f.} = 0.58$ and yields:

$$\Delta E_{0,\text{phys}} = (-99.25 \pm 39.08)\ \text{MeV}, \qquad \lambda = (0.00036 \pm 0.00031)\ \text{MeV}^{-1} \tag{6.78}$$

The ground state energy for all five ensembles as well as the extrapolated binding energy are summarized in Table 6.8. The graphical representation of the extrapolation is shown in Fig. 6.7. We have performed a detailed statistical and systematic error analysis while applying the methods discussed in Sec. 3. The given uncertainties are representing the total error.

Ensemble	Fit range	ΔE_0 [MeV]
C005	6 . . . 18	$-62.8\,^{+21.5}_{-36.3}$
C01	6 . . . 20	$-44.0\,^{+21.7}_{-64.8}$
F004	6 . . . 22	$-54.0\,^{+32.7}_{-35.2}$
F006	7 . . . 24	$-59.8\,^{+36.9}_{-33.6}$
C00078	4 . . . 14	$-171.2\,^{+139.2}_{-80.7}$
Extrapolation		$-99.3\,^{+39.1}_{-39.1}$

Table 6.8: Binding energies for the presented ensembles relative to the threshold energy $E_B + E_{B^*}$ and extrapolation to the physical pion mass.

As a result, we found a bound $\bar{b}\bar{b}ud$ tetraquark state with a binding energy of $E_{\bar{b}\bar{b}ud} = -99\,^{+39}_{-39}$ MeV which is located within the errors clearly below the BB^*-threshold. This

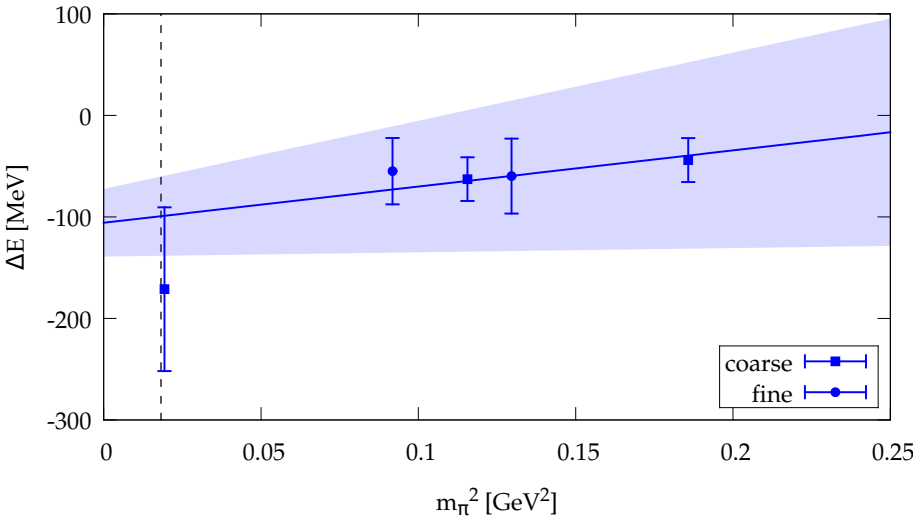

Figure 6.7: Chiral extrapolation for the ground state energy ΔE_0.

result coincides with previous studies of the $\bar{b}\bar{b}ud$ system in the Born-Oppenheimer approximation which reveal a bound state with $E_{\bar{b}\bar{b}ud} \simeq -90$ MeV (cf. [16, 17]). Our results are supported by further publications: In recent papers considering also $\bar{b}\bar{b}ud$ tetraquarks in NRQCD (cf. [23, 24]), evidence for a bound four-quark system has been found as well. However, in [23] a bound state with $E_{\bar{b}\bar{b}ud} \simeq -190$ MeV is predicted. Thus, a more detailed and elaborate comparison of the extracted results and applied analysis methods is necessary to make a more precise statement about the quantitative value of the binding energy.

We would like to emphasise that we intentionally did not perform the chiral extrapolation for the first excited state. Referring to Sec. 6.4.1, we found clear evidence that the lowest effective mass contains admixture of the first excitation for small t separations when considering only mesonic operators. Consequently, we suppose that the extracted effective mass for the first excited state includes further higher excitations and therefore cannot be identified with the pure physical energy level of the first excited state. Accordingly, an extrapolation is not assumed to yield reliable results and thus we renounce it.

In this work, we focus solely on the GEP and thus consider only the 3×3 submatrix. However, as shown in Sec. 6.4.1, we achieve a better separation of the lowest and first excited state when including the scattering operators, i.e. considering the whole 5×3 matrix. In this case, the binding energy has been decreased clearly so one assumes that the same behaviour will be detected for all other ensembles.
Nevertheless, the 5×3 matrix is only accessible when applying exponential fitting. Therefore, analysing the complete 5×3 correlation matrix including all scattering operators will be the subject of further investigations.

Chapter 7

Conclusion

In this thesis, I investigated the heavy-light $\bar{b}\bar{b}ud$ four-quark system in the framework of lattice non-relativistic QCD (NRQCD). This system allows interesting insights in the formation of heavy-light tetraquarks, and the detailed study of this system therefore provides an important step towards a theoretical understanding of occurring tetraquark states in nature and will support future experimental research.

Before considering tetraquarks, we successfully computed the masses of the bottomonium states $\eta_B(1S)$ and $\Upsilon(1S)$ using lattice NRQCD and illustrated the scale setting in NRQCD.

Continuing with four-quark states, we started with a preliminary study of the heavy tetraquark $\bar{b}\bar{b}bb$ in the $J^{PC} = 1^{+-}$ channel by means of NRQCD. Searching for bound states, we did not receive any evidence for a bound tetraquark state which is in agreement with recent lattice NRQCD studies ([36]).

The main part of the thesis focuses nevertheless on the $\bar{b}\bar{b}ud$ system in NRQCD which has been discussed in Chapter 6. We included five different creation operators in the correlation matrix for the $I(J^P) = 0(1^+)$ channel. We distinguish between three mesonic structures and two scattering structures. In the first step of our analysis, we included only the three mesonic operators and evaluated the 3×3 correlation matrix using the GEP. Calculations were executed for several different pion masses, and we finally performed an extrapolation to the physical pion mass. We have found strong indication for a bound state with a binding energy $E_{\bar{b}\bar{b}ud} = -99\,^{+39}_{-39}$ MeV at physical pion mass. Previous studies of the $\bar{b}\bar{b}ud$ system in the Born-Oppenheimer approximation have predicted a bound state with $E_{\bar{b}\bar{b}ud} = -90^{+43}_{-36}$ ([16, 17]). Consequently we successfully confirm these results in a qualitative as well as quantitative way.

Moreover, we performed calculations for an unphysical heavy bottom quark mass which is five times the physical bottom quark mass $m_Q = 5m_b$. In terms of quality we discovered a decrease of the bound state and supported previous studies stating the heavy quark mass dependence of the bound state energy ([15, 24]).

Additionally, we included the scattering operators in our analysis to study their influence on creating a tetraquark system. However, we did not perform a chiral extrapolation in this case but consider only one specific ensemble. Our studies reveal that the scattering operators decrease the bound state significantly and improve the extracted signal for the

lowest state. For the ensemble used, the extracted ground state energy has been lowered from $E_{\bar{b}\bar{b}ud} \simeq -60$ MeV to $E_{\bar{b}\bar{b}ud} \simeq -100$ MeV. We assume that the scattering state has an excellent overlap with the first excited state and therefore removes excited admixtures from the ground state so that we are able to extract the lowest energy level more precisely. It will be part of further investigations to extrapolate these results to the physical pion mass.

Finally, this project can be continued in the following directions.
The next logical step with regard to the presented results will be a detailed analysis of scattering states (cf. [46]). All currently observed tetraquark systems seem to be resonances, so a deeper theoretical understanding of tetraquark resonances is essential. Recent studies based on the Born-Oppenheimer approximation have already predicted a resonance in the $\bar{b}\bar{b}ud$ system for $I(J^P) = 0(1^-)$ (cf. [22]). Thus, the $\bar{b}\bar{b}ud$ four-quark system is a promising candidate to apply lattice QCD studies for scattering processes and to search for resonances. However, investigating such states, which are unstable under the strong interactions, is much more challenging than focusing on stable states: The same dynamics that provides binding of quarks and gluons into resonances is also responsible for their decay.
A powerful tool to study scattering processes on the lattice has been established by Lüscher some decades ago and is today known as the "Lüscher method" (cf. [47, 48, 49]). Due to the periodic final volume used in lattice calculations, we receive a discrete spectrum of QCD eigenstates. This spectrum can be related to scattering amplitudes applying Lüscher's method and we can perform an analytical continuation into the complex energy plane. There, resonances appear as pole singularities and can easily be detected.

Pursuing this ambitious project, the first part has been successfully achieved in this thesis by extracting the energy spectrum for the chosen operator basis. Implementing the Lüscher method to extend this investigation to scattering amplitudes and resonances will be the subject of ongoing research efforts.

Appendix A

Conventions and Formulas

Three-dimensional vectors are expressed by bold symbols $\mathbf{x} = (x_1, x_2, x_3)$, while four-dimensional vectors are defined by $x \equiv (\mathbf{x}, t)$. In this thesis we use natural units, i.e. $\hbar = c = 1$. Unless otherwise stated, we work in Euclidean space and therefore use the Euclidean formulation of the gamma matrices in the non-relativistic representation.

A.1 Gamma Matrices

The gamma matrices in the Euclidean representation fulfil the following relations:

- $\gamma_0 = \begin{pmatrix} 1 & 0 \\ 0 & -1 \end{pmatrix} \equiv \gamma_4, \qquad \gamma_j = \begin{pmatrix} 0 & -i\sigma_j \\ i\sigma_j & 0 \end{pmatrix}$

  with the Pauli matrices σ_i:

  $\sigma_1 = \begin{pmatrix} 0 & 1 \\ 1 & 0 \end{pmatrix}, \qquad \sigma_2 = \begin{pmatrix} 0 & -i \\ i & 0 \end{pmatrix}, \qquad \sigma_3 = \begin{pmatrix} 1 & 0 \\ 0 & -1 \end{pmatrix}$

- $\{\gamma_\mu, \gamma_\nu\} = 2\, g_{\mu\nu}$
- $\gamma_0^\dagger = \gamma_0, \qquad \gamma_i^\dagger = \gamma_i$
- $(\gamma_0)^2 = 1, \qquad (\gamma_i)^2 = 1$
- $\gamma_5 = \gamma_1\gamma_2\gamma_3\gamma_0$
- $\{\gamma_\mu, \gamma_5\} = 0$
- $(\gamma_5)^2 = 1, \qquad \gamma_5^\dagger = \gamma_5$
- $\gamma_0\gamma_i^\dagger\gamma_0 = -\gamma_i$
- $\gamma_0^T = \gamma_0, \quad \gamma_1^T = -\gamma_1, \quad \gamma_2^T = \gamma_2, \quad \gamma_3^T = -\gamma_3, \quad \gamma_5^T = \gamma_5,$

A.2 Quantum Number Operators

In this section we list the transformation behaviour of a spinor Ψ when applying the different quantum number operators.

Parity Operator:

$$\mathcal{P}(\Psi) = \gamma_0 \Psi \tag{A.1}$$

Charge Conjugation Operator:

$$\begin{aligned} \Psi &\xrightarrow{\mathcal{C}} \mathcal{C}^{-1}\overline{\Psi}^T \\ \overline{\Psi} &\xrightarrow{\mathcal{C}} -\Psi^T \mathcal{C} \end{aligned} \tag{A.2}$$

with the charge conjugation matrix $\mathcal{C} = \gamma_2\gamma_0$.

Angular Momentum Operator:

$$\begin{aligned} \mathcal{R}_j(\alpha)(\Psi) &= \exp\left(\alpha\epsilon_{jkl}\frac{\gamma_k\gamma_l}{4}\right)\Psi = \left[1 + \alpha\epsilon_{jkl}\frac{\gamma_k\gamma_l}{4}\right]\Psi + \mathcal{O}(\alpha^2) \\ &= \exp(i\alpha J_j)\,\Psi = \Big[1 + i\alpha J_j\Big]\,\Psi + \mathcal{O}(\alpha^2) \end{aligned} \tag{A.3}$$

with J_j the angular momentum for the j-th component.

Isospin Operator:

$$\begin{aligned} \mathcal{I}_j(\alpha)(\Psi) &= \exp\left(\frac{i\alpha}{2}\sigma_j\right)\Psi = \left[1 + \frac{i\alpha}{2}\sigma_j\right]\Psi + \mathcal{O}(\alpha^2) \\ &= \exp(i\alpha I_j)\,\Psi = \Big[1 + i\alpha I_j\Big]\,\Psi + \mathcal{O}(\alpha^2) \end{aligned} \tag{A.4}$$

with I_j the isospin for the j-th component.

Appendix B

FWT Transformation - Detailed Calculations

In this section we collect the complete and detailed calculations necessary to perform the FWT transformation including terms of $\mathcal{O}\left(1/m_Q^2\right)$. All higher orders $\mathcal{O}\left(1/m_Q^3\right)$ will be neglected. To preserve readability we introduce the notation:

$$\mathcal{L}_{(n)m} = \overline{\Psi}_{(n)} \widetilde{\mathcal{O}}_{(n)m} \Psi_{(n)} \tag{B.1}$$

where the index (n) numerates the performed redefinition and m denotes the highest included order in $1/m_Q$. In some calculations we omit the spinors and consider only $\widetilde{\mathcal{O}}_{(n)m}$ instead of the complete Lagrangian $\mathcal{L}_{(n)m}$.

B.1 Cancelling Anti-Commuting Terms of Leading Order

First, we redefine the spinors as presented in (2.23):

$$\begin{aligned} \Psi &= \exp\left(-\frac{1}{2m_Q} i\gamma^j D_j\right) \Psi_{(1)} \\ \overline{\Psi} &= \overline{\Psi}_{(1)} \exp\left(-\frac{1}{2m_Q} i\gamma^j D_j\right) \end{aligned} \tag{B.2}$$

Applying these spinors to the Lagrangian $\mathcal{L}$ and including all terms up to $1/m_Q^2$ eliminates the leading order anti-commuting terms and yields the new Lagrangian $\mathcal{L}_{(1)2}$. The index (1) labels the performed redefinition, and the index 2 indicates the highest order included. As discussed above, we compute the redefined Dirac operator $\widetilde{\mathcal{O}}_{(1)2}$ and omit the spinors $\Psi_{(1)}$ and $\overline{\Psi}_{(1)}$.

$$\widetilde{\mathcal{O}}_{(1)2} = \exp\left(-\frac{1}{2m_Q} i\gamma^j D_j\right) \left(i\gamma^0 D_0 - i\gamma^j D_j - m_Q\right) \exp\left(-\frac{1}{2m_Q} i\gamma^j D_j\right)$$

$$
\begin{aligned}
&= \left(1 - \frac{i}{2m_Q}\gamma^j D_j - \frac{1}{2}\frac{1}{4m_Q^2}\left(\gamma^j D_j\right)^2 + \frac{1}{6}\frac{i}{8m_Q^3}\left(\gamma^j D_j\right)^3 + \dots\right)\left(i\gamma^0 D_0 - i\gamma^j D_j - m_Q\right) \\
&\quad \times \left(1 - \frac{i}{2m_Q}\gamma^j D_j - \frac{1}{2}\frac{1}{4m_Q^2}\left(\gamma^j D_j\right)^2 + \frac{1}{6}\frac{i}{8m_Q^3}\left(\gamma^j D_j\right)^3 + \dots\right) \\
&= \Bigg[\left(i\gamma^0 D_0 - i\gamma^j D_j - m_Q\right) - \frac{i}{2m_Q}\gamma^j D_j\left(i\gamma^0 D_0 - i\gamma^j D_j - m_Q\right) \\
&\quad - \frac{1}{2}\frac{1}{4m_Q^2}\left(\gamma^j D_j\right)^2\left(i\gamma^0 D_0 - i\gamma^j D_j - m_Q\right) + \frac{1}{6}\frac{i}{8m_Q^3}\left(\gamma^j D_j\right)^3\left(i\gamma^0 D_0 - i\gamma^j D_j - m_Q\right)\Bigg] \\
&\quad \times \left(1 - \frac{i}{2m_Q}\gamma^j D_j - \frac{1}{2}\frac{1}{4m_Q^2}\left(\gamma^j D_j\right)^2 + \frac{1}{6}\frac{i}{8m_Q^3}\left(\gamma^j D_j\right)^3 + \dots\right) \\
&= \Bigg[\left(i\gamma^0 D_0 - i\gamma^j D_j - m_Q\right) - \frac{i}{2m_Q}\gamma^j D_j\left(i\gamma^0 D_0 - i\gamma^j D_j - m_Q\right) \\
&\quad - \frac{1}{2}\frac{1}{4m_Q^2}\left(\gamma^j D_j\right)^2\left(i\gamma^0 D_0 - i\gamma^j D_j - m_Q\right) + \frac{1}{6}\frac{i}{8m_Q^3}\left(\gamma^j D_j\right)^3\left(i\gamma^0 D_0 - i\gamma^j D_j - m_Q\right)\Bigg] \\
&\quad - \Bigg[\left(i\gamma^0 D_0 - i\gamma^j D_j - m_Q\right) - \frac{i}{2m_Q}\gamma^j D_j\left(i\gamma^0 D_0 - i\gamma^j D_j - m_Q\right) \\
&\quad - \frac{1}{2}\frac{1}{4m_Q^2}\left(\gamma^j D_j\right)^2\left(i\gamma^0 D_0 - i\gamma^j D_j - m_Q\right) + \frac{1}{6}\frac{i}{8m_Q^3}\left(\gamma^j D_j\right)^3\left(i\gamma^0 D_0 - i\gamma^j D_j - m_Q\right)\Bigg] \\
&\quad \times \frac{1}{2m_Q} i\gamma^j D_j \\
&\quad - \Bigg[\left(i\gamma^0 D_0 - i\gamma^j D_j - m_Q\right) - \frac{i}{2m_Q}\gamma^j D_j\left(i\gamma^0 D_0 - i\gamma^j D_j - m_Q\right) \\
&\quad - \frac{1}{2}\frac{1}{4m_Q^2}\left(\gamma^j D_j\right)^2\left(i\gamma^0 D_0 - i\gamma^j D_j - m_Q\right) + \frac{1}{6}\frac{i}{8m_Q^3}\left(\gamma^j D_j\right)^3\left(i\gamma^0 D_0 - i\gamma^j D_j - m_Q\right)\Bigg] \\
&\quad \times \frac{1}{2}\frac{1}{4m_Q^2}\left(\gamma^j D_j\right)^2 \\
&\quad + \Bigg[\left(i\gamma^0 D_0 - i\gamma^j D_j - m_Q\right) - \frac{i}{2m_Q}\gamma^j D_j\left(i\gamma^0 D_0 - i\gamma^j D_j - m_Q\right) \\
&\quad - \frac{1}{2}\frac{1}{4m_Q^2}\left(\gamma^j D_j\right)^2\left(i\gamma^0 D_0 - i\gamma^j D_j - m_Q\right) + \frac{1}{6}\frac{i}{8m_Q^3}\left(\gamma^j D_j\right)^3\left(i\gamma^0 D_0 - i\gamma^j D_j - m_Q\right)\Bigg] \\
&\quad \times \frac{1}{6}\frac{i}{8m_Q^3}\left(\gamma^j D_j\right)^3
\end{aligned}
$$

$$
\begin{aligned}
=& - m_Q + i\gamma^0 D_0 \\
&+ \frac{1}{m_Q}\left\{+\frac{1}{2}\gamma^j D_j \gamma^0 D_0 + \frac{1}{2}\gamma^0 D_0 \gamma^j D_j - \frac{1}{2}\left(\gamma^j D_j\right)^2\right\} \\
&+ \frac{1}{m_Q^2}\left\{-\frac{1}{8}\left(\gamma^j D_j\right)^2\left(i\gamma^0 D_0 - i\gamma^j D_j\right) - \frac{i}{48}\left(\gamma^j D_j\right)^3\right. \\
&- \frac{1}{4}\gamma^j D_j\left(i\gamma^0 D_0 - i\gamma^j D_j\right)\gamma^j D_j - \frac{i}{16}\left(\gamma^j D_j\right)^3 - \frac{1}{8}\left(i\gamma^0 D_0 - i\gamma^j D_j\right)\left(\gamma^j D_j\right)^2 \\
&\left.- \frac{i}{16}\left(\gamma^j D_j\right)^3 - \frac{i}{48}\left(\gamma^j D_j\right)^3\right\} + \mathcal{O}\left(\frac{1}{m_Q^3}\right) \\
=& - m_Q + i\gamma^0 D_0 \\
&+ \frac{1}{m_Q}\left\{+\frac{1}{2}\gamma^j D_j \gamma^0 D_0 + \frac{1}{2}\gamma^0 D_0 \gamma^j D_j - \frac{1}{2}\left(\gamma^j D_j\right)^2\right\} \\
&+ \frac{1}{m_Q^2}\left\{-\frac{i}{8}\left(\gamma^j D_j\right)^2\gamma^0 D_0 - \frac{i}{8}\gamma^0 D_0\left(\gamma^j D_j\right)^2 - \frac{i}{4}\gamma^j D_j \gamma^0 D_0 \gamma^k D_k\right. \\
&\left.- \frac{i}{6}\left(\gamma^j D_j\right)^3 + \frac{i}{2}\left(\gamma^j D_j\right)^3\right\} + \mathcal{O}\left(\frac{1}{m_Q^3}\right) \\
=& - m_Q + i\gamma^0 D_0 \\
&+ \frac{1}{m_Q}\left\{+\frac{1}{2}\gamma^j D_j \gamma^0 D_0 + \frac{1}{2}\gamma^0 D_0 \gamma^j D_j - \frac{1}{2}\left(\gamma^j D_j\right)^2\right\} \\
&+ \frac{1}{m_Q^2}\left\{-\frac{i}{8}\left(\gamma^j D_j\right)^2\gamma^0 D_0 - \frac{i}{8}\gamma^0 D_0\left(\gamma^j D_j\right)^2 - \frac{i}{4}\gamma^j D_j \gamma^0 D_0 \gamma^k D_k + \frac{i}{3}\left(\gamma^j D_j\right)^3\right\} \\
&+ \mathcal{O}\left(\frac{1}{m_Q^3}\right)
\end{aligned}
$$

As expected the leading order anti-commuting term has been cancelled.

B.2 Cancelling Anti-Commuting Terms of Order $\mathcal{O}(1/m_Q)$

After grouping the $1/m_Q$ contribution in commuting and anti-commuting terms, we apply the second redefined spinors (2.31) to $\mathcal{L}_{(1)2}$ in order to cancel the anti-commuting terms of order $1/m_Q$. The second redefinition is given by:

$$\begin{aligned}\Psi_{(1)} &= \exp\left(\frac{1}{2m_Q^2}O^A_{(1)1}\right)\Psi_{(2)}\\ \overline{\Psi}_{(1)} &= \overline{\Psi}_{(2)}\exp\left(\frac{1}{2m_Q^2}O^A_{(1)1}\right)\end{aligned} \tag{B.3}$$

The associated Dirac operator is computed as follows:

$$\begin{aligned}\widetilde{\mathcal{O}}_{(2)2} =& \exp\left(\frac{1}{2m_Q^2}\frac{ig}{2}\gamma^j\gamma^0F_{j0}\right)\left(-m_Q+i\gamma^0D_0\right)\exp\left(\frac{1}{2m_Q^2}\frac{ig}{2}\gamma^j\gamma^0F_{j0}\right)\\
&+\exp\left(\frac{1}{2m_Q^2}\frac{ig}{2}\gamma^j\gamma^0F_{j0}\right)\frac{1}{m_Q}\left\{-\frac{1}{2}D_jD^j-\frac{ig}{8}\left[\gamma^j,\gamma^k\right]F_{jk}+\frac{ig}{2}\gamma^j\gamma^0F_{j0}\right\}\\
&\times\exp\left(\frac{1}{2m_Q^2}\frac{ig}{2}\gamma^j\gamma^0F_{j0}\right)\\
&+\exp\left(\frac{1}{2m_Q^2}\frac{ig}{2}\gamma^j\gamma^0F_{j0}\right)\\
&\times\frac{1}{m_Q^2}\left\{-\frac{i}{8}\left(\gamma^jD_j\right)^2\gamma^0D_0-\frac{i}{8}\gamma^0D_0\left(\gamma^jD_j\right)^2-\frac{i}{4}\gamma^jD_j\gamma^0D_0\gamma^kD_k+\frac{i}{3}\left(\gamma^jD_j\right)^3\right\}\\
&\times\exp\left(\frac{1}{2m_Q^2}\frac{ig}{2}\gamma^j\gamma^0F_{j0}\right)\\
=&\left(1+\frac{1}{2m_Q^2}\frac{ig}{2}\gamma^j\gamma^0F_{j0}+\dots\right)\left(-m_Q+i\gamma^0D_0\right)\left(1+\frac{1}{2m_Q^2}\frac{ig}{2}\gamma^j\gamma^0F_{j0}+\dots\right)\\
&+\left(1+\frac{1}{2m_Q^2}\frac{ig}{2}\gamma^j\gamma^0F_{j0}+\dots\right)\frac{1}{m_Q}\left\{-\frac{1}{2}D_jD^j-\frac{ig}{8}\left[\gamma^j,\gamma^k\right]F_{jk}+\frac{ig}{2}\gamma^j\gamma^0F_{j0}\right\}\\
&\times\left(1+\frac{1}{2m_Q^2}\frac{ig}{2}\gamma^j\gamma^0F_{j0}+\dots\right)\\
&+\left(1+\frac{1}{2m_Q^2}\frac{ig}{2}\gamma^j\gamma^0F_{j0}+\dots\right)\\
&\times\frac{1}{m_Q^2}\left\{-\frac{i}{8}\left(\gamma^jD_j\right)^2\gamma^0D_0-\frac{i}{8}\gamma^0D_0\left(\gamma^jD_j\right)^2-\frac{i}{4}\gamma^jD_j\gamma^0D_0\gamma^kD_k+\frac{i}{3}\left(\gamma^jD_j\right)^3\right\}\\
&\times\left(1+\frac{1}{2m_Q^2}\frac{ig}{2}\gamma^j\gamma^0F_{j0}+\dots\right)\end{aligned}$$

$$
\begin{aligned}
&= \left(-m_Q + i\gamma^0 D_0\right) - \frac{1}{m_Q}\frac{ig}{2}\gamma^j\gamma^0 F_{j0} \\
&\quad + \frac{1}{2m_Q^2}\frac{ig}{2}\gamma^j\gamma^0 F_{j0} i\gamma^0 D_0 + i\gamma^0 D_0 \frac{1}{2m_Q^2}\frac{ig}{2}\gamma^j\gamma^0 F_{j0} \\
&\quad + \frac{1}{m_Q}\left\{-\frac{1}{2}D_j D^j - \frac{ig}{8}\left[\gamma^j, \gamma^k\right] F_{jk} + \frac{ig}{2}\gamma^j\gamma^0 F_{j0}\right\} \\
&\quad + \frac{1}{m_Q^2}\left\{-\frac{i}{8}\left(\gamma^j D_j\right)^2 \gamma^0 D_0 - \frac{i}{8}\gamma^0 D_0 \left(\gamma^j D_j\right)^2 - \frac{i}{4}\gamma^j D_j \gamma^0 D_0 \gamma^k D_k + \frac{i}{3}\left(\gamma^j D_j\right)^3\right\} \\
&= \left(-m_Q + i\gamma^0 D_0\right) + \frac{1}{m_Q}\left\{-\frac{1}{2}D_j D^j - \frac{ig}{8}\left[\gamma^j, \gamma^k\right] F_{jk}\right\} \\
&\quad + \frac{1}{m_Q^2}\left\{-\frac{i}{8}\left(\gamma^j D_j\right)^2 \gamma^0 D_0 - \frac{i}{8}\gamma^0 D_0 \left(\gamma^j D_j\right)^2 - \frac{i}{4}\gamma^j D_j \gamma^0 D_0 \gamma^k D_k + \frac{i}{3}\left(\gamma^j D_j\right)^3\right. \\
&\quad \left. - \frac{g}{4}\gamma^j\gamma^0 F_{j0}\gamma^0 D_0 - \frac{g}{4}\gamma^0 D_0 \gamma^j\gamma^0 F_{j0}\right\} + \mathcal{O}\left(\frac{1}{m_Q^3}\right) \\
&= \left(-m_Q + i\gamma^0 D_0\right) + \frac{1}{m_Q}\left\{-\frac{1}{2}D_j D^j - \frac{ig}{8}\left[\gamma^j, \gamma^k\right] F_{jk}\right\} \\
&\quad + \frac{1}{m_Q^2}\left\{-\frac{i}{8}\left(\gamma^j D_j\right)^2 \gamma^0 D_0 - \frac{i}{8}\gamma^0 D_0 \left(\gamma^j D_j\right)^2 - \frac{i}{4}\gamma^j D_j \gamma^0 D_0 \gamma^k D_k\right. \\
&\quad \left. + \frac{i}{3}\gamma^j\gamma^k\gamma^l D_j D_k D_l + \frac{g}{4}\gamma^j\left[D_0, F_{j0}\right]\right\} + \mathcal{O}\left(\frac{1}{m_Q^3}\right) \\
&= \left(-m_Q + i\gamma^0 D_0\right) + \frac{1}{m_Q}\left\{-\frac{1}{2}D_j D^j - \frac{ig}{8}\left[\gamma^j, \gamma^k\right] F_{jk}\right\} \\
&\quad - \frac{i}{8m_Q^2}\left\{\left(\gamma^j D_j\right)^2 \gamma^0 D_0 + \gamma^0 D_0 \left(\gamma^j D_j\right)^2 + 2\gamma^j D_j \gamma^0 D_0 \gamma^k D_k\right\} \\
&\quad + \frac{1}{m_Q^2}\left\{\frac{i}{3}\gamma^j\gamma^k\gamma^l D_j D_k D_l + \frac{g}{4}\gamma^j\left[D_0, F_{j0}\right]\right\} + \mathcal{O}\left(\frac{1}{m_Q^3}\right) \\
&= \left(-m_Q + i\gamma^0 D_0\right) + \frac{1}{m_Q}\left\{-\frac{1}{2}D_j D^j - \frac{ig}{8}\left[\gamma^j, \gamma^k\right] F_{jk}\right\} \\
&\quad - \frac{i}{8m_Q^2}\left\{\gamma^j D_j\left(\gamma^k D_k \gamma^0 D_0 + \gamma^0 D_0 \gamma^k D_k\right)\right. \\
&\quad \left. + \left(\gamma^k D_k \gamma^0 D_0 + \gamma^0 D_0 \gamma^k D_k\right)\gamma^j D_j\right\} \\
&\quad + \frac{1}{m_Q^2}\left\{\frac{i}{3}\gamma^j\gamma^k\gamma^l D_j D_k D_l + \frac{g}{4}\gamma^j\left[D_0, F_{j0}\right]\right\} + \mathcal{O}\left(\frac{1}{m_Q^3}\right)
\end{aligned}
$$

with: $\gamma^k D_k \gamma^0 D_0 + \gamma^0 D_0 \gamma^k D_k = ig\gamma^k\gamma^0 F_{k0}$

$$
\begin{aligned}
&= \left(-m_Q + i\gamma^0 D_0\right) + \frac{1}{m_Q}\left\{-\frac{1}{2}D_j D^j - \frac{ig}{8}\left[\gamma^j, \gamma^k\right] F_{jk}\right\} \\
&\quad + \frac{g}{8m_Q^2}\left\{\gamma^j D_j \gamma^k \gamma^0 F_{k0} + \gamma^k \gamma^0 F_{k0} \gamma^j D_j\right\} \\
&\quad + \frac{1}{m_Q^2}\left\{\frac{i}{3}\gamma^j\gamma^k\gamma^l D_j D_k D_l + \frac{g}{4}\gamma^j \left[D_0, F_{j0}\right]\right\} + \mathcal{O}\left(\frac{1}{m_Q^3}\right) \\
&= \left(-m_Q + i\gamma^0 D_0\right) + \frac{1}{m_Q}\left\{-\frac{1}{2}D_j D^j - \frac{ig}{8}\left[\gamma^j, \gamma^k\right] F_{jk}\right\} \\
&\quad + \frac{g}{8m_Q^2}\gamma^0\left\{\gamma^j \gamma^k D_j F_{k0} - \gamma^k \gamma^j F_{k0} D_j\right\} \\
&\quad + \frac{1}{m_Q^2}\left\{\frac{i}{3}\gamma^j\gamma^k\gamma^l D_j D_k D_l + \frac{g}{4}\gamma^j \left[D_0, F_{j0}\right]\right\} + \mathcal{O}\left(\frac{1}{m_Q^3}\right)
\end{aligned}
$$

In order to rewrite this expression in commuting and anti-commuting terms, we consider:

$$
\begin{aligned}
&\gamma^j\gamma^k D_j F_{k0} - \gamma^k\gamma^j F_{k0} D_j \\
=&\frac{1}{2}\left(\gamma^j\gamma^k D_j F_{k0} + \gamma^j\gamma^k D_j F_{k0} - \gamma^k\gamma^j F_{k0} D_j - \gamma^k\gamma^j F_{k0} D_j\right) \\
=&\frac{1}{2}\left(\gamma^j\gamma^k D_j F_{k0} + \left(2\eta^{jk} - \gamma^k\gamma^j\right) D_j F_{k0} - \gamma^k\gamma^j F_{k0} D_j - \left(2\eta^{jk} - \gamma^j\gamma^k\right) F_{k0} D_j\right) \\
=&\frac{1}{2}\left(\gamma^j\gamma^k D_j F_{k0} - \gamma^k\gamma^j D_j F_{k0} - \gamma^k\gamma^j F_{k0} D_j + \gamma^j\gamma^k F_{k0} D_j\right) \\
&+ \eta^{jk} D_j F_{k0} - \eta^{jk} F_{k0} D_j \\
=&\frac{1}{2}\left(\left(\gamma^j\gamma^k - \gamma^k\gamma^j\right) D_j F_{k0} + \left(\gamma^j\gamma^k - \gamma^k\gamma^j\right) F_{k0} D_j\right) \\
&+ \eta^{jk} D_j F_{k0} - \eta^{jk} F_{k0} D_j \\
=&\frac{1}{2}\left[\gamma^j, \gamma^k\right]\left\{D_j, F_{k0}\right\} + \eta^{jk} D_j F_{k0} - \eta^{jk} F_{k0} D_j
\end{aligned}
$$

with:

$$
\begin{aligned}
&\eta^{jk}\left(D_j F_{k0} - F_{k0} D_j\right)\Psi = \eta^{jk}\left[\left(D_j F_{k0}\right)\Psi + F_{k0}\left(D_j\Psi\right) - F_{k0}\left(D_j\Psi\right)\right] \\
=&\eta^{jk}\left(D_j F_{k0}\right)\Psi \equiv \eta^{jk}\left(D_j^* F_{k0}\right)\Psi = -D_j^* F_{j0}\Psi
\end{aligned}
$$

where D_j^* means that the derivative acts only on the electromagnetic field on the right but not on the spinor.

Finally, we get:

$$\begin{aligned}\widetilde{\mathcal{O}}_{(2)2} = &\left(-m_Q + i\gamma^0 D_0\right) + \frac{1}{m_Q}\left\{-\frac{1}{2}D_j D^j - \frac{ig}{8}\left[\gamma^j, \gamma^k\right] F_{jk}\right\} \\ &+ \frac{1}{m_Q^2}\left\{-\frac{g}{8m}\gamma^0\left(D_j^* F_{j0} - \frac{1}{2}\left[\gamma^j, \gamma^k\right]\{D_j, F_{k0}\}\right)\right. \\ &\left.+\frac{i}{3}\gamma^j\gamma^k\gamma^l D_j D_k D_l + \frac{g}{4}\gamma^j\left[D_0, F_{j0}\right]\right\} + \mathcal{O}\left(\frac{1}{m_Q^3}\right)\end{aligned} \tag{B.4}$$

(B.5)

B.3 Cancelling Quark Mass Term

To eliminate the quark mass term we apply the transformation (2.37). In the following, we illustrate the proof. Note that it is sufficient to consider only the leading terms and neglect all contributions of $\mathcal{O}(1/m_Q)$, since they do not contain further time derivatives and thus commute with the exponentials.

$$\begin{aligned}&\overline{\widetilde{\Psi}}\exp\left(im_Q x^0\gamma^0\right)\left[-m_Q + i\gamma^0 D_0 + \mathcal{O}\left(\frac{1}{m_Q}\right)\right]\exp\left(-im_Q x^0\gamma^0\right)\widetilde{\Psi} \\ =&\overline{\widetilde{\Psi}}\exp\left(im_Q x^0\gamma^0\right)\left[-m_Q + i\gamma^0 D_0\right]\exp\left(-im_Q x^0\gamma^0\right)\widetilde{\Psi} + \mathcal{O}\left(\frac{1}{m_Q}\right) \\ =&\overline{\widetilde{\Psi}}\exp\left(im_Q x^0\gamma^0\right)\exp\left(-im_Q x^0\gamma^0\right)\left[-m_Q + i\gamma^0\left(-im_Q\gamma^0\right) + i\gamma^0 D_0\right]\widetilde{\Psi} + \mathcal{O}\left(\frac{1}{m_Q}\right) \\ =&\overline{\widetilde{\Psi}}\left[-m_Q + m_Q + i\gamma^0 D_0\right]\widetilde{\Psi} + \mathcal{O}\left(\frac{1}{m_Q}\right) \\ =&\overline{\widetilde{\Psi}} i\gamma^0 D_0\widetilde{\Psi} + \mathcal{O}\left(\frac{1}{m_Q}\right)\end{aligned} \tag{B.6}$$

As we can see, the quark mass contribution has vanished while all other terms remain unaffected.

Appendix C

Calculation of Quantum Numbers

C.1 Angular Momentum for $\Upsilon(1S)$

In the following, the computation of the angular momentum for the $\Upsilon(1S)$ is illustrated. In this case, all three spatial directions have to be considered and therefore evaluation will be performed for $j = 1, 2, 3$.

$$\begin{aligned}\mathcal{R}_3(\alpha)|\Phi_{\Upsilon,j}\rangle =& \mathcal{R}_3(\alpha)(\bar{b}\gamma_j b)\ |\Omega\rangle \\ =& \left[\left(1+\frac{\alpha}{4}\left[\gamma_1,\gamma_2\right]\right)\ b\right]^\dagger \gamma_0\gamma_j\left(1+\frac{\alpha}{4}\left[\gamma_1,\gamma_2\right]\right)\ b\ |\Omega\rangle + \mathcal{O}(\alpha^2) \\ =& b^\dagger\left(1-\frac{\alpha}{4}\left[\gamma_1,\gamma_2\right]\right)\gamma_0\gamma_j\left(1+\frac{\alpha}{4}\left[\gamma_1,\gamma_2\right]\right)\ b\ |\Omega\rangle + \mathcal{O}(\alpha^2)\end{aligned} \tag{C.1}$$

for $j = 1$:

$$\begin{aligned}=& b^\dagger\gamma_0\gamma_1 b|\Omega\rangle + \alpha b^\dagger\gamma_0\gamma_2 b|\Omega\rangle + \mathcal{O}(\alpha^2) \\ =& |\Phi_{\Upsilon,1}\rangle + \alpha|\Phi_{\Upsilon,2}\rangle + \mathcal{O}(\alpha^2)\end{aligned} \tag{C.2}$$

for $j = 2$:

$$\begin{aligned}=& b^\dagger\gamma_0\gamma_2 b|\Omega\rangle - \alpha b^\dagger\gamma_0\gamma_1 b|\Omega\rangle + \mathcal{O}(\alpha^2) \\ =& |\Phi_{\Upsilon,2}\rangle - \alpha|\Phi_{\Upsilon,1}\rangle + \mathcal{O}(\alpha^2)\end{aligned} \tag{C.3}$$

for $j = 3$:

$$\begin{aligned}=& b^\dagger\gamma_0\gamma_3 b|\Omega\rangle + \mathcal{O}(\alpha^2) \\ =& |\Phi_{\Upsilon,3}\rangle + \mathcal{O}(\alpha^2)\end{aligned} \tag{C.4}$$

Regarding the associated three-dimensional spinor, the transformation behaviour results in:

$$\mathcal{R}_3(\alpha)|\Phi_\Upsilon\rangle = \begin{pmatrix} 1 & \alpha & 0 \\ -\alpha & 1 & 0 \\ 0 & 0 & 1 \end{pmatrix} |\Phi_\Upsilon\rangle = |\Phi_\Upsilon\rangle + i\alpha \begin{pmatrix} 0 & -i & 0 \\ i & 0 & 0 \\ 0 & 0 & 0 \end{pmatrix} |\Phi_\Upsilon\rangle \tag{C.5}$$

We can identify the matrix with J_3 via $\mathcal{R}_3(\alpha)|\Phi_\Upsilon\rangle = (1 + i\alpha J_3)|\Phi_\Upsilon\rangle$. $J_{1,2}$ can be obtained by cyclic permutation. The rotation matrices are given by:

$$J_1 = \begin{pmatrix} 0 & 0 & 0 \\ 0 & 0 & -i \\ 0 & i & 0 \end{pmatrix}, \quad J_2 = \begin{pmatrix} 0 & 0 & i \\ 0 & 0 & 0 \\ -i & 0 & 0 \end{pmatrix}, \quad J_3 = \begin{pmatrix} 0 & -i & 0 \\ i & 0 & 0 \\ 0 & 0 & 0 \end{pmatrix} \tag{C.6}$$

Finally, we get $J^2 = J_1^2 + J_2^2 + J_3^2 = 2 \cdot \mathbb{1} \stackrel{!}{=} J(J+1) \cdot \mathbb{1}$ so that the angular momentum is $J = 1$.

C.2 Quantum Numbers for $\bar{b}\bar{b}ud$

In this section we will compute explicitly the quantum numbers $I(J^P)$ for the three creation operator structures used in this work. Note that it is not necessary to distinguish between different momentum projections, and therefore, in the following, we omit the space-time arguments and consider only the general expressions. The three operators are given by:

$$\mathcal{O}_{BB^*} = \bar{b}\Gamma_1 d\, \bar{b}\Gamma_2 u - \bar{b}\Gamma_1 u\, \bar{b}\Gamma_2 d \tag{C.7}$$

with $\Gamma_1 = \gamma_5, \quad \Gamma_2 = \gamma_j$.

$$\mathcal{O}_{B^*B^*} = \bar{b}\Gamma_1 d\, \bar{b}\Gamma_2 u - \bar{b}\Gamma_1 u\, \bar{b}\Gamma_2 d \tag{C.8}$$

with ϵ_{ijk} ($\Gamma_1 = \gamma_j, \quad \Gamma_2 = \gamma_k$).

$$\mathcal{O}_{Dd} = \epsilon^{abc}\bar{b}^b\Gamma_1 \left[\bar{b}^c\right]^T \epsilon^{ade}\left(\left[d^d\right]^T \Gamma_2 u^e - \left[u^d\right]^T \Gamma_2 d^e\right) \tag{C.9}$$

with $\Gamma_1 = \gamma_j\mathcal{C}, \quad \Gamma_2 = \mathcal{C}\gamma_5$.

A spinor describing one of these particles is constructed via $|\Psi_j\rangle = \mathcal{O}_j|\Omega\rangle$ with $j \in \{BB^*, B^*B^*, Dd\}$ and the vacuum state $|\Omega\rangle$. In this section we are working in Minkowski space.

C.2.1 Parity

First, we compute the parity $\mathcal{P}$ for all three operators. We use the parity operator given in (A.1).

For $\mathcal{O}_{BB^*}$ and $\mathcal{O}_{B^*B^*}$:

For evaluating case one and two together we keep the Γ matrices general:

$$\begin{aligned}\mathcal{P}|\Phi\rangle =& \mathcal{P}\left(\bar{b}\Gamma_1 d\, \bar{b}\Gamma_2 u - \bar{b}\Gamma_1 u\, \bar{b}\Gamma_2 d\right)|\Omega\rangle \\ =& \bar{b}\gamma_0\Gamma_1\gamma_0 d\, \bar{b}\gamma_0\Gamma_2\gamma_0 u - \bar{b}\gamma_0\Gamma_1\gamma_0 u\, \bar{b}\gamma_0\Gamma_2\gamma_0 d|\Omega\rangle \\ =& \bar{b}\Gamma_1 d\, \bar{b}\Gamma_2 u - \bar{b}\Gamma_1 u\, \bar{b}\Gamma_2 d|\Omega\rangle \\ =& + |\Phi\rangle\end{aligned} \tag{C.10}$$

We apply $\{\gamma_0, \gamma_5\} = 0$ and $\{\gamma_0, \gamma_j\} = 0$ which is valid for $\mathcal{O}_{BB^*}$ as well as $\mathcal{O}_{B^*B^*}$.

For $\mathcal{O}_{Dd}$:

$$\begin{aligned}
&\mathcal{P}|\Phi\rangle \\
=&\mathcal{P}\left[\epsilon^{abc}\bar{b}^b\Gamma_1\left[\bar{b}^c\right]^T\epsilon^{ade}\left(\left[d^d\right]^T\Gamma_2 u^e-\left[u^d\right]^T\Gamma_2 d^e\right)\right]|\Omega\rangle \\
=&\epsilon^{abc}\bar{b}^b\gamma_0\Gamma_1\gamma_0\left[\bar{b}^c\right]^T\epsilon^{ade}\left(\left[d^d\right]^T\gamma_0\Gamma_2\gamma_0 u^e-\left[u^d\right]^T\gamma_0\Gamma_2\gamma_0 d^e\right)|\Omega\rangle \\
=&\epsilon^{abc}\bar{b}^b\Gamma_1\left[\bar{b}^c\right]^T\epsilon^{ade}\left(\left[d^d\right]^T\Gamma_2 u^e-\left[u^d\right]^T\Gamma_2 d^e\right)|\Omega\rangle \\
=&+|\Phi\rangle
\end{aligned} \tag{C.11}$$

We use the commutators $[\gamma_0,\gamma_j\mathcal{C}]=0$ and $[\gamma_0,\mathcal{C}\gamma_5]=0$.

Hence, the parity is positive for all three operators ($\mathcal{P}=+$).

C.2.2 Angular momentum

We proceed computing the angular momentum for all operators applying (A.3). We consider the z-component and set $j=3$. The rotation operator for small angular α can be expressed by:

$$\mathcal{R}_3(\alpha)\left(\Psi\right)=\exp\left(\frac{\alpha}{4}\left[\gamma_1,\gamma_2\right]\right)\Psi=\left(1+\frac{\alpha}{4}\left[\gamma_1,\gamma_2\right]\right)\Psi+\mathcal{O}(\alpha^2) \tag{C.12}$$

For $\mathcal{O}_{BB^*}$ and $\mathcal{O}_{B^*B^*}$:

Again, we consider $\mathcal{O}_{BB^*}$ and $\mathcal{O}_{B^*B^*}$ in a common approach and insert the Γ matrices at the end of the calculation. The general expression is found to be:

$$\begin{aligned}
&\mathcal{R}_3(\alpha)\left(\bar{b}\Gamma_1 d\,\bar{b}\Gamma_2 u-\bar{b}\Gamma_1 u\,\bar{b}\Gamma_2 d\right)|\Omega\rangle \\
=\Big\{&\quad\left[\left(1+\frac{\alpha}{4}\left[\gamma_1,\gamma_2\right]\right)b\right]^\dagger\gamma_0\Gamma_1\left(1+\frac{\alpha}{4}\left[\gamma_1,\gamma_2\right]\right)d \\
&\times\left[\left(1+\frac{\alpha}{4}\left[\gamma_1,\gamma_2\right]\right)b\right]^\dagger\gamma_0\Gamma_2\left(1+\frac{\alpha}{4}\left[\gamma_1,\gamma_2\right]\right)u \\
&-\left[\left(1+\frac{\alpha}{4}\left[\gamma_1,\gamma_2\right]\right)b\right]^\dagger\gamma_0\Gamma_1\left(1+\frac{\alpha}{4}\left[\gamma_1,\gamma_2\right]\right)u \\
&\times\left[\left(1+\frac{\alpha}{4}\left[\gamma_1,\gamma_2\right]\right)b\right]^\dagger\gamma_0\Gamma_2\left(1+\frac{\alpha}{4}\left[\gamma_1,\gamma_2\right]\right)d\Big\}|\Omega\rangle
\end{aligned}$$

$$
\begin{aligned}
&= \Big\{ \quad b^\dagger \left(1 + \frac{\alpha}{4}\left(\gamma_1\gamma_2 - \gamma_2\gamma_1\right)^\dagger\right)\gamma_0\Gamma_1\left(1 + \frac{\alpha}{4}\left(\gamma_1\gamma_2 - \gamma_2\gamma_1\right)\right) d \\
&\quad \times b^\dagger \left(1 + \frac{\alpha}{4}\left(\gamma_1\gamma_2 - \gamma_2\gamma_1\right)^\dagger\right)\gamma_0\Gamma_2\left(1 + \frac{\alpha}{4}\left(\gamma_1\gamma_2 - \gamma_2\gamma_1\right)\right) u \\
&\quad - b^\dagger \left(1 + \frac{\alpha}{4}\left(\gamma_1\gamma_2 - \gamma_2\gamma_1\right)^\dagger\right)\gamma_0\Gamma_1\left(1 + \frac{\alpha}{4}\left(\gamma_1\gamma_2 - \gamma_2\gamma_1\right)\right) u \\
&\quad \times b^\dagger \left(1 + \frac{\alpha}{4}\left(\gamma_1\gamma_2 - \gamma_2\gamma_1\right)^\dagger\right)\gamma_0\Gamma_2\left(1 + \frac{\alpha}{4}\left(\gamma_1\gamma_2 - \gamma_2\gamma_1\right)\right) d \Big\} |\Omega\rangle \\
&= \Big\{ \quad \bar{b}\left(\Gamma_1 + \frac{\alpha}{4}\left[\left(\gamma_2\gamma_1 - \gamma_1\gamma_2\right)\Gamma_1 + \Gamma_1\left(\gamma_1\gamma_2 - \gamma_2\gamma_1\right)\right]\right) d \\
&\quad \times \bar{b}\left(\Gamma_2 + \frac{\alpha}{4}\left[\left(\gamma_2\gamma_1 - \gamma_1\gamma_2\right)\Gamma_2 + \Gamma_2\left(\gamma_1\gamma_2 - \gamma_2\gamma_1\right)\right]\right) u \\
&\quad - \bar{b}\left(\Gamma_1 + \frac{\alpha}{4}\left[\left(\gamma_2\gamma_1 - \gamma_1\gamma_2\right)\Gamma_1 + \Gamma_1\left(\gamma_1\gamma_2 - \gamma_2\gamma_1\right)\right]\right) u \\
&\quad \times \bar{b}\left(\Gamma_2 + \frac{\alpha}{4}\left[\left(\gamma_2\gamma_1 - \gamma_1\gamma_2\right)\Gamma_2 + \Gamma_2\left(\gamma_1\gamma_2 - \gamma_2\gamma_1\right)\right]\right) d \Big\} |\Omega\rangle \\
&= \Big\{ \left(\bar{b}\Gamma_1 d\,\bar{b}\Gamma_2 u - \bar{b}\Gamma_1 u\,\bar{b}\Gamma_2 d\right) \\
&\quad - \frac{\alpha}{2}\left(\bar{b}\left[\gamma_1\gamma_2, \Gamma_1\right] d\bar{b}\Gamma_2 u + \bar{b}\Gamma_1 d\bar{b}\left[\gamma_1\gamma_2, \Gamma_2\right] u\right. \\
&\quad \left. -\bar{b}\left[\gamma_1\gamma_2, \Gamma_1\right] u\bar{b}\Gamma_2 d - \bar{b}\Gamma_1 u\bar{b}\left[\gamma_1\gamma_2, \Gamma_2\right] d\right) \Big\} |\Omega\rangle
\end{aligned}
\tag{C.13}
$$

Now we insert the Γ matrices explicitly and therefore distinguish between $\mathcal{O}_{BB^*}$ and $\mathcal{O}_{B^*B^*}$.

For $\mathcal{O}_{BB^*}$:

For $\mathcal{O}_{BB^*}$, we insert $\Gamma_1 = \gamma_5$ and $\Gamma_2 = \gamma_j$. We evaluate (C.13) for all spatial directions $j = 1, 2, 3$ and use the commutation relation $[\gamma_1\gamma_2, \gamma_5] = 0$:

$\underline{j = 1}$:

$$
\left[\gamma_1\gamma_2, \gamma_1\right] = 2\gamma_2 \tag{C.14}
$$

thus:

$$
\begin{aligned}
\mathcal{R}_3(\alpha)|\Psi_1\rangle = &\Big\{\left(\bar{b}\gamma_5 d\,\bar{b}\gamma_1 u - \bar{b}\gamma_5 u\,\bar{b}\gamma_1 d\right) \\
&- \alpha\left(\bar{b}\gamma_5 d\bar{b}\gamma_2 u - \bar{b}\gamma_5 u\bar{b}\gamma_2 d\,\right)\Big\}|\Omega\rangle = |\Psi_1\rangle - \alpha|\Psi_2\rangle
\end{aligned}
\tag{C.15}
$$

$\underline{j = 2}$:

$$
\left[\gamma_1\gamma_2, \gamma_2\right] = -2\gamma_1 \tag{C.16}
$$

thus:

$$
\begin{aligned}
\mathcal{R}_3(\alpha)|\Psi_2\rangle = &\Big\{\left(\bar{b}\gamma_5 d\,\bar{b}\gamma_2 u - \bar{b}\gamma_5 u\,\bar{b}\gamma_2 d\right) \\
&+ \alpha\left(\bar{b}\gamma_5 d\bar{b}\gamma_1 u - \bar{b}\gamma_5 u\bar{b}\gamma_1 d\,\right)\Big\}|\Omega\rangle = |\Psi_2\rangle + \alpha|\Psi_1\rangle
\end{aligned}
\tag{C.17}
$$

$\underline{j=3}$:

$$[\gamma_1\gamma_2, \gamma_3] = 0 \tag{C.18}$$

thus:

$$\mathcal{R}_3(\alpha)|\Psi_1\rangle = \left\{ \left(\bar{b}\gamma_5 d\, \bar{b}\gamma_1 u - \bar{b}\gamma_5 u\, \bar{b}\gamma_1 d \right) \right\} |\Omega\rangle = |\Psi_3\rangle \tag{C.19}$$

Hence, the spinor transforms like:

$$\mathcal{R}_3(\alpha)|\Psi\rangle = \begin{pmatrix} 1 & -\alpha & 0 \\ \alpha & 1 & 0 \\ 0 & 0 & 1 \end{pmatrix} |\Psi\rangle = |\Psi\rangle + i\alpha \begin{pmatrix} 0 & i & 0 \\ -i & 0 & 0 \\ 0 & 0 & 0 \end{pmatrix} |\Psi\rangle \tag{C.20}$$

Using (A.3) to rewrite $\mathcal{R}_3(\alpha) = \exp(i\alpha J_3) = 1 + i\alpha J_3 + \mathcal{O}(\alpha^2)$ we get:

$$J_3 = \begin{pmatrix} 0 & i & 0 \\ -i & 0 & 0 \\ 0 & 0 & 0 \end{pmatrix} \tag{C.21}$$

Repeating the calculation for $\mathcal{R}_1(\alpha)$ and $\mathcal{R}_2(\alpha)$ or deviating the results from circular permutation of the gamma matrices' indices, we find:

$$J_1 = \begin{pmatrix} 0 & 0 & 0 \\ 0 & 0 & i \\ 0 & -i & 0 \end{pmatrix}, \qquad J_2 = \begin{pmatrix} 0 & 0 & -i \\ 0 & 0 & 0 \\ i & 0 & 0 \end{pmatrix} \tag{C.22}$$

The total angular momentum is given by:

$$J^2 = J_1^2 + J_2^2 + J_3^2 = 2 \cdot \mathbb{1} \stackrel{!}{=} (J+1)J \cdot \mathbb{1} \tag{C.23}$$

so that the total angular momentum is $J = 1$.

For $\mathcal{O}_{B^*B^*}$:

We repeat the same calculation for $\mathcal{O}_{B^*B^*}$ with ϵ_{ijk} ($\Gamma_1 = \gamma_j, \Gamma_2 = \gamma_k$) and distinguish again the three components $i = 1, 2, 3$.

$\underline{i=1}$:

$$\begin{aligned} [\gamma_1\gamma_2, \gamma_2] &= -2\gamma_1 \\ [\gamma_1\gamma_2, \gamma_3] &= 0 \end{aligned} \tag{C.24}$$

$$\begin{aligned} \mathcal{R}_3(\alpha)|\Psi_1\rangle =& \left\{ \left(\bar{b}\gamma_2 d\, \bar{b}\gamma_3 u - \bar{b}\gamma_2 u\, \bar{b}\gamma_3 d \right) - \left(\bar{b}\gamma_3 d\, \bar{b}\gamma_2 u - \bar{b}\gamma_3 u\, \bar{b}\gamma_2 d \right) \right. \\ & \left. - \alpha \left(- \left(\bar{b}\gamma_1 d \bar{b}\gamma_3 u - \bar{b}\gamma_1 u \bar{b}\gamma_3 d \right) + \left(\bar{b}\gamma_3 d \bar{b}\gamma_1 u - \bar{b}\gamma_3 u \bar{b}\gamma_1 d \right) \right) \right\} |\Omega\rangle \\ =& |\Psi_1\rangle - \alpha|\Psi_2\rangle \end{aligned} \tag{C.25}$$

$\underline{i=2}$:

$$\begin{aligned}[\gamma_1\gamma_2,\gamma_1] &= 2\gamma_2\\ [\gamma_1\gamma_2,\gamma_3] &= 0\end{aligned} \tag{C.26}$$

$$\begin{aligned}\mathcal{R}_3(\alpha)|\Psi_2\rangle =& \Big\{\Big(\bar{b}\gamma_3 d\,\bar{b}\gamma_1 u - \bar{b}\gamma_3 u\,\bar{b}\gamma_1 d\Big) - \Big(\bar{b}\gamma_1 d\,\bar{b}\gamma_3 u - \bar{b}\gamma_1 u\,\bar{b}\gamma_3 d\Big)\\ &+ \alpha\Big(-\Big(\bar{b}\gamma_3 d\bar{b}\gamma_2 u - \bar{b}\gamma_3 u\bar{b}\gamma_2 d\Big) + \Big(\bar{b}\gamma_2 d\bar{b}\gamma_3 u - \bar{b}\gamma_2 u\bar{b}\gamma_3 d\Big)\Big)\Big\}|\Omega\rangle\\ =&|\Psi_2\rangle + \alpha|\Psi_1\rangle\end{aligned} \tag{C.27}$$

$\underline{i=3}$:

$$\begin{aligned}[\gamma_1\gamma_2,\gamma_1] &= +2\gamma_2\\ [\gamma_1\gamma_2,\gamma_2] &= -2\gamma_1\end{aligned} \tag{C.28}$$

$$\begin{aligned}\mathcal{R}_3(\alpha)|\Psi_1\rangle =& \Big\{\Big(\bar{b}\gamma_1 d\,\bar{b}\gamma_2 u - \bar{b}\gamma_1 u\,\bar{b}\gamma_2 d\Big) - \Big(\bar{b}\gamma_2 d\,\bar{b}\gamma_1 u - \bar{b}\gamma_2 u\,\bar{b}\gamma_1 d\Big)\\ &- \alpha\Big[\Big(-\bar{b}\gamma_1 d\bar{b}\gamma_1 u + \bar{b}\gamma_2 d\bar{b}\gamma_2 u - \bar{b}\gamma_1 u\bar{b}\gamma_1 d + \bar{b}\gamma_2 u\bar{b}\gamma_2 d\Big)\\ &- \Big(\bar{b}\gamma_2 d\bar{b}\gamma_2 u - \bar{b}\gamma_1 d\bar{b}\gamma_1 u + \bar{b}\gamma_2 u\bar{b}\gamma_2 d - \bar{b}\gamma_1 u\bar{b}\gamma_1 d\Big)\,]\Big\}|\Omega\rangle\\ =&|\Psi_3\rangle\end{aligned} \tag{C.29}$$

Therefore, we obtain the same transformation behaviour for $|\Psi\rangle$ compared to $\mathcal{O}_{BB^*}$, i.e. $J=1$ is also valid for $\mathcal{O}_{B^*B^*}$.

For $\mathcal{O}_{Dd}$:

Finally, we consider the diquark-antidiquark operator.

$$
\begin{aligned}
&\mathcal{R}_3(\alpha)\left(\epsilon^{abc}\bar{b}^b\Gamma_1\left(\bar{b}^c\right)^T\epsilon^{ade}\left(\left(d^d\right)^T\Gamma_2 u^e-\left(u^d\right)^T\Gamma_2 d^e\right)\right)|\Omega\rangle\\
=&\epsilon^{abc}\epsilon^{ade}\Bigg\{\ b^{b\dagger}\left(1+\frac{\alpha}{4}\left(\gamma_1\gamma_2-\gamma_2\gamma_1\right)^\dagger\right)\gamma_0\Gamma_1\left[b^{c\dagger}\left(1+\frac{\alpha}{4}\left(\gamma_1\gamma_2-\gamma_2\gamma_1\right)^\dagger\right)\gamma_0\right]^T\\
&\left(\left[\left(1+\frac{\alpha}{4}\left(\gamma_1\gamma_2-\gamma_2\gamma_1\right)\right)d^d\right]^T\Gamma_2\left(1+\frac{\alpha}{4}\left(\gamma_1\gamma_2-\gamma_2\gamma_1\right)\right)u^e\right.\\
&\left.-\left[\left(1+\frac{\alpha}{4}\left(\gamma_1\gamma_2-\gamma_2\gamma_1\right)\right)u^d\right]^T\Gamma_2\left(1+\frac{\alpha}{4}\left(\gamma_1\gamma_2-\gamma_2\gamma_1\right)\right)d^e\right)\Bigg\}|\Omega\rangle\\
=&\epsilon^{abc}\epsilon^{ade}\Bigg\{\ \bar{b}^b\left(1-\frac{\alpha}{4}\left(\gamma_1\gamma_2-\gamma_2\gamma_1\right)\right)\Gamma_1\left(1-\frac{\alpha}{4}\left(\gamma_1\gamma_2-\gamma_2\gamma_1\right)\right)\left[\bar{b}^c\right]^T\\
&\left(\left[d^d\right]^T\left(1+\frac{\alpha}{4}\left(\gamma_1\gamma_2-\gamma_2\gamma_1\right)\right)\Gamma_2\left(1+\frac{\alpha}{4}\left(\gamma_1\gamma_2-\gamma_2\gamma_1\right)\right)u^e\right.\\
&\left.-\left[u^d\right]^T\left(1+\frac{\alpha}{4}\left(\gamma_1\gamma_2-\gamma_2\gamma_1\right)\right)\Gamma_2\left(1+\frac{\alpha}{4}\left(\gamma_1\gamma_2-\gamma_2\gamma_1\right)\right)d^e\right)\Bigg\}|\Omega\rangle\\
=&\epsilon^{abc}\epsilon^{ade}\Bigg\{\ \bar{b}^b\left[\Gamma_1-\frac{\alpha}{4}\left(\gamma_1\gamma_2-\gamma_2\gamma_1\right)\Gamma_1-\Gamma_1\frac{\alpha}{4}\left(\gamma_1\gamma_2-\gamma_2\gamma_1\right)\right]\left[\bar{b}^c\right]^T\\
&\left(\left[d^d\right]^T\left[\Gamma_2+\frac{\alpha}{4}\left(\gamma_1\gamma_2-\gamma_2\gamma_1\right)\Gamma_2+\Gamma_2\frac{\alpha}{4}\left(\gamma_1\gamma_2-\gamma_2\gamma_1\right)\right]u^e\right.\\
&\left.-\left[u^d\right]^T\left[\Gamma_2+\frac{\alpha}{4}\left(\gamma_1\gamma_2-\gamma_2\gamma_1\right)\Gamma_2+\Gamma_2\frac{\alpha}{4}\left(\gamma_1\gamma_2-\gamma_2\gamma_1\right)\right]d^e\right)\Bigg\}|\Omega\rangle\\
=&\epsilon^{abc}\epsilon^{ade}\Bigg\{\ \bar{b}^b\left(\Gamma_1-\frac{\alpha}{2}\left\{\gamma_1\gamma_2,\Gamma_1\right\}\right)\left[\bar{b}^c\right]^T\\
&\left(\left[d^d\right]^T\left(\Gamma_2+\frac{\alpha}{2}\left\{\gamma_1\gamma_2,\Gamma_2\right\}\right)u^e-\left[u^d\right]^T\left(\Gamma_2+\frac{\alpha}{2}\left\{\gamma_1\gamma_2,\Gamma_2\right\}\right)d^e\right)\Bigg\}|\Omega\rangle\\
=&\epsilon^{abc}\epsilon^{ade}\Bigg\{\ \bar{b}^b\Gamma_1\left[\bar{b}^c\right]^T\left(\left[d^d\right]^T\Gamma_2 u^e-\left[u^d\right]^T\Gamma_2 d^e\right)\\
&-\frac{\alpha}{2}\left[-\bar{b}^b\Gamma_1\left[\bar{b}^c\right]^T\left(\left[d^d\right]^T\left\{\gamma_1\gamma_2,\Gamma_2\right\}u^e-\left[u^d\right]^T\left\{\gamma_1\gamma_2,\Gamma_2\right\}d^e\right)\right.\\
&\left.+\bar{b}^b\left\{\gamma_1\gamma_2,\Gamma_1\right\}\left[\bar{b}^c\right]^T\left(\left[d^d\right]^T\Gamma_2 u^e-\left[u^d\right]^T\Gamma_2 d^e\right)\right]\Bigg\}|\Omega\rangle
\end{aligned}
\tag{C.30}
$$

Evaluating this expression with $\Gamma_1=\gamma_j\mathcal{C}$, $\Gamma_2=\mathcal{C}\gamma_5$, and $\mathcal{C}=i\gamma_2\gamma_0$, and considering again all three spatial directions $j=1,2,3$, we find:

$$
\begin{aligned}
\{\gamma_1\gamma_2,\mathcal{C}\gamma_5\}&=0\\
\{\gamma_1\gamma_2,\gamma_1\mathcal{C}\}&=+2\gamma_2\mathcal{C}\\
\{\gamma_1\gamma_2,\gamma_2\mathcal{C}\}&=-2\gamma_1\mathcal{C}\\
\{\gamma_1\gamma_2,\gamma_3\mathcal{C}\}&=0
\end{aligned}
\tag{C.31}
$$

$\underline{j=1}$:

$$\begin{aligned}
&\mathcal{R}_3(\alpha)|\Psi_1\rangle \\
=&\epsilon^{abc}\epsilon^{ade}\Big\{\bar{b}^b\mathcal{C}\gamma_1\left[\bar{b}^c\right]^T\left(\left[d^d\right]^T\mathcal{C}\gamma_5 u^e-\left[u^d\right]^T\mathcal{C}\gamma_5 d^e\right) \\
&-\alpha\left[\bar{b}^b\mathcal{C}\gamma_2\left[\bar{b}^c\right]^T\left(\left[d^d\right]^T\mathcal{C}\gamma_5 u^e-\left[u^d\right]^T\mathcal{C}\gamma_5 d^e\right)\right]\Big\}|\Omega\rangle=|\Psi_1\rangle-\alpha|\Psi_2\rangle
\end{aligned} \tag{C.32}$$

$\underline{j=2}$:

$$\begin{aligned}
&\mathcal{R}_3(\alpha)|\Psi_2\rangle \\
=&\epsilon^{abc}\epsilon^{ade}\Big\{\bar{b}^b\mathcal{C}\gamma_2\left[\bar{b}^c\right]^T\left(\left[d^d\right]^T\mathcal{C}\gamma_5 u^e-\left[u^d\right]^T\mathcal{C}\gamma_5 d^e\right) \\
&+\alpha\left[\bar{b}^b\mathcal{C}\gamma_1\left[\bar{b}^c\right]^T\left(\left[d^d\right]^T\mathcal{C}\gamma_5 u^e-\left[u^d\right]^T\mathcal{C}\gamma_5 d^e\right)\right]\Big\}|\Omega\rangle=|\Psi_2\rangle+\alpha|\Psi_1\rangle
\end{aligned} \tag{C.33}$$

$\underline{j=3}$:

$$\begin{aligned}
&\mathcal{R}_3(\alpha)|\Psi_3\rangle \\
=&\epsilon^{abc}\epsilon^{ade}\left\{\bar{b}^b\mathcal{C}\gamma_2\left[\bar{b}^c\right]^T\left(\left[d^d\right]^T\mathcal{C}\gamma_5 u^e-\left[u^d\right]^T\mathcal{C}\gamma_5 d^e\right)\right\}|\Omega\rangle=|\Psi_3\rangle
\end{aligned} \tag{C.34}$$

Hence, we find the same transformation behaviour for the spinor $|\Psi\rangle$ as illustrated for the previous operators. Therefore, with the analogous computation, we conclude that the angular momentum is $J=1$.

Consequently, we have proven that all operators generate angular momentum $J=1$.

C.2.3 Isospin

Finally, we consider the isospin for the three creating operators using the isospin operator (A.4) and the vector notation for the u and d spinors in the SU(2) isospin space:

$$u=\begin{pmatrix}1\\0\end{pmatrix}\qquad d=\begin{pmatrix}0\\1\end{pmatrix} \tag{C.35}$$

We compute the I_3 component and apply the expansion:

$$\mathcal{I}_3(\alpha)=\exp\left(\frac{i\alpha}{2}\sigma_3\right)=1+\frac{i\alpha}{2}\sigma_3+\mathcal{O}(\alpha^2) \tag{C.36}$$

The operator I_3 acts only on the SU(2) spinors u and d. The b quarks are unaffected.

We start again with the Isospin for $\mathcal{O}_{BB^*}$ and $\mathcal{O}_{B^*B^*}$ and conclude with $\mathcal{O}_{Dd}$.

For $\mathcal{O}_{BB^*}$ and $\mathcal{O}_{B^*B^*}$:

For the two mesonic operators, we find:

$$
\begin{aligned}
&\mathcal{I}_3(\alpha)\left\{\bar{b}\Gamma_1 d\,\bar{b}\Gamma_2 u - \bar{b}\Gamma_1 u\,\bar{b}\Gamma_2 d\right\}|\Omega\rangle \\
=&\mathcal{I}_3(\alpha)\left\{\bar{b}\Gamma_1\begin{pmatrix}0\\1\end{pmatrix}\bar{b}\Gamma_2\begin{pmatrix}1\\0\end{pmatrix} - \bar{b}\Gamma_1\begin{pmatrix}1\\0\end{pmatrix}\bar{b}\Gamma_2\begin{pmatrix}0\\1\end{pmatrix}\right\}|\Omega\rangle \\
=&\left\{\bar{b}\Gamma_1\left[1+\frac{i\alpha}{2}\sigma_3\right]\begin{pmatrix}0\\1\end{pmatrix}\bar{b}\Gamma_2\left[1+\frac{i\alpha}{2}\sigma_3\right]\begin{pmatrix}1\\0\end{pmatrix}\right. \\
&\left.-\bar{b}\Gamma_1\left[1+\frac{i\alpha}{2}\sigma_3\right]\begin{pmatrix}1\\0\end{pmatrix}\bar{b}\Gamma_2\left[1+\frac{i\alpha}{2}\sigma_3\right]\begin{pmatrix}0\\1\end{pmatrix}\right\}|\Omega\rangle \\
=&\left\{\left[\bar{b}\Gamma_1\begin{pmatrix}0\\1\end{pmatrix}+\bar{b}\Gamma_1\frac{i\alpha}{2}\begin{pmatrix}0\\-1\end{pmatrix}\right]\left[\bar{b}\Gamma_2\begin{pmatrix}1\\0\end{pmatrix}+\bar{b}\Gamma_2\frac{i\alpha}{2}\begin{pmatrix}1\\0\end{pmatrix}\right]\right. \\
&\left.-\left[\bar{b}\Gamma_1\begin{pmatrix}1\\0\end{pmatrix}+\bar{b}\Gamma_1\frac{i\alpha}{2}\begin{pmatrix}1\\0\end{pmatrix}\right]\left[\bar{b}\Gamma_2\begin{pmatrix}0\\1\end{pmatrix}+\bar{b}\Gamma_2\frac{i\alpha}{2}\begin{pmatrix}0\\-1\end{pmatrix}\right]\right\}|\Omega\rangle \\
=&\left\{\bar{b}\Gamma_1\begin{pmatrix}0\\1\end{pmatrix}\bar{b}\Gamma_2\begin{pmatrix}1\\0\end{pmatrix} - \bar{b}\Gamma_1\begin{pmatrix}1\\0\end{pmatrix}\bar{b}\Gamma_2\begin{pmatrix}0\\1\end{pmatrix}\right. \\
&+i\frac{\alpha}{2}\left[\bar{b}\Gamma_1\begin{pmatrix}0\\1\end{pmatrix}\bar{b}\Gamma_2\begin{pmatrix}1\\0\end{pmatrix} - \bar{b}\Gamma_1\begin{pmatrix}0\\1\end{pmatrix}\bar{b}\Gamma_2\begin{pmatrix}1\\0\end{pmatrix}\right. \\
&\left.\left.+\bar{b}\Gamma_1\begin{pmatrix}1\\0\end{pmatrix}\bar{b}\Gamma_2\begin{pmatrix}0\\1\end{pmatrix} - \bar{b}\Gamma_1\begin{pmatrix}1\\0\end{pmatrix}\bar{b}\Gamma_2\begin{pmatrix}0\\1\end{pmatrix}\right]\right\}|\Omega\rangle \\
=&\left\{\bar{b}\Gamma_1 d\bar{b}\Gamma_2 u - \bar{b}\Gamma_1 u\bar{b}\Gamma_2 d\right\}|\Omega\rangle
\end{aligned}
\tag{C.37}
$$

Using $\mathcal{I}_3(\alpha) = \exp(i\alpha I_3) = 1 + i\alpha I_3 + \mathcal{O}(\alpha^2)$ we conclude that $I_3 = 0$. Repeating the analogous calculation for the other two components yields $I_1 = 0$ and $I_2 = 0$. Consequently, the total isospin is zero ($I = 0$).

For $\mathcal{O}_{Dd}$:

We conclude with the isospin for the diquark-antidiquark operator:

$$
\begin{aligned}
&\mathcal{I}_3(\alpha)\left\{\epsilon^{abc}\bar{b}^b\Gamma_1\left[\bar{b}^c\right]^T\epsilon^{ade}\left(\left[d^d\right]^T\Gamma_2 u^e-\left[u^d\right]^T\Gamma_2 d^e\right)\right\}|\Omega\rangle\\
=&\mathcal{I}_3(\alpha)\left\{\epsilon^{abc}\bar{b}^b\Gamma_1\left[\bar{b}^c\right]^T\epsilon^{ade}\left(\left[\left(\begin{array}{c}0\\1\end{array}\right)^d\right]^T\Gamma_2\left(\begin{array}{c}1\\0\end{array}\right)^e\right.\right.\\
&\left.\left.-\left[\left(\begin{array}{c}1\\0\end{array}\right)^d\right]^T\Gamma_2\left(\begin{array}{c}0\\1\end{array}\right)^e\right)\right\}|\Omega\rangle\\
=&\left\{\epsilon^{abc}\bar{b}^b\Gamma_1\left[\bar{b}^c\right]^T\epsilon^{ade}\left(\left[\left[1+\frac{i\alpha}{2}\sigma_3\right]\left(\begin{array}{c}0\\1\end{array}\right)^d\right]^T\Gamma_2\left[1+\frac{i\alpha}{2}\sigma_3\right]\left(\begin{array}{c}1\\0\end{array}\right)^e\right.\right.\\
&\left.\left.-\left[\left[1+\frac{i\alpha}{2}\sigma_3\right]\left(\begin{array}{c}1\\0\end{array}\right)^d\right]^T\Gamma_2\left[1+\frac{i\alpha}{2}\sigma_3\right]\left(\begin{array}{c}0\\1\end{array}\right)^e\right)\right\}|\Omega\rangle\\
=&\left\{\epsilon^{abc}\bar{b}^b\Gamma_1\left[\bar{b}^c\right]^T\epsilon^{ade}\left(\left[\left(\begin{array}{c}0\\1\end{array}\right)^d+\frac{i\alpha}{2}\left(\begin{array}{c}0\\-1\end{array}\right)^d\right]^T\Gamma_2\left[\left(\begin{array}{c}1\\0\end{array}\right)^e+\frac{i\alpha}{2}\left(\begin{array}{c}1\\0\end{array}\right)^e\right]\right.\right.\\
&\left.\left.-\left[\left(\begin{array}{c}1\\0\end{array}\right)^d+\frac{i\alpha}{2}\left(\begin{array}{c}1\\0\end{array}\right)^d\right]^T\Gamma_2\left[\left(\begin{array}{c}0\\1\end{array}\right)^e+\frac{i\alpha}{2}\left(\begin{array}{c}0\\-1\end{array}\right)^e\right]\right)\right\}|\Omega\rangle\\
=&\left\{\epsilon^{abc}\bar{b}^b\Gamma_1\left[\bar{b}^c\right]^T\epsilon^{ade}\left(\left[\left(\begin{array}{c}0\\1\end{array}\right)^d\right]^T\Gamma_2\left(\begin{array}{c}1\\0\end{array}\right)^e-\left[\left(\begin{array}{c}1\\0\end{array}\right)^d\right]^T\Gamma_2\left(\begin{array}{c}0\\1\end{array}\right)^e\right)\right.\\
&+\frac{i\alpha}{2}\left[-\left[\left(\begin{array}{c}0\\1\end{array}\right)^d\right]^T\Gamma_2\left(\begin{array}{c}1\\0\end{array}\right)^e+\left[\left(\begin{array}{c}0\\1\end{array}\right)^d\right]^T\Gamma_2\left(\begin{array}{c}1\\0\end{array}\right)^e\right.\\
&\left.\left.\left.-\left[\left(\begin{array}{c}1\\0\end{array}\right)^d\right]^T\Gamma_2\left(\begin{array}{c}0\\1\end{array}\right)^e+\left[\left(\begin{array}{c}1\\0\end{array}\right)^d\right]^T\Gamma_2\left(\begin{array}{c}0\\1\end{array}\right)^e\right]\right\}|\Omega\rangle\\
=&\left\{\epsilon^{abc}\bar{b}^b\Gamma_1\left[\bar{b}^c\right]^T\epsilon^{ade}\left(\left[d^d\right]^T\Gamma_2 u^e-\left[u^d\right]^T\Gamma_2 d^e\right)\right\}|\Omega\rangle
\end{aligned}
\tag{C.38}
$$

Finally, we find that $I_3 = 0$. Calculating the other components of the isospin, we get $I_1 = 0$ and $I_2 = 0$. So, the total isospin is $I = 0$.

In conclusion, we have proven that all three creation operators possess the quantum numbers $I(J^P) = 0(1^+)$.

Appendix D

Correlation Matrix Elements

D.1 Type I Correlation Function

For the first class of correlation functions we consider the operator:

$$\mathcal{O}_{BB}(t) = \sum_{\mathbf{x},\mathbf{y}} \bar{b}\Gamma_1^{(1)} d(\mathbf{x},t)\, \bar{b}\Gamma_2^{(1)} u(\mathbf{y},t) - \bar{b}\Gamma_1^{(1)} u(\mathbf{x},t)\, \bar{b}\Gamma_2^{(1)} d(\mathbf{y},t) \tag{D.1}$$

and the associated daggered operator:

$$\mathcal{O}^\dagger_{BB}(t) = \sum_{\mathbf{z},\mathbf{u}} \bar{d}\Gamma_1'^{(2)} b(\mathbf{z},t)\, \bar{u}\Gamma_2'^{(2)} b(\mathbf{u},t) - \bar{u}\Gamma_1'^{(2)} b(\mathbf{z},t)\, \bar{d}\Gamma_2'^{(2)} b(\mathbf{u},t) \tag{D.2}$$

with $\Gamma_1'^{(2)} = \gamma_0 \Gamma_1^{(2)\dagger} \gamma_0$ and $\Gamma_2'^{(2)} = \gamma_0 \Gamma_2^{(2)\dagger} \gamma_0$. We have introduced the upper indices $(1), (2)$ to distinguish between the gamma matrices of the daggered and non-daggered operator. Thus, we are also able to compute off-diagonal matrix elements.

We will now calculate the correlation function $C(t)$ for the two operators $\mathcal{O}_{BB}(t)$ and $\mathcal{O}^\dagger_{BB}(0)$ in Eq. (D.1) and (D.2) using the different Γ matrices presented in (6.35) to (6.38). Note that we use fixed source point locations, so the sums over $\mathbf{z}, \mathbf{u}$ are omitted and $\mathbf{u} = \mathbf{z}$. The correlation function is given by:

$$C(t) = \left\langle \mathcal{O}_{BB}(t) \mathcal{O}^\dagger_{BB}(0) \right\rangle \tag{D.3}$$

$$\begin{aligned} &= \sum_{\mathbf{x},\mathbf{y}} \Big\langle \Big[\bar{b}\Gamma_1^{(1)} d(\mathbf{x},t)\, \bar{b}\Gamma_2^{(1)} u(\mathbf{y},t) - \bar{b}\Gamma_1^{(1)} u(\mathbf{x},t)\, \bar{b}\Gamma_2^{(1)} d(\mathbf{y},t) \Big] \\ &\quad \times \Big[\bar{d}\Gamma_1'^{(2)} b(\mathbf{z},0)\, \bar{u}\Gamma_2'^{(2)} b(\mathbf{z},0) - \bar{u}\Gamma_1'^{(2)} b(\mathbf{z},0)\, \bar{d}\Gamma_2'^{(2)} b(\mathbf{z},0) \Big] \Big\rangle \end{aligned} \tag{D.4}$$

For simplicity, we omit the upper indices of the Γ's but keep in mind that:

$$\Gamma_i \equiv \Gamma_i^{(1)} \qquad \Gamma_i' \equiv \Gamma_i'^{(2)} = \gamma_0 \Gamma_i^{\dagger(2)} \gamma_0 \tag{D.5}$$

Furthermore, we include the space-time arguments of the spinors in the colour and Dirac indices. The replacement condition is:

$$(\mathbf{x},t) \leftrightarrow a \qquad (\mathbf{y},t) \leftrightarrow b \qquad (\mathbf{z},0) \leftrightarrow a',b' \tag{D.6}$$

These conventions improve the readability of the formula while they permit a distinct reassignment at the end of the calculation.
Applying the described proceeding, the correlation function is written as:

$$\begin{aligned} C(t) = \sum_{\mathbf{x},\mathbf{y}} & \Big\langle \Big[\bar{b}^a_A \Gamma_{1AB} d^a_B \, \bar{b}^b_C \Gamma_{2CD} u^b_D - \bar{b}^a_A \Gamma_{1AB} u^a_B \, \bar{b}^b_C \Gamma_{2CD} d^b_D\Big] \\ & \times \Big[\bar{d}^{a'}_{A'} \Gamma'_{1A'B'} b^{a'}_{B'} \, \bar{u}^{b'}_{C'} \Gamma'_{2C'D'} b^{b'}_{D'} - \bar{u}^{a'}_{A'} \Gamma'_{1A'B'} b^{a'}_{B'} \, \bar{d}^{b'}_{C'} \Gamma'_{2C'D'} b^{b'}_{D'}\Big]\Big\rangle \end{aligned} \tag{D.7}$$

$$\begin{aligned} = \sum_{\mathbf{x},\mathbf{y}} & \Gamma_{1AB}\Gamma_{2CD}\Gamma'_{1A'B'}\Gamma'_{2C'D'} \\ & \times \Big\langle \bar{b}^a_A d^a_B \, \bar{b}^b_C u^b_D \, \bar{d}^{a'}_{A'} b^{a'}_{B'} \, \bar{u}^{b'}_{C'} b^{b'}_{D'} - \bar{b}^a_A d^a_B \, \bar{b}^b_C u^b_D \, \bar{u}^{a'}_{A'} b^{a'}_{B'} \, \bar{d}^{b'}_{C'} b^{b'}_{D'} \\ & - \bar{b}^a_A u^a_B \, \bar{b}^b_C d^b_D \, \bar{d}^{a'}_{A'} b^{a'}_{B'} \, \bar{u}^{b'}_{C'} b^{b'}_{D'} + \bar{b}^a_A u^a_B \, \bar{b}^b_C d^b_D \, \bar{u}^{a'}_{A'} b^{a'}_{B'} \, \bar{d}^{b'}_{C'} b^{b'}_{D'} \Big\rangle \end{aligned} \tag{D.8}$$

$$\begin{aligned} = \sum_{\mathbf{x},\mathbf{y}} & \Gamma_{1AB}\Gamma_{2CD}\Gamma'_{1A'B'}\Gamma'_{2C'D'} \\ & \times \Big\langle d^a_B \bar{d}^{a'}_{A'} \, u^b_D \bar{u}^{b'}_{C'} \, \Big(b^{a'}_{B'} \bar{b}^a_A \, b^{b'}_{D'} \bar{b}^b_C - b^{a'}_{B'} \bar{b}^b_C \, b^{b'}_{D'} \bar{b}^a_A\Big) \\ & + \; d^a_B \bar{d}^{b'}_{C'} \, u^b_D \bar{u}^{a'}_{A'} \, \Big(b^{a'}_{B'} \bar{b}^a_A \, b^{b'}_{D'} \bar{b}^b_C - b^{a'}_{B'} \bar{b}^b_C \, b^{b'}_{D'} \bar{b}^a_A\Big) \\ & + \; d^b_D \bar{d}^{a'}_{A'} \, u^a_B \bar{u}^{b'}_{C'} \, \Big(b^{a'}_{B'} \bar{b}^a_A \, b^{b'}_{D'} \bar{b}^b_C - b^{a'}_{B'} \bar{b}^b_C \, b^{b'}_{D'} \bar{b}^a_A\Big) \\ & + \; d^b_D \bar{d}^{b'}_{C'} \, u^a_B \bar{u}^{a'}_{A'} \, \Big(b^{a'}_{B'} \bar{b}^a_A \, b^{b'}_{D'} \bar{b}^b_C - b^{a'}_{B'} \bar{b}^b_C \, b^{b'}_{D'} \bar{b}^a_A\Big)\Big\rangle \end{aligned} \tag{D.9}$$

Now rewriting the quark propagators as $u^a_A \bar{u}^b_B \equiv U^{ab}_{AB}$ and using the isospin symmetry $D = U$ yields:

$$\begin{aligned} = \sum_{\mathbf{x},\mathbf{y}} & \Gamma_{1AB}\Gamma_{2CD}\Gamma'_{1A'B'}\Gamma'_{2C'D'} \\ & \times \Big\langle U^{aa'}_{BA'} \, U^{bb'}_{DC'} \, \Big(B^{a'a}_{B'A} \, B^{b'b}_{D'C} - B^{a'b}_{B'C} \, B^{b'a}_{D'A}\Big) \\ & + \; U^{ab'}_{BC'} \, U^{ba'}_{DA'} \, \Big(B^{a'a}_{B'A} \, B^{b'b}_{D'C} - B^{a'b}_{B'C} \, B^{b'a}_{D'A}\Big) \\ & + \; U^{ba'}_{DA'} \, U^{ab'}_{BC'} \, \Big(B^{a'a}_{B'A} \, B^{b'b}_{D'C} - B^{a'b}_{B'C} \, B^{b'a}_{D'A}\Big) \\ & + \; U^{bb'}_{DC'} \, U^{aa'}_{BA'} \, \Big(B^{a'a}_{B'A} \, B^{b'b}_{D'C} - B^{a'b}_{B'C} \, B^{b'a}_{D'A}\Big)\Big\rangle \end{aligned} \tag{D.10}$$

$$\begin{aligned} = \sum_{\mathbf{x},\mathbf{y}} & 2 \cdot \Gamma_{1AB}\Gamma_{2CD}\Gamma'_{1A'B'}\Gamma'_{2C'D'} \\ & \times \Big\langle U^{aa'}_{BA'} \, U^{bb'}_{DC'} \, B^{a'a}_{B'A} \, B^{b'b}_{D'C} - U^{aa'}_{BA'} \, U^{bb'}_{DC'} B^{a'b}_{B'C} \, B^{b'a}_{D'A} \\ & + \; U^{ab'}_{BC'} \, U^{ba'}_{DA'} \, B^{a'a}_{B'A} \, B^{b'b}_{D'C} - U^{ab'}_{BC'} \, U^{ba'}_{DA'} B^{a'b}_{B'C} \, B^{b'a}_{D'A}\Big\rangle \end{aligned} \tag{D.11}$$

Multiplying the Γ matrices to each addend, we can express the correlation function by traces. Furthermore, in the next step the space-time arguments are re-established due to the conventions given in Eq. (D.6). To improve readability, we use four-vector notation for the space-time arguments. We apply the γ_5-hermiticity for the heavy quark propagators.

$$\begin{aligned}
&= 2 \cdot \sum_{\mathbf{x},\mathbf{y}} \langle \mathrm{Tr}\left[U(x,z)\Gamma_1' B(z,x)\Gamma_1\right] \mathrm{Tr}\left[U(y,z)\Gamma_2' B(z,y)\Gamma_2\right] \\
&\quad - \mathrm{Tr}\left[U(x,z)\Gamma_1' B(z,y)\Gamma_2 U(y,z)\Gamma_2' B(z,x)\Gamma_1\right] \\
&\quad + \mathrm{Tr}\left[U(x,z)\Gamma_2' B(z,y)\Gamma_2 U(y,z)\Gamma_1' B(z,x)\Gamma_1\right] \\
&\quad - \mathrm{Tr}\left[U(x,z)\Gamma_2' B(z,x)\Gamma_1\right] \mathrm{Tr}\left[U(y,z)\Gamma_1' B(z,y)\Gamma_2\right] \rangle
\end{aligned} \tag{D.12}$$

$$\begin{aligned}
&= 2 \cdot \sum_{\mathbf{x},\mathbf{y}} \Big\langle \mathrm{Tr}\Big[U(x,z)\Gamma_1'\gamma_5 B(x,z)^\dagger \gamma_5 \Gamma_1\Big] \mathrm{Tr}\Big[U(y,z)\Gamma_2'\gamma_5 B(y,z)^\dagger \gamma_5 \Gamma_2\Big] \\
&\quad - \mathrm{Tr}\Big[U(x,z)\Gamma_1'\gamma_5 B(y,z)^\dagger \gamma_5 \Gamma_2 U(y,z)\Gamma_2'\gamma_5 B(x,z)^\dagger \gamma_5 \Gamma_1\Big] \\
&\quad + \mathrm{Tr}\Big[U(x,z)\Gamma_2'\gamma_5 B(y,z)^\dagger \gamma_5 \Gamma_2 U(y,z)\Gamma_1'\gamma_5 B(x,z)^\dagger \gamma_5 \Gamma_1\Big] \\
&\quad - \mathrm{Tr}\Big[U(x,z)\Gamma_2'\gamma_5 B(x,z)^\dagger \gamma_5 \Gamma_1\Big] \mathrm{Tr}\Big[U(y,z)\Gamma_1'\gamma_5 B(y,z)^\dagger \gamma_5 \Gamma_2\Big] \Big\rangle
\end{aligned} \tag{D.13}$$

We can use the correlation function in Eq. (D.13) now to compute the different correlation functions by inserting the appropriate Γ matrices for the cases of interest. For completeness, the Γ's for the different operators are again listed below:

- $\left\langle \mathcal{O}_{[BB^*](0)}(t)\mathcal{O}^\dagger_{[BB^*](0)}(0)\right\rangle$:

$$\begin{aligned}
\Gamma_1 &= \gamma_5 & \Gamma_2 &= \gamma_j \\
\Gamma_1' &= \gamma_0\gamma_5^\dagger\gamma_0 = -\gamma_5 & \Gamma_2' &= \gamma_0\gamma_j^\dagger\gamma_0 = -\gamma_j
\end{aligned} \tag{D.14}$$

- $\left\langle \mathcal{O}_{[BB^*](0)}(t)\mathcal{O}^\dagger_{[B^*B^*](0)}(0)\right\rangle$:

$$\begin{aligned}
\Gamma_1 &= \gamma_5 & \Gamma_2 &= \gamma_i \\
\epsilon_{ijk}\ \Big(\Gamma_1' &= \gamma_0\gamma_j^\dagger\gamma_0 = -\gamma_j & \Gamma_2' &= \gamma_0\gamma_k^\dagger\gamma_0 = -\gamma_k\Big)
\end{aligned} \tag{D.15}$$

- $\left\langle \mathcal{O}_{[B^*B^*](0)}(t)\mathcal{O}^\dagger_{[BB^*](0)}(0)\right\rangle$:

$$\begin{aligned}
\epsilon_{ijk}\ \Big(\Gamma_1 &= \gamma_j & \Gamma_2 &= \gamma_k\Big) \\
\Gamma_1' &= \gamma_0\gamma_5^\dagger\gamma_0 = -\gamma_5 & \Gamma_2' &= \gamma_0\gamma_i^\dagger\gamma_0 = -\gamma_i
\end{aligned} \tag{D.16}$$

- $\left\langle \mathcal{O}_{[B^*B^*](0)}(t)\mathcal{O}^\dagger_{[B^*B^*](0)}(0)\right\rangle$:

$$\begin{aligned}
\epsilon_{ilm}\ \Big(\Gamma_1 &= \gamma_l & \Gamma_2 &= \gamma_m\ \Big) \\
\epsilon_{ijk}\ \Big(\Gamma_1' &= \gamma_0\gamma_j^\dagger\gamma_0 = -\gamma_j & \Gamma_2' &= \gamma_0\gamma_k^\dagger\gamma_0 = -\gamma_k\ \Big)
\end{aligned} \tag{D.17}$$

Inserting this in Eq. (D.13) yields the specific correlation function. Derivations and the final complete expressions are listed below:

Matrix element C_{11}:

$$\begin{aligned}
&\left\langle \mathcal{O}_{[BB^*](0)}(t)\mathcal{O}^\dagger_{[BB^*](0)}(0)\right\rangle \\
&= 2\cdot\sum_{\mathbf{x}}\Big\langle \mathrm{Tr}\left[U(x,z)B(x,z)^\dagger\right]\mathrm{Tr}\left[U(x,z)\gamma_j\gamma_5 B(x,z)^\dagger\gamma_5\gamma_j\right] \\
&\quad -\mathrm{Tr}\left[U(x,z)B(x,z)^\dagger\gamma_5\gamma_j U(x,z)\gamma_j\gamma_5 B(x,z)^\dagger\right] \\
&\quad +\mathrm{Tr}\left[U(x,z)\gamma_j\gamma_5 B(x,z)^\dagger\gamma_5\gamma_j U(x,z)B(x,z)^\dagger\right] \\
&\quad -\mathrm{Tr}\left[U(x,z)\gamma_j\gamma_5 B(x,z)^\dagger\right]\mathrm{Tr}\left[U(x,z)B(x,z)^\dagger\gamma_5\gamma_j\right]\Big\rangle
\end{aligned} \tag{D.18}$$

Matrix element C_{12}:

$$\begin{aligned}
&\left\langle \mathcal{O}_{[BB^*](0)}(t)\mathcal{O}^\dagger_{[B^*B^*](0)}(0)\right\rangle \\
&= 2\cdot\sum_{\mathbf{x}}\Big\langle \epsilon_{ijk}\mathrm{Tr}\left[U(x,z)\gamma_0\gamma_j^\dagger\gamma_0\gamma_5 B(x,z)^\dagger\right]\mathrm{Tr}\left[U(x,z)\gamma_0\gamma_k^\dagger\gamma_0\gamma_5 B(x,z)^\dagger\gamma_5\gamma_i\right] \\
&\quad -\epsilon_{ijk}\mathrm{Tr}\left[U(x,z)\gamma_0\gamma_j^\dagger\gamma_0\gamma_5 B(x,z)^\dagger\gamma_5\gamma_i U(x,z)\gamma_0\gamma_k^\dagger\gamma_0\gamma_5 B(x,z)^\dagger\right] \\
&\quad +\epsilon_{ijk}\mathrm{Tr}\left[U(x,z)\gamma_0\gamma_k^\dagger\gamma_0\gamma_5 B(x,z)^\dagger\gamma_5\gamma_i U(x,z)\gamma_0\gamma_j^\dagger\gamma_0\gamma_5 B(x,z)^\dagger\right] \\
&\quad -\epsilon_{ijk}\mathrm{Tr}\left[U(x,z)\gamma_0\gamma_k^\dagger\gamma_0\gamma_5 B(x,z)^\dagger\right]\mathrm{Tr}\left[U(x,z)\gamma_0\gamma_j^\dagger\gamma_0\gamma_5 B(x,z)^\dagger\gamma_5\gamma_i\right]\Big\rangle \\
&= 4\cdot\sum_{\mathbf{x}}\Big\langle \mathrm{Tr}\left[U(x,z)\gamma_2\gamma_5 B(x,z)^\dagger\right]\mathrm{Tr}\left[U(x,z)\gamma_3\gamma_5 B(x,z)^\dagger\gamma_5\gamma_1\right] \\
&\quad +\mathrm{Tr}\left[U(x,z)\gamma_1\gamma_5 B(x,z)^\dagger\right]\mathrm{Tr}\left[U(x,z)\gamma_2\gamma_5 B(x,z)^\dagger\gamma_5\gamma_3\right] \\
&\quad +\mathrm{Tr}\left[U(x,z)\gamma_3\gamma_5 B(x,z)^\dagger\right]\mathrm{Tr}\left[U(x,z)\gamma_1\gamma_5 B(x,z)^\dagger\gamma_5\gamma_2\right] \\
&\quad -\mathrm{Tr}\left[U(x,z)\gamma_2\gamma_5 B(x,z)^\dagger\gamma_5\gamma_1 U(x,z)\gamma_3\gamma_5 B(x,z)^\dagger\right] \\
&\quad -\mathrm{Tr}\left[U(x,z)\gamma_3\gamma_5 B(x,z)^\dagger\gamma_5\gamma_2 U(x,z)\gamma_1\gamma_5 B(x,z)^\dagger\right] \\
&\quad -\mathrm{Tr}\left[U(x,z)\gamma_1\gamma_5 B(x,z)^\dagger\gamma_5\gamma_3 U(x,z)\gamma_2\gamma_5 B(x,z)^\dagger\right] \\
&\quad +\mathrm{Tr}\left[U(x,z)\gamma_3\gamma_5 B(x,z)^\dagger\gamma_5\gamma_1 U(x,z)\gamma_2\gamma_5 B(x,z)^\dagger\right] \\
&\quad +\mathrm{Tr}\left[U(x,z)\gamma_2\gamma_5 B(x,z)^\dagger\gamma_5\gamma_3 U(x,z)\gamma_1\gamma_5 B(x,z)^\dagger\right] \\
&\quad +\mathrm{Tr}\left[U(x,z)\gamma_1\gamma_5 B(x,z)^\dagger\gamma_5\gamma_2 U(x,z)\gamma_3\gamma_5 B(x,z)^\dagger\right] \\
&\quad -\mathrm{Tr}\left[U(x,z)\gamma_3\gamma_5 B(x,z)^\dagger\right]\mathrm{Tr}\left[U(x,z)\gamma_2\gamma_5 B(x,z)^\dagger\gamma_5\gamma_1\right] \\
&\quad -\mathrm{Tr}\left[U(x,z)\gamma_2\gamma_5 B(x,z)^\dagger\right]\mathrm{Tr}\left[U(x,z)\gamma_1\gamma_5 B(x,z)^\dagger\gamma_5\gamma_3\right] \\
&\quad -\mathrm{Tr}\left[U(x,z)\gamma_1\gamma_5 B(x,z)^\dagger\right]\mathrm{Tr}\left[U(x,z)\gamma_3\gamma_5 B(x,z)^\dagger\gamma_5\gamma_2\right]\Big\rangle
\end{aligned} \tag{D.19}$$

Matrix element C_{21}:

$$\begin{aligned}
&\left\langle \mathcal{O}_{[B^*B^*](0)}(t)\mathcal{O}^\dagger_{[BB^*](0)}(0)\right\rangle \\
&= 2\cdot\sum_{\mathbf{x}}\epsilon_{ijk}\Big\langle \mathrm{Tr}\left[U(x,z)B(x,z)^\dagger\gamma_5\gamma_j\right]\mathrm{Tr}\left[U(x,z)\gamma_i\gamma_5 B(x,z)^\dagger\gamma_5\gamma_k\right] \\
&\quad -\mathrm{Tr}\left[U(x,z)B(x,z)^\dagger\gamma_5\gamma_k U(x,z)\gamma_i\gamma_5 B(x,z)^\dagger\gamma_5\gamma_j\right] \\
&\quad +\mathrm{Tr}\left[U(x,z)\gamma_i\gamma_5 B(x,z)^\dagger\gamma_5\gamma_k U(x,z)B(x,z)^\dagger\gamma_5\gamma_j\right] \\
&\quad -\mathrm{Tr}\left[U(x,z)\gamma_i\gamma_5 B(x,z)^\dagger\gamma_5\gamma_j\right]\mathrm{Tr}\left[U(x,z)B(x,z)^\dagger\gamma_5\gamma_k\right]\Big\rangle
\end{aligned} \tag{D.21}$$

$$\begin{aligned}
&= 4\cdot\sum_{\mathbf{x}}\Big\langle \mathrm{Tr}\left[U(x,z)B(x,z)^\dagger\gamma_5\gamma_2\right]\mathrm{Tr}\left[U(x,z)\gamma_1\gamma_5 B(x,z)^\dagger\gamma_5\gamma_3\right] \\
&\quad \mathrm{Tr}\left[U(x,z)B(x,z)^\dagger\gamma_5\gamma_3\right]\mathrm{Tr}\left[U(x,z)\gamma_2\gamma_5 B(x,z)^\dagger\gamma_5\gamma_1\right] \\
&\quad \mathrm{Tr}\left[U(x,z)B(x,z)^\dagger\gamma_5\gamma_1\right]\mathrm{Tr}\left[U(x,z)\gamma_3\gamma_5 B(x,z)^\dagger\gamma_5\gamma_2\right] \\
&\quad -\mathrm{Tr}\left[U(x,z)B(x,z)^\dagger\gamma_5\gamma_3 U(x,z)\gamma_1\gamma_5 B(x,z)^\dagger\gamma_5\gamma_2\right] \\
&\quad -\mathrm{Tr}\left[U(x,z)B(x,z)^\dagger\gamma_5\gamma_1 U(x,z)\gamma_2\gamma_5 B(x,z)^\dagger\gamma_5\gamma_3\right] \\
&\quad -\mathrm{Tr}\left[U(x,z)B(x,z)^\dagger\gamma_5\gamma_2 U(x,z)\gamma_3\gamma_5 B(x,z)^\dagger\gamma_5\gamma_1\right] \\
&\quad +\mathrm{Tr}\left[U(x,z)\gamma_1\gamma_5 B(x,z)^\dagger\gamma_5\gamma_3 U(x,z)B(x,z)^\dagger\gamma_5\gamma_2\right] \\
&\quad +\mathrm{Tr}\left[U(x,z)\gamma_2\gamma_5 B(x,z)^\dagger\gamma_5\gamma_1 U(x,z)B(x,z)^\dagger\gamma_5\gamma_3\right] \\
&\quad +\mathrm{Tr}\left[U(x,z)\gamma_3\gamma_5 B(x,z)^\dagger\gamma_5\gamma_2 U(x,z)B(x,z)^\dagger\gamma_5\gamma_1\right] \\
&\quad -\mathrm{Tr}\left[U(x,z)\gamma_1\gamma_5 B(x,z)^\dagger\gamma_5\gamma_2\right]\mathrm{Tr}\left[U(x,z)B(x,z)^\dagger\gamma_5\gamma_3\right] \\
&\quad -\mathrm{Tr}\left[U(x,z)\gamma_2\gamma_5 B(x,z)^\dagger\gamma_5\gamma_3\right]\mathrm{Tr}\left[U(x,z)B(x,z)^\dagger\gamma_5\gamma_1\right] \\
&\quad -\mathrm{Tr}\left[U(x,z)\gamma_3\gamma_5 B(x,z)^\dagger\gamma_5\gamma_1\right]\mathrm{Tr}\left[U(x,z)B(x,z)^\dagger\gamma_5\gamma_2\right]\Big\rangle
\end{aligned} \tag{D.22}$$

Matrix element C_{22}:

$$\begin{aligned}
&\left\langle \mathcal{O}_{[B^*B^*](0)}(t)\mathcal{O}^\dagger_{[B^*B^*](0)}(0)\right\rangle \\
&= 2\cdot\sum_{\mathbf{x}}\Big\langle \mathrm{Tr}\left[U(x,z)\Gamma_1'\gamma_5 B(x,z)^\dagger\gamma_5\Gamma_1\right]\mathrm{Tr}\left[U(x,z)\Gamma_2'\gamma_5 B(x,z)^\dagger\gamma_5\Gamma_2\right] \\
&\quad -\mathrm{Tr}\left[U(x,z)\Gamma_1'\gamma_5 B(x,z)^\dagger\gamma_5\Gamma_2 U(x,z)\Gamma_2'\gamma_5 B(x,z)^\dagger\gamma_5\Gamma_1\right] \\
&\quad +\mathrm{Tr}\left[U(x,z)\Gamma_2'\gamma_5 B(x,z)^\dagger\gamma_5\Gamma_2 U(x,z)\Gamma_1'\gamma_5 B(x,z)^\dagger\gamma_5\Gamma_1\right] \\
&\quad -\mathrm{Tr}\left[U(x,z)\Gamma_2'\gamma_5 B(x,z)^\dagger\gamma_5\Gamma_1\right]\mathrm{Tr}\left[U(x,z)\Gamma_1'\gamma_5 B(x,z)^\dagger\gamma_5\Gamma_2\right]\Big\rangle
\end{aligned} \tag{D.23}$$

$$
\begin{aligned}
&= 2 \cdot \sum_{\mathbf{x}} \epsilon_{ijk}\epsilon_{ilm} \\
&\quad \Big\langle \mathrm{Tr}\left[U(x,z)\gamma_j\gamma_5 B(x,z)^\dagger \gamma_5\gamma_l\right] \mathrm{Tr}\left[U(x,z)\gamma_k\gamma_5 B(x,z)^\dagger\gamma_5\gamma_m\right] \\
&\quad -\mathrm{Tr}\left[U(x,z)\gamma_j\gamma_5 B(x,z)^\dagger\gamma_5\gamma_m U(x,z)\gamma_k\gamma_5 B(x,z)^\dagger\gamma_5\gamma_l\right] \\
&\quad +\mathrm{Tr}\left[U(x,z)\gamma_k\gamma_5 B(x,z)^\dagger\gamma_5\gamma_m U(x,z)\gamma_j\gamma_5 B(x,z)^\dagger\gamma_5\gamma_l\right] \\
&\quad -\mathrm{Tr}\left[U(x,z)\gamma_k\gamma_5 B(x,z)^\dagger\gamma_5\gamma_l\right] \mathrm{Tr}\left[U(x,z)\gamma_j\gamma_5 B(x,z)^\dagger\gamma_5\gamma_m\right]\Big\rangle
\end{aligned}
\tag{D.24}
$$

$$
\begin{aligned}
&= 4 \cdot \sum_{\mathbf{x}} \sum_{j,k;j\neq k} \\
&\quad \Big\langle \mathrm{Tr}\left[U(x,z)\gamma_j\gamma_5 B(x,z)^\dagger \gamma_5\gamma_j\right] \mathrm{Tr}\left[U(x,z)\gamma_k\gamma_5 B(x,z)^\dagger\gamma_5\gamma_k\right] \\
&\quad -\mathrm{Tr}\left[U(x,z)\gamma_j\gamma_5 B(x,z)^\dagger\gamma_5\gamma_k U(x,z)\gamma_k\gamma_5 B(x,z)^\dagger\gamma_5\gamma_j\right] \\
&\quad +\mathrm{Tr}\left[U(x,z)\gamma_j\gamma_5 B(x,z)^\dagger\gamma_5\gamma_j U(x,z)\gamma_k\gamma_5 B(x,z)^\dagger\gamma_5\gamma_k\right] \\
&\quad -\mathrm{Tr}\left[U(x,z)\gamma_j\gamma_5 B(x,z)^\dagger\gamma_5\gamma_k\right] \mathrm{Tr}\left[U(x,z)\gamma_k\gamma_5 B(x,z)^\dagger\gamma_5\gamma_j\right]\Big\rangle
\end{aligned}
\tag{D.25}
$$

Matrix element C_{41}:

$$
\begin{aligned}
&\left\langle \mathcal{O}_{B(0)B^*(0)}(t)\mathcal{O}^\dagger_{[BB^*](0)}(0)\right\rangle \\
&= 2 \cdot \sum_{\mathbf{x},\mathbf{y}} \Big\langle \mathrm{Tr}\left[U(x,z)B(x,z)^\dagger\right] \mathrm{Tr}\left[U(y,z)\gamma_j\gamma_5 B(y,z)^\dagger\gamma_5\gamma_j\right] \\
&\quad -\mathrm{Tr}\left[U(x,z)B(y,z)^\dagger\gamma_5\gamma_j U(y,z)\gamma_j\gamma_5 B(x,z)^\dagger\right] \\
&\quad +\mathrm{Tr}\left[U(x,z)\gamma_j\gamma_5 B(y,z)^\dagger\gamma_5\gamma_j U(y,z)B(x,z)^\dagger\right] \\
&\quad -\mathrm{Tr}\left[U(x,z)\gamma_j\gamma_5 B(x,z)^\dagger\right] \mathrm{Tr}\left[U(y,z)B(y,z)^\dagger\gamma_5\gamma_j\right]\Big\rangle
\end{aligned}
\tag{D.26}
$$

Matrix element C_{42}:

$$
\begin{aligned}
&\left\langle \mathcal{O}_{B(0)B^*(0)}(t)\mathcal{O}^\dagger_{[B^*B^*](0)}(0)\right\rangle \\
&= 2\cdot\sum_{\mathbf{x},\mathbf{y}}\Big\langle \epsilon_{ijk}\mathrm{Tr}\left[U(x,z)\gamma_0\gamma_j^\dagger\gamma_0\gamma_5 B(x,z)^\dagger\right]\mathrm{Tr}\left[U(y,z)\gamma_0\gamma_k^\dagger\gamma_0\gamma_5 B(y,z)^\dagger\gamma_5\gamma_i\right] \\
&\quad -\epsilon_{ijk}\mathrm{Tr}\left[U(x,z)\gamma_0\gamma_j^\dagger\gamma_0\gamma_5 B(y,z)^\dagger\gamma_5\gamma_i U(y,z)\gamma_0\gamma_k^\dagger\gamma_0\gamma_5 B(x,z)^\dagger\right] \\
&\quad +\epsilon_{ijk}\mathrm{Tr}\left[U(x,z)\gamma_0\gamma_k^\dagger\gamma_0\gamma_5 B(y,z)^\dagger\gamma_5\gamma_i U(y,z)\gamma_0\gamma_j^\dagger\gamma_0\gamma_5 B(x,z)^\dagger\right] \\
&\quad -\epsilon_{ijk}\mathrm{Tr}\left[U(x,z)\gamma_0\gamma_k^\dagger\gamma_0\gamma_5 B(x,z)^\dagger\right]\mathrm{Tr}\left[U(y,z)\gamma_0\gamma_j^\dagger\gamma_0\gamma_5 B(y,z)^\dagger\gamma_5\gamma_i\right]\Big\rangle
\end{aligned}
\tag{D.27}
$$

$$
\begin{aligned}
&= 4\cdot\sum_{\mathbf{x},\mathbf{y}}\Big\langle \mathrm{Tr}\left[U(x,z)\gamma_2\gamma_5 B(x,z)^\dagger\right]\mathrm{Tr}\left[U(y,z)\gamma_3\gamma_5 B(y,z)^\dagger\gamma_5\gamma_1\right] \\
&\quad +\mathrm{Tr}\left[U(x,z)\gamma_1\gamma_5 B(x,z)^\dagger\right]\mathrm{Tr}\left[U(y,z)\gamma_2\gamma_5 B(y,z)^\dagger\gamma_5\gamma_3\right] \\
&\quad +\mathrm{Tr}\left[U(x,z)\gamma_3\gamma_5 B(x,z)^\dagger\right]\mathrm{Tr}\left[U(y,z)\gamma_1\gamma_5 B(y,z)^\dagger\gamma_5\gamma_2\right] \\
&\quad -\mathrm{Tr}\left[U(x,z)\gamma_2\gamma_5 B(y,z)^\dagger\gamma_5\gamma_1 U(y,z)\gamma_3\gamma_5 B(x,z)^\dagger\right] \\
&\quad -\mathrm{Tr}\left[U(x,z)\gamma_3\gamma_5 B(y,z)^\dagger\gamma_5\gamma_2 U(y,z)\gamma_1\gamma_5 B(x,z)^\dagger\right] \\
&\quad -\mathrm{Tr}\left[U(x,z)\gamma_1\gamma_5 B(y,z)^\dagger\gamma_5\gamma_3 U(y,z)\gamma_2\gamma_5 B(x,z)^\dagger\right] \\
&\quad +\mathrm{Tr}\left[U(x,z)\gamma_3\gamma_5 B(y,z)^\dagger\gamma_5\gamma_1 U(y,z)\gamma_2\gamma_5 B(x,z)^\dagger\right] \\
&\quad +\mathrm{Tr}\left[U(x,z)\gamma_2\gamma_5 B(y,z)^\dagger\gamma_5\gamma_3 U(y,z)\gamma_1\gamma_5 B(x,z)^\dagger\right] \\
&\quad +\mathrm{Tr}\left[U(x,z)\gamma_1\gamma_5 B(y,z)^\dagger\gamma_5\gamma_2 U(y,z)\gamma_3\gamma_5 B(x,z)^\dagger\right] \\
&\quad -\mathrm{Tr}\left[U(x,z)\gamma_3\gamma_5 B(x,z)^\dagger\right]\mathrm{Tr}\left[U(y,z)\gamma_2\gamma_5 B(y,z)^\dagger\gamma_5\gamma_1\right] \\
&\quad -\mathrm{Tr}\left[U(x,z)\gamma_2\gamma_5 B(x,z)^\dagger\right]\mathrm{Tr}\left[U(y,z)\gamma_1\gamma_5 B(y,z)^\dagger\gamma_5\gamma_3\right] \\
&\quad -\mathrm{Tr}\left[U(x,z)\gamma_1\gamma_5 B(x,z)^\dagger\right]\mathrm{Tr}\left[U(y,z)\gamma_3\gamma_5 B(y,z)^\dagger\gamma_5\gamma_2\right]\Big\rangle
\end{aligned}
\tag{D.28}
$$

Matrix element C_{51}:

$$
\begin{aligned}
&\left\langle \mathcal{O}_{B^*(0)B^*(0)}(t)\mathcal{O}^\dagger_{[BB^*](0)}(0)\right\rangle \\
&= 4\cdot\sum_{\mathbf{x},\mathbf{y}}\Big\langle \mathrm{Tr}\left[U(x,z)B(x,z)^\dagger\gamma_5\gamma_2\right]\mathrm{Tr}\left[U(y,z)\gamma_1\gamma_5 B(y,z)^\dagger\gamma_5\gamma_3\right] \\
&\quad \mathrm{Tr}\left[U(x,z)B(x,z)^\dagger\gamma_5\gamma_3\right]\mathrm{Tr}\left[U(y,z)\gamma_2\gamma_5 B(y,z)^\dagger\gamma_5\gamma_1\right] \\
&\quad \mathrm{Tr}\left[U(x,z)B(x,z)^\dagger\gamma_5\gamma_1\right]\mathrm{Tr}\left[U(y,z)\gamma_3\gamma_5 B(y,z)^\dagger\gamma_5\gamma_2\right] \\
&\quad -\mathrm{Tr}\left[U(x,z)B(y,z)^\dagger\gamma_5\gamma_3 U(y,z)\gamma_1\gamma_5 B(x,z)^\dagger\gamma_5\gamma_2\right] \\
&\quad -\mathrm{Tr}\left[U(x,z)B(y,z)^\dagger\gamma_5\gamma_1 U(y,z)\gamma_2\gamma_5 B(x,z)^\dagger\gamma_5\gamma_3\right] \\
&\quad -\mathrm{Tr}\left[U(x,z)B(y,z)^\dagger\gamma_5\gamma_2 U(y,z)\gamma_3\gamma_5 B(x,z)^\dagger\gamma_5\gamma_1\right] \\
&\quad +\mathrm{Tr}\left[U(x,z)\gamma_1\gamma_5 B(y,z)^\dagger\gamma_5\gamma_3 U(y,z)B(x,z)^\dagger\gamma_5\gamma_2\right] \\
&\quad +\mathrm{Tr}\left[U(x,z)\gamma_2\gamma_5 B(y,z)^\dagger\gamma_5\gamma_1 U(y,z)B(x,z)^\dagger\gamma_5\gamma_3\right] \\
&\quad +\mathrm{Tr}\left[U(x,z)\gamma_3\gamma_5 B(y,z)^\dagger\gamma_5\gamma_2 U(y,z)B(x,z)^\dagger\gamma_5\gamma_1\right] \\
&\quad -\mathrm{Tr}\left[U(x,z)\gamma_1\gamma_5 B(x,z)^\dagger\gamma_5\gamma_2\right]\mathrm{Tr}\left[U(y,z)B(y,z)^\dagger\gamma_5\gamma_3\right] \\
&\quad -\mathrm{Tr}\left[U(x,z)\gamma_2\gamma_5 B(x,z)^\dagger\gamma_5\gamma_3\right]\mathrm{Tr}\left[U(y,z)B(y,z)^\dagger\gamma_5\gamma_1\right] \\
&\quad -\mathrm{Tr}\left[U(x,z)\gamma_3\gamma_5 B(x,z)^\dagger\gamma_5\gamma_1\right]\mathrm{Tr}\left[U(y,z)B(y,z)^\dagger\gamma_5\gamma_2\right]\Big\rangle
\end{aligned}
\tag{D.29}
$$

Matrix element C_{52}:

$$
\begin{aligned}
&\left\langle \mathcal{O}_{B^*(0)B^*(0)}(t)\mathcal{O}^\dagger_{[B^*B^*](0)}(0)\right\rangle \\
&= 2\cdot\sum_{\mathbf{x},\mathbf{y}}\Big\langle \mathrm{Tr}\left[U(x,z)\Gamma'_1\gamma_5 B(x,z)^\dagger\gamma_5\Gamma_1\right]\mathrm{Tr}\left[U(y,z)\Gamma'_2\gamma_5 B(y,z)^\dagger\gamma_5\Gamma_2\right] \\
&\quad -\mathrm{Tr}\left[U(x,z)\Gamma'_1\gamma_5 B(y,z)^\dagger\gamma_5\Gamma_2 U(y,z)\Gamma'_2\gamma_5 B(x,z)^\dagger\gamma_5\Gamma_1\right] \\
&\quad +\mathrm{Tr}\left[U(x,z)\Gamma'_2\gamma_5 B(y,z)^\dagger\gamma_5\Gamma_2 U(y,z)\Gamma'_1\gamma_5 B(x,z)^\dagger\gamma_5\Gamma_1\right] \\
&\quad -\mathrm{Tr}\left[U(x,z)\Gamma'_2\gamma_5 B(x,z)^\dagger\gamma_5\Gamma_1\right]\mathrm{Tr}\left[U(y,z)\Gamma'_1\gamma_5 B(y,z)^\dagger\gamma_5\Gamma_2\right]\Big\rangle
\end{aligned}
\tag{D.30}
$$

$$
\begin{aligned}
&= 2\cdot\sum_{\mathbf{x},\mathbf{y}}\epsilon_{ijk}\epsilon_{ilm} \\
&\quad \Big\langle \mathrm{Tr}\left[U(x,z)\gamma_j\gamma_5 B(x,z)^\dagger\gamma_5\gamma_l\right]\mathrm{Tr}\left[U(y,z)\gamma_k\gamma_5 B(y,z)^\dagger\gamma_5\gamma_m\right] \\
&\quad -\mathrm{Tr}\left[U(x,z)\gamma_j\gamma_5 B(y,z)^\dagger\gamma_5\gamma_m U(y,z)\gamma_k\gamma_5 B(x,z)^\dagger\gamma_5\gamma_l\right] \\
&\quad +\mathrm{Tr}\left[U(x,z)\gamma_k\gamma_5 B(y,z)^\dagger\gamma_5\gamma_m U(y,z)\gamma_j\gamma_5 B(x,z)^\dagger\gamma_5\gamma_l\right] \\
&\quad -\mathrm{Tr}\left[U(x,z)\gamma_k\gamma_5 B(x,z)^\dagger\gamma_5\gamma_l\right]\mathrm{Tr}\left[U(y,z)\gamma_j\gamma_5 B(y,z)^\dagger\gamma_5\gamma_m\right]\Big\rangle
\end{aligned}
\tag{D.31}
$$

$$
\begin{aligned}
&= 4 \cdot \sum_{\mathbf{x},\mathbf{y}} \sum_{j,k;j\neq k} \\
&\quad \Big\langle \mathrm{Tr}\left[U(x,z)\gamma_j\gamma_5 B(x,z)^\dagger \gamma_5\gamma_j\right] \mathrm{Tr}\left[U(y,z)\gamma_k\gamma_5 B(y,z)^\dagger\gamma_5\gamma_k\right] \\
&\quad -\mathrm{Tr}\left[U(x,z)\gamma_j\gamma_5 B(y,z)^\dagger\gamma_5\gamma_k U(y,z)\gamma_k\gamma_5 B(x,z)^\dagger\gamma_5\gamma_j\right] \\
&\quad +\mathrm{Tr}\left[U(x,z)\gamma_j\gamma_5 B(y,z)^\dagger\gamma_5\gamma_j U(y,z)\gamma_k\gamma_5 B(x,z)^\dagger\gamma_5\gamma_k\right] \\
&\quad -\mathrm{Tr}\left[U(x,z)\gamma_j\gamma_5 B(x,z)^\dagger\gamma_5\gamma_k\right] \mathrm{Tr}\left[U(y,z)\gamma_k\gamma_5 B(y,z)^\dagger\gamma_5\gamma_j\right]\Big\rangle
\end{aligned}
\tag{D.32}
$$

Since the double sum is extremely expensive for numerical calculation, we factorise these terms to improve run time. The angled brackets can be omitted because the calculation is executed for several configurations and finally averaged. For example, C_{41} will be implemented as follows:

Matrix element C_{41}:

$$
\begin{aligned}
&\left\langle \mathcal{O}_{B(0)B^*(0)}(t)\mathcal{O}^\dagger_{[BB^*](0)}(0)\right\rangle \\
C_{41}(t) =& 2 \cdot \left(\sum_{\mathbf{x}} \mathrm{Tr}\left[U(x,z)B(x,z)^\dagger\right]\right)\left(\sum_{\mathbf{y}} \mathrm{Tr}\left[U(y,z)\gamma_j\gamma_5 B(y,z)^\dagger\gamma_5\gamma_j\right]\right) \\
& -2 \cdot \mathrm{Tr}\left[\left(\sum_{\mathbf{x}} B(x,z)^\dagger U(x,z)\right)\left(\sum_{\mathbf{y}} B(y,z)^\dagger\gamma_5\gamma_j U(y,z)\right)\gamma_j\gamma_5\right] \\
& +2 \cdot \mathrm{Tr}\left[\left(\sum_{\mathbf{x}} B(x,z)^\dagger U(x,z)\right)\gamma_j\gamma_5\left(\sum_{\mathbf{y}} B(y,z)^\dagger\gamma_5\gamma_j U(y,z)\right)\right] \\
& -2 \cdot \left(\sum_{\mathbf{x}} \mathrm{Tr}\left[U(x,z)\gamma_j\gamma_5 B(x,z)^\dagger\right]\right)\left(\sum_{\mathbf{y}} \mathrm{Tr}\left[U(y,z)B(y,z)^\dagger\gamma_5\gamma_j\right]\right)
\end{aligned}
\tag{D.33}
$$

D.2 Time Reversal

In the following, we present the explicit computation of time reversal $\mathcal{T}$ for all 15 correlation matrix elements.

$$\begin{aligned}\mathcal{T}\left[C_{11}(t)\right] = \mathcal{T}\Big\{&\Big[\bar{b}\gamma_5 d(x,t)\,\bar{b}\gamma_j u(x,t) - \bar{b}\gamma_5 u(x,t)\,\bar{b}\gamma_j d(x,t)\Big] \\ &\times \Big[\bar{d}\gamma_5 b(z,0)\,\bar{u}\gamma_j b(z,0) - \bar{u}\gamma_5 b(z,0)\,\bar{d}\gamma_j b(z,0)\Big]\Big\} = C_{11}(-t)\end{aligned} \tag{D.34}$$

$$\begin{aligned}\mathcal{T}\left[C_{12}(t)\right] = \mathcal{T}\Big\{&\Big[\bar{b}\gamma_5 d(x,t)\,\bar{b}\gamma_i u(x,t) - \bar{b}\gamma_5 u(x,t)\,\bar{b}\gamma_i d(x,t)\Big] \\ &\times \Big[\bar{d}\gamma_j b(z,0)\,\bar{u}\gamma_k b(z,0) - \bar{u}\gamma_j b(z,0)\,\bar{d}\gamma_k b(z,0)\Big]\Big\} = -C_{12}(-t)\end{aligned} \tag{D.35}$$

$$\begin{aligned}\mathcal{T}\left[C_{13}(t)\right] = \mathcal{T}\Big\{&\Big[\bar{b}\gamma_5 d(x,t)\,\bar{b}\gamma_j u(x,t) - \bar{b}\gamma_5 u(x,t)\,\bar{b}\gamma_j d(x,t)\Big] \\ &\times \Big[\epsilon^{a'd'e'}\left(\bar{u}^{d'}\mathcal{C}\gamma_5\bar{d}^{e'}(z,0) - \bar{d}^{d'}\mathcal{C}\gamma_5\bar{u}^{e'}(z,0)\right)\epsilon^{a'b'c'}b^{b'}\gamma_0\left(\gamma_j\mathcal{C}\right)^\dagger\gamma_0 b^{c'}(z,0)\Big]\Big\} \\ &= C_{13}(-t)\end{aligned} \tag{D.36}$$

$$\begin{aligned}\mathcal{T}\left[C_{21}(t)\right] = \mathcal{T}\Big\{&\Big[\bar{b}\gamma_j d(x,t)\,\bar{b}\gamma_k u(x,t) - \bar{b}\gamma_j u(x,t)\,\bar{b}\gamma_k d(x,t)\Big] \\ &\times \Big[\bar{d}\gamma_5 b(z,0)\,\bar{u}\gamma_i b(z,0) - \bar{u}\gamma_5 b(z,0)\,\bar{d}\gamma_i b(z,0)\Big]\Big\} = -C_{21}(-t)\end{aligned} \tag{D.37}$$

$$\begin{aligned}\mathcal{T}\left[C_{22}(t)\right] = \mathcal{T}\Big\{&\Big[\bar{b}\gamma_l d(x,t)\,\bar{b}\gamma_m u(x,t) - \bar{b}\gamma_l u(x,t)\,\bar{b}\gamma_m d(x,t)\Big] \\ &\times \Big[\bar{d}\gamma_j b(z,0)\,\bar{u}\gamma_k b(z,0) - \bar{u}\gamma_j b(z,0)\,\bar{d}\gamma_k b(z,0)\Big]\Big\} = C_{22}(-t)\end{aligned} \tag{D.38}$$

$$\begin{aligned}\mathcal{T}\left[C_{23}(t)\right] = \mathcal{T}\Big\{&\Big[\bar{b}\gamma_i d(x,t)\,\bar{b}\gamma_j u(x,t) - \bar{b}\gamma_i u(x,t)\,\bar{b}\gamma_j d(x,t)\Big] \\ &\times \Big[\epsilon^{a'd'e'}\left(\bar{u}^{d'}\mathcal{C}\gamma_5\bar{d}^{e'}(z,0) - \bar{d}^{d'}\mathcal{C}\gamma_5\bar{u}^{e'}(z,0)\right)\epsilon^{a'b'c'}b^{b'}\gamma_0\left(\gamma_k\mathcal{C}\right)^\dagger\gamma_0 b^{c'}(z,0)\Big]\Big\} \\ &= -C_{23}(-t)\end{aligned} \tag{D.39}$$

$$\begin{aligned}\mathcal{T}\left[C_{31}(t)\right] = \mathcal{T}\Big\{&\Big[\epsilon^{abc}\bar{b}^b\gamma_j\mathcal{C}\bar{b}^c(x,t)\epsilon^{ade}\left(d^d\mathcal{C}\gamma_5 u^e(x,t) - u^d\mathcal{C}\gamma_5 d^e(x,t)\right)\Big] \\ &\times \Big[\bar{d}\gamma_5 b(z,0)\,\bar{u}\gamma_j b(z,0) - \bar{u}\gamma_5 b(z,0)\,\bar{d}\gamma_j b(z,0)\Big]\Big\} = C_{31}(-t)\end{aligned} \tag{D.40}$$

$$\begin{aligned}\mathcal{T}\left[C_{32}(t)\right] = \mathcal{T}\Big\{&\Big[\epsilon^{abc}\bar{b}^b\gamma_j\mathcal{C}\bar{b}^c(x,t)\epsilon^{ade}\left(d^d\mathcal{C}\gamma_5 u^e(x,t) - u^d\mathcal{C}\gamma_5 d^e(x,t)\right)\Big] \\ &\times \Big[\bar{d}\gamma_k b(z,0)\,\bar{u}\gamma_l b(z,0) - \bar{u}\gamma_k b(z,0)\,\bar{d}\gamma_l b(z,0)\Big]\Big\} = -C_{32}(-t)\end{aligned} \tag{D.41}$$

$$\begin{aligned}\mathcal{T}\left[C_{33}(t)\right] &= \mathcal{T}\Big\{\Big[\epsilon^{abc}\bar{b}^{b}\gamma_j\mathcal{C}\bar{b}^{c}(x,t)\epsilon^{ade}\left(d^{d}\mathcal{C}\gamma_5 u^{e}(x,t)-u^{d}\mathcal{C}\gamma_5 d^{e}(x,t)\right)\Big] \\ &\times\Big[\epsilon^{a'd'e'}\left(\bar{u}^{d'}\mathcal{C}\gamma_5\bar{d}^{e'}(z,0)-\bar{d}^{d'}\mathcal{C}\gamma_5\bar{u}^{e'}(z,0)\right)\epsilon^{a'b'c'}b^{b'}\gamma_0\left(\gamma_j\mathcal{C}\right)^{\dagger}\gamma_0 b^{c'}(z,0)\Big]\Big\} \\ &= C_{33}(-t)\end{aligned} \tag{D.42}$$

$$\begin{aligned}\mathcal{T}\left[C_{41}(t)\right] &= \mathcal{T}\Big\{\Big[\bar{b}\gamma_5 d(x,t)\,\bar{b}\gamma_j u(y,t)-\bar{b}\gamma_5 u(x,t)\,\bar{b}\gamma_j d(y,t)\Big] \\ &\times\Big[\bar{d}\gamma_5 b(z,0)\,\bar{u}\gamma_j b(z,0)\;-\bar{u}\gamma_5 b(z,0)\,\bar{d}\gamma_j b(z,0)\Big]\Big\} = C_{41}(-t)\end{aligned} \tag{D.43}$$

$$\begin{aligned}\mathcal{T}\left[C_{42}(t)\right] &= \mathcal{T}\Big\{\Big[\bar{b}\gamma_5 d(x,t)\,\bar{b}\gamma_i u(y,t)-\bar{b}\gamma_5 u(x,t)\,\bar{b}\gamma_i d(y,t)\Big] \\ &\times\Big[\bar{d}\gamma_j b(z,0)\,\bar{u}\gamma_k b(z,0)\;-\bar{u}\gamma_j b(z,0)\,\bar{d}\gamma_k b(z,0)\Big]\Big\} = -C_{42}(-t)\end{aligned} \tag{D.44}$$

$$\begin{aligned}\mathcal{T}\left[C_{43}(t)\right] &= \mathcal{T}\Big\{\Big[\bar{b}\gamma_5 d(x,t)\,\bar{b}\gamma_j u(y,t)-\bar{b}\gamma_5 u(x,t)\,\bar{b}\gamma_j d(y,t)\Big] \\ &\times\Big[\epsilon^{a'd'e'}\left(\bar{u}^{d'}\mathcal{C}\gamma_5\bar{d}^{e'}(z,0)-\bar{d}^{d'}\mathcal{C}\gamma_5\bar{u}^{e'}(z,0)\right)\epsilon^{a'b'c'}b^{b'}\gamma_0\left(\gamma_j\mathcal{C}\right)^{\dagger}\gamma_0 b^{c'}(z,0)\Big]\Big\} \\ &= C_{43}(-t)\end{aligned} \tag{D.45}$$

$$\begin{aligned}\mathcal{T}\left[C_{51}(t)\right] &= \mathcal{T}\Big\{\Big[\bar{b}\gamma_j d(x,t)\,\bar{b}\gamma_k u(y,t)-\bar{b}\gamma_j u(x,t)\,\bar{b}\gamma_k d(y,t)\Big] \\ &\times\Big[\bar{d}\gamma_5 b(z,0)\,\bar{u}\gamma_i b(z,0)\;-\bar{u}\gamma_5 b(z,0)\,\bar{d}\gamma_i b(z,0)\Big]\Big\} = -C_{51}(-t)\end{aligned} \tag{D.46}$$

$$\begin{aligned}\mathcal{T}\left[C_{52}(t)\right] &= \mathcal{T}\Big\{\Big[\bar{b}\gamma_l d(x,t)\,\bar{b}\gamma_m u(y,t)-\bar{b}\gamma_l u(x,t)\,\bar{b}\gamma_m d(y,t)\Big] \\ &\times\Big[\bar{d}\gamma_j b(z,0)\,\bar{u}\gamma_k b(z,0)\;-\bar{u}\gamma_j b(z,0)\,\bar{d}\gamma_k b(z,0)\Big]\Big\} = C_{52}(-t)\end{aligned} \tag{D.47}$$

$$\begin{aligned}\mathcal{T}\left[C_{53}(t)\right] &= \mathcal{T}\Big\{\Big[\bar{b}\gamma_i d(x,t)\,\bar{b}\gamma_j u(y,t)-\bar{b}\gamma_i u(x,t)\,\bar{b}\gamma_j d(y,t)\Big] \\ &\times\Big[\epsilon^{a'd'e'}\left(\bar{u}^{d'}\mathcal{C}\gamma_5\bar{d}^{e'}(z,0)-\bar{d}^{d'}\mathcal{C}\gamma_5\bar{u}^{e'}(z,0)\right)\epsilon^{a'b'c'}b^{b'}\gamma_0\left(\gamma_k\mathcal{C}\right)^{\dagger}\gamma_0 b^{c'}(z,0)\Big]\Big\} \\ &= -C_{53}(-t)\end{aligned} \tag{D.48}$$

Bibliography

[1] C. Patrignani et al. (Particle Data Group): Chin. Phys. C, **40**, 100001 (2016) and 2017 update

[2] J. J. Dudek, R. G. Edwards, D. J. Wilson: "*An a_0 resonance in strongly coupled $\pi\eta, KK$ scattering from lattice QCD*", Phys. Rev. **D93** 094506 (2016), arXiv:1602.05122 [hep-ph]

[3] The Belle Collaboration: K. Abe, et al.: "*Observation of a New Narrow Charmonium State in Exclusive $B^{\pm} \to K^{\pm}\pi^{+}\pi^{-}J/\psi$ Decays*", Phys. Rev. Lett. **91**, 262001 (2003), arXiv:hep-ex/0308029v1

[4] The LHCb Collaboration: R. Aaij et al.: "*Observation of the resonant character of the $Z(4430)^{-}$ state*", Phys. Rev. Lett. **112**, 222002 (2014), arXiv:1404.1903v1 [hep-ex]

[5] The Belle Collaboration: S.-K. Choi, S. L. Olsen, et al.: "*Observation of a resonance-like structure in the $\pi^{\pm}\psi'$ mass distribution in exclusive $B \to K\pi^{\pm}\psi'$ decays*", Phys. Rev. Lett. **100**, 142001 (2008), arXiv:0708.1790v2 [hep-ex]

[6] The Belle Collaboration: R. Mizuk et al.: "*Dalitz analysis of $B \to K\pi^{+}\psi'$ decays and the $Z(4430)^{+}$*", Phys. Rev. D **80**, 031104(R) (2009), arXiv:0905.2869v2 [hep-ex]

[7] The Belle Collaboration: K. Chilikin, R. Mizuk et al.: "*Observation of a new charged charmoniumlike state in $\bar{B}^0 \to J/\psi K^{-}\pi^{+}$ decays*", Phys. Rev. D **90**, 112009 (2014) arXiv:1408.6457v3 [hep-ex]

[8] The Belle Collaboration: A. Bondar et al.: "*Observation of two charged bottomonium-like resonances in $\Upsilon(5S)$ decays*", Phys. Rev. Lett. **108**, 122001 (2012), arXiv:1110.2251 [hep-ex]

[9] BESIII Collaboration: M. Ablikim et al.: "*Observation of $Z_c(3900)^0$ in $e^{+}e^{-} \to \pi^0\pi^0 J/\psi$*", Phys. Rev. Lett. **115**, 112003 (2015), arXiv:1506.06018v2 [hep-ex]

[10] The Belle Collaboration: Z. Q. Liu et al.: "*Study of $e^{+}e^{-} \to \pi^{+}\pi^{-}J/\psi$ and Observation of a Charged Charmonium-like State at Belle*", Phys. Rev. Lett. **110**, 252002 (2013), arXiv:1304.0121v2 [hep-ex]

[11] BESIII Collaboration: M. Ablikim, M. N. Achasov et al.: "*Observation of a charged charmoniumlike structure in $e^{+}e^{-} \to \pi^{+}\pi^{-}J/\psi$ at $\sqrt{s} = 4.26$ GeV*", Phys. Rev. Lett. **110**, 252001 (2013), arXiv:1303.5949 [hep-ex]

[12] T. Xiao, S. Dobbs, A. Tomaradze, Kamal K. Seth: "*Observation of the Charged Hadron $Z_c^{\pm}(3900)$ and Evidence for the Neutral $Z_c^0(3900)$ in $e^+e^- \to \pi\pi J/\psi$ at $\sqrt{s} =$ 4170 MeV*", Phys. Lett. B **727** (2013) 366-370, arXiv:1304.3036 [hep-ex]

[13] D0 Collaboration: V. M. Abazov et al.: "*Evidence for a $B_s^0\pi^{\pm}$ State*", Phys. Rev. Lett. **117**, 022003 (2016), arXiv:1602.07588 [hep-ex]

[14] Z. S. Brown, K. Orginos: "*Tetraquark bound states in the heavy-light heavy-light system*", Phys. Rev. D **86**, 114506 (2012), arXiv:1210.1953 [hep-lat]

[15] P. Bicudo, M. Wagner: "*Lattice QCD signal for a bottom-bottom tetraquark*", Phys. Rev. D **87**, 114511 (2013), arXiv:1209.6274 [hep-ph]

[16] P. Bicudo, K. Cichy, A. Peters, B. Wagenbach, M. Wagner: "*Evidence for the existence of $ud\bar{b}\bar{b}$ and the non-existence of $ss\bar{b}\bar{b}$ and $cc\bar{b}\bar{b}$ tetraquarks from lattice QCD*", Phys. Rev. D **92**, 014507 (2015), arXiv:1505.00613v2 [hep-lat]

[17] P. Bicudo, K. Cichy, A. Peters, M. Wagner: "*B B interactions with static bottom quarks from Lattice QCD*", Phys. Rev. D **93**, 034501 (2016), arXiv:1510.03441v1 [hep-lat]

[18] A. Peters, P. Bicudo, L. Leskovec, S. Meinel, A. Peters, M. Wagner: "*Lattice QCD study of heavy-heavy-light-light tetraquark candidates*", arXiv:1609.00181v1 [hep-lat]

[19] Martin Pflaumer: "*Resonanzen in $\bar{b}\bar{b}ud$-Tetraquark-Systemen basierend auf statisch-leichten Gitter-QCD-Vier-Quark-Potentialen*", Bachelor thesis, Goethe University Frankfurt am Main, 2016.

[20] P. Bicudo, J. Scheunert, M. Wagner: "*Including heavy spin effects in the prediction of a $\bar{b}\bar{b}ud$ tetraquark with lattice QCD potentials*", Phys. Rev. D **95**, 034502 (2017), arXiv:1612.02758 [hep-lat]

[21] Antje Peters: "*Investigation of heavy-light four-quark systems by means of Lattice QCD*", PhD thesis, Goethe University Frankfurt am Main, 2017.

[22] P. Bicudo, M. Cardoso, A. Peters, M. Pflaumer, M. Wagner: "*$ud\bar{b}\bar{b}$ tetraquark resonances with lattice QCD potentials and the Born-Oppenheimer approximation*", Phys. Rev. D **96**, 054510 (2017), arXiv:1704.02383 [hep-lat]

[23] A. Francis, R. J. Hudspith, R. Lewis, K. Maltman: "*Lattice Prediction for Deeply Bound Doubly Heavy Tetraquarks*", Phys. Rev. Lett. **118**, 142001 (2017), arXiv:1607.05214 [hep-lat]

[24] A. Francis, R. J. Hudspith, R. Lewis, K. Maltman: "*More on heavy tetraquarks in lattice QCD at almost physical pion mass*", arXiv:1711.03380v1 [hep-lat]

[25] S. Hashimoto, T. Onogi: "*Heavy Quarks on the Lattice*", Ann. Rev. Nucl. Part. Sci. **54** (2004) 451–486, arXiv:hep-ph/0407221

[26] C. Amsler et al. (Particle Data Group): Phys. Lett. B **667**, 1 (2008)

[27] Christof Gattringer, Christian B. Lang: "*Quantum Chromodynamics on the Lattice*", Springer-Verlag, 2010.

[28] S. Meinel: "*Heavy quark physics on the lattice with improved nonrelativistic actions*", PhD thesis, University of Cambridge, 2009.

[29] Lewis H. Ryder: "*Quantum Field Theory*", Cambridge University Press, 1985.

[30] G. P. Lepage, L. Magnea, C. Nakhleh: "*Improved Nonrelativistic QCD for Heavy Quark Physics*", Phys. Rev. **D46**, 4052 (1992), arXiv:9205007v1 [hep-lat]

[31] B. A. Thacker, G. P. Lepage: "*Heavy-quark bound states in lattice QCD*", Phys. Rev. D **43**, 196 (1991)

[32] G.P. Lepage, P.B. Mackenzie: "*On the Viability of Lattice Perturbation Theory*", Phys. Rev. D **48**, 2250 (1993), arXiv:hep-lat/9209022

[33] N. H. Shakespeare, H. D. Trottier: "*Tadpole renormalization and relativistic corrections in lattice NRQCD*", Phys. Rev. D **58**, 034502 (1998), arXiv:hep-lat/9802038

[34] K. Cichy, V. Drach, E. Garcia-Ramos, G. Herdoiza, K. Jansen: "*Overlap valence quarks on a twisted mass sea: a case study for mixed action Lattice QCD*", Nucl. Phys.B **869** (2013) 131–163, arXiv:1211.1605 [hep-lat]

[35] M. Wingate, J. Shigemitsu, C. T. H. Davies, G. P. Lepage, H. D. Trottier: "*Heavy-light mesons with staggered light quarks*", Phys. Rev. D **67**, 054505 (2003), arXiv:hep-lat/0211014v2

[36] C. Hughes, E. Eichten, C. T. H. Davies: "*The Search for Beauty-fully Bound Tetraquarks Using Lattice Non-Relativistic QCD*", Phys. Rev. D **97**, 054505 (2018), arXiv:1710.03236v1 [hep-lat]

[37] Z.-G. Wang, Z.-Y. Di: "*Analysis of the vector and axialvector $QQ\bar{Q}\bar{Q}$ tetraquark states with QCD sum rules*", arXiv:1807.08520 [hep-ph]

[38] A. Esposito, A. D. Polosa: "*A $bb\bar{b}\bar{b}$ di-bottomonium at the LHC?*", arXiv:1807.06040 [hep-ph]

[39] B. Blossier, M. Della Morte, G. von Hippel, T. Mendes, R. Sommer: "*On the generalized eigenvalue method for energies and matrix elements in lattice field theory*", JHEP **04** (2009) 094, arXiv:0902.1265v2 [hep-lat]

[40] B. Blossier, G. von Hippel, T. Mendes, R. Sommer, M. Della Morte: "*Efficient use of the Generalized Eigenvalue Problem*", arXiv:0808.1017v1 [hep-lat]

[41] A. Abdel-Rehim, C. Alexandrou, J. Berlin, M. Dalla Brida, J. Finkenrath, M. Wagner: "*Investigating efficient methods for computing four-quark correlation functions*", arXiv:1701.07228v1 [hep-lat]

[42] Z. S. Brown, W. Detmold, S. Meinel, K. Orginos: "*Charmed bottom baryon spectroscopy from lattice QCD*", Phys. Rev. D **90**, 094507 (2014), arXiv:1409.0497 [hep-lat]

[43] S.Meinel: "*User manual for QMBF and MBF*", 7 June 2013, stefan-meinel.com/software/QMBF_MBF/

[44] L. Leskovec, S. Meinel, A. Peters, G. Rendon: "*The BB tetraquark with NRQCD*", January 9, 2017, *not published*.

[45] S.Meinel: "*Available domain-wall propagators with AMA on the RBC/UKQCD ensembles*", 28 November 2017, *not published*.

[46] R. A. Briceno, J. J. Dudek, R. D. Young: "*Scattering processes and resonances from lattice QCD*", Rev. Mod. Phys. **90**, 025001 (2018), arXiv:1706.06223 [hep-lat]

[47] M.Lüscher: "*Volume dependence of the energy spectrum in massive quantum field theories - I. Stable Particle States*", Commun. Math. Phys. **104**, 177-206 (1986)

[48] M.Lüscher: "*Volume dependence of the energy spectrum in massive quantum field theories - II. Scattering States*", Commun. Math. Phys. **105**, 153-188 (1986)

[49] M.Lüscher: "*Two-particle states on a torus and their relation to the scattering matrix*", Nucl. Phys. **B354**, 531-578 (1991)

Acknowledgements

At the end, I would like to thank all those supporting me writing this thesis.
First of all, I thank Marc Wagner for his excellent supervision and his patience in our numerous discussions. Whenever I knocked at his door, he took the time to debate thoroughly my ideas and suggested new ways how to proceed. This work would not have been possible without his helpful advice.
Next, I want to thank my second examiner Stefan Meinel for providing his NRQCD code and lattice configurations and explaining how to include the quark propagators. Our audio conferences have been very gainful and I have benefited a lot from his comprehensive explanations.
My thanks go also to Luka Leskovec for discussing and comparing our numerical results and answering patiently all my questions.
I would also like to say thank you to Antje Peters for kindly introducing me to the field of NRQCD.
Finally, I would like to express my gratitude to my family who supported me all the time and spent lots of hours proofreading my thesis.